Xi'an Technological University (XATU)

Xi'an Technological University(XATU) was founded in 1955. After more than fifty years of development, the school has become a multidisciplinary university with distinctive features and great impact. The school covers an area of 1290 mu, with building area of nearly 475,000 square meters, 1773 full-time regular teachers, including 126 professors, 483 teachers with senior professional titles; 430 teachers with doctor's degree.

At present there are 14 secondary colleges, 4 direct departments, one industrial center, more than 1,700 graduate students and 19000 undergraduates of various disciplines. The school now has three doctoral project construction disciplines: "Optical Engineering", "Materials Processing Engineering" and "Mechanical Engineering", two doctoral project construction support disciplines: "Computer Science and Technology", "Management Science and Engineering", 6 subjects and disciplines with characteristics at the provincial level, 15 master degree authorization disciplines at first level, 62 master degree authorization centers and 13 master degree authorization centers for Master of Engineering and Master of Business Administration (MBA), 46 undergraduate majors, covering Engineering, Science, Management Science, Economics, Science of Law, Literature, Education and other seven disciplines. In the process of discipline construction and development, the school focus on highlighting science industry characteristics, take the road of production, teaching and research integration, promote the full integration of school and the local economic development, meets development requirements of weapons industry. The school has already had two national key research base, an international cooperative research centre and 11 provincial and ministerial key laboratories, with the ability to undertake large-scale military and civilian research projects in Optics, Machinery, Materials and other disciplines.

The school strengthens international exchange and cooperation, has established intercollegiate exchange relationship of research collaboration, student exchange programs with more than 20 renowned universities in more than 20 countries, such as United States, Japan, Britain, France, Germany, Australia and so on. Each year there are a number of teachers, students or the school senior managers go abroad for learning, short-term training or investigation.

Website: www.xatu.edu.cn

Publisher: State and Local Joint Engineering Lab. of Advanced Network and Monitoring Control (ANMC)

Cooperate: Xi'an Technological University (CHINA)
West Virginia University (USA)
Huddersfield University of UK (UK)
Missouri Western State University (USA)
National University of Singapore (Singapore)

Approval: Library of Congress of the United States
Shaanxi provincial Bureau of Press, Publication, Radio and Television

Address: 4525 Downs Drive, St. Joseph, MO64507 , USA
No. 2 Xuefu Road,weiyang District, Xi'an, 710021, China

Telephone: +1-816-2715618 (USA) +86-29-86173290 (China)

Website: www.ijanmc.org
E-mail: ijanmc@jianmc.org
xxwlcn@163.com
ISSN: 2470-8038

Print No (China): 61-94101
Publication Date: Mar. 28, 2017

Editorial board

Language Editor

CONTENTS

An Investigation on Tree-Based Tags Anti-Collision Algorithms in RFID

Su Xiaohao [1], Liu Baolong [2]

[1] School of Computer Science and Engineering, Xi'an Technological University,

Xi'an 710021, China, Email:529489890@qq.com

[2] School of Computer Science and Engineering, Xi'an Technological University,

Xi'an 710021, China, Email:liu.bao.long@hotmail.com

Abstract. The tree-based tags anti-collision algorithm is an important method in the anti-collision algorithms. In this paper, several typical tree algorithms are evaluated. The comparison of algorithms is summarized including time complexity, communication complexity and recognition, and the characteristics and disadvantages of each algorithm are pointed out. Finally, the improvement strategies of tree anti-collision algorithm are proposed, and the future research directions are also prospected.

Keywords: Radio Frequency Identification, Anti-collision algorithm, Electronic tags, Deterministic algorithm

1. Introduction

With the rapid development of the Internet of things technology, Radio frequency identification (RFID) technology has been used more and more in life and production. RFID technology is an important part of the Internet of Things system. It is a non-contact intelligent identification technology. Compared with the traditional automatic identification technology, it has many advantages such as small size, low cost, large amount of data storage, high security and reusable. It has great application value in industrial production, logistics and transport and cargo management, commodity trade, health and safety inspection and intelligent transportation and other fields. RFID system mainly consists of reader (including antenna), the application system and a large number of electronic tags [1-3] as shown in Fig.1. Label is mainly used to store the information encoded by the marked object and security encryption, the reader used to read, change and verify the label information. However, there are several problems in the application of RFID system.

1.1 Collision problem

When multiple tags and readers in the same channel and signal transmission, collision problem is generated because of mutual interferences between tags and readers.

1.2 Security authentication and privacy protection

The security problem is how to ensure the authenticity and validity of the label information and the

reader when there are eavesdropping attacks and replay attacks.

1.3 Efficient storage of large amounts of data

RFID devices in real-world applications continue to generate large amounts of data. How to build an efficient data storage model to reduce system overhead and improve query efficiency is an urgent problem to be solved.

1.4 Precise target location and tracking

How to obtain the accurate position information of the location object in outdoor and indoor environment will be a hot research field in the future.

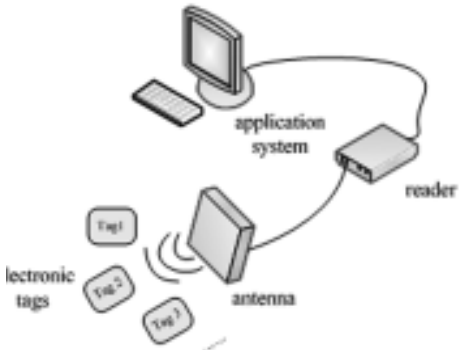

Figure.1 Diagram of RFID system composition

The collision problem is a key problem affecting the performance of RFID identification, which restricts the recognition efficiency in large-scale label recognition environment. When multiple readers or multiple tags at the same time, the same frequency to send data, the data signal will interfere with each other in the wireless channel, resulting in data loss, missing, misreading and other phenomena [4]. According to the different reasons of the collision, it can be divided into three categories: tag-tag collision, tag-reader collision and reader-reader collision [5]. As for tag-tag collision problem, the anti-collision algorithm has been divided into three categories [6-10]: (1) Non deterministic anti-collision algorithms based on ALOHA; (2) Deterministic anti-collision algorithms based on tree structure; (3) Hybrid algorithms.

This paper summarizes the tag-tag anti-collision algorithms based on tree structure. Some of the typical algorithms at present are analyzed and compared for algorithm on time complexity, communication complexity and recognition efficiency. The way to improve the existing algorithm is discussed, and the future research directions are points out. This provides reference for the research on anti-collision algorithms the structure of the tree.

2. Reviews of Several Typical Tree-Based Anti-Collision Algorithms

The tree-based anti-collision algorithms transform the label number to a binary string consisting of '0' and '1'. When a collision occurs, it is divided into "0" and "1" branches according to the label number. In each branch, the algorithm repeats the query process until it can correctly identify a label. In the end, a tree structure is built. Compared to ALOHA algorithm for random reading of labels, tree-based algorithm can avoid the label hunger phenomenon. In this section, we have selected several tree-based algorithms with the most research at present, and analyzed the implementation process of the

algorithm and the latest research progress。

2.1 BT (Binary Tree) Algorithm

The binary tree algorithm (BT) is a basic binary anti-collision algorithm, in which each tag contains a counter and a random number generator [11].When the counter value is 0, the label sends the tag information. When the counter value is not 0, the label is in a wait state and does not respond, and the value of each counter is 0 in initial state. The algorithm steps are as follows.

1) After the reader sends the query command for the first time, all the tags responses within the recognition range and sent the respective tag numbers.

2) If a collision occurs, each tag with a counter value of 0 randomly generates 0 or 1 and assigns it to the counter. If the counter value is greater than 0, the counter value is incremented by 1.

3) If no collision occurs, it indicates that a label has been identified or a free node is generated, and the counter value for all tags is decremented by one.

4) Cycle the step 2 until all the tags are identified.

Fig. 2 shows an example of using the BT algorithm to identify tags. With the increasing of the number of tags, the number of queries increases dramatically. This leads to a large number of idle time slots and reduces the efficiency of the system recognition. Otherwise, the BT algorithm needs to update the value of the tag counter for each identification cycle with requiring the tag to have storage and counting function [12]. As the result, it increases the overhead of the system. In [13], the ABS algorithm was proposed based on the BT algorithm. Each tag in the algorithm has two counters: the reader’s allocates slot counter Rc and the label’s progress slot counter Pc [14]. These two counters and random numbers make the tags identically identifiable, but the algorithm is designed to be more complex. There are still idle slots in the recognition process. The value of the counter is also stored every time, which increases the time complexity of the algorithm. Jiang et al [15] introduced a fallback strategy and search tree algorithm to improve the ABS algorithm. The algorithm eliminates idle time, and reduces the identification delay, but it does not reduce the system overhead because each query still needs to change the value of the counters.

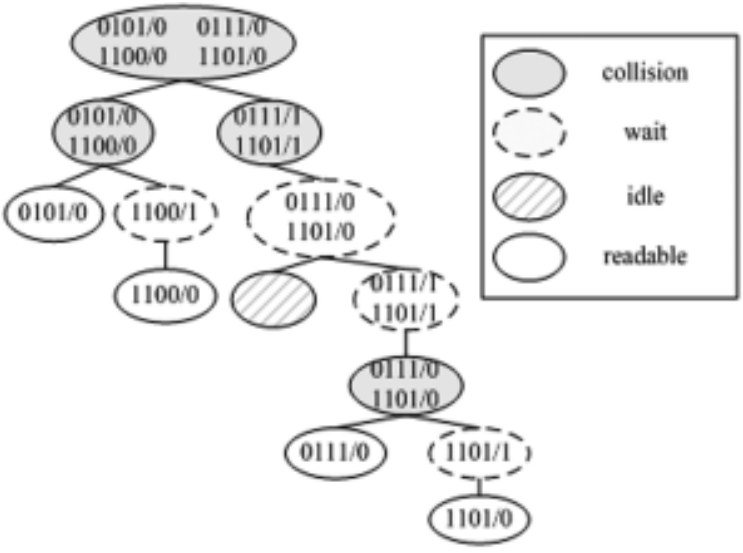

Figure.2 An example diagram for BT algorithm

2.2 BS (Binary Search) Algorithm

Binary search tree anti-collision algorithm (BS) is a memory less classic tree-based anti-collision algorithm [16]. In the algorithm, the label does not need to store any information, when the collision occurs, the reader can change the query string to identify labels. The algorithm steps are as follows.

1) The reader sends the query command to tags in binary string. The query string length is equal to the label number length and the initial value is composed of all ’1’. All tags to be identified in the recognition range response and send the numbers to the reader.

2) If no collision occurs, there is only one tag identified. If the collision occurs, the reader will set query string’s the highest collision position ‘0’ and the encoding higher than the highest collision bit unchanged, the highest collision to the lowest are set to “1” to form a new query string.

3) The reader broadcasts a new query string, looping the step 2. When a tag is recognized, the reader reads its number and sends the command to the “dormant” state.

4) Restart from step 1 until all tags are identified.

The binary search algorithm (BS) eliminates the idle time slot and does not need to store additional data. However, each recognition after the query string will start from the initial state, and it increases the number of queries. At the same time, when the reader sends a binary string, the tag needs to send a complete binary string. In fact, the same part of the binary string sent by the reader does not need to be sent to the reader. Given the three labels A, B, C {110100101011011010101101}, using the BS algorithm to identify the process of these three labels are shown in table 1.

Table 1 Binary search algorithm identification table

	First search	Second search	Third search
Reqest	11111111	10111111	10101111
Label A	11010010	——	——
Label B	10110110	10110110	——
Label C	10101101	10101101	10101101
Collision bit decoding results	1×××××××	101××1××	
Identified label	null	null	C

The improved algorithm based on BS algorithm includes dynamic binary search algorithm (DBS), dynamic back off binary search algorithm [20] and so on. Compared to the BS algorithm, the DBS algorithm has the same number of queries, but the data between the label and the reader is reduced by half and the query efficiency is improved. Dynamic binary back off algorithm is improved on the basis of the DBS algorithm, which reduces the number of queries while ensuring that DBS transmits less data. On the basis of BS algorithm, the BS - BLG algorithm is proposed by Di Chunyu from Jilin University [21], whose main improvement is to increase the lock bit group and group paging instructions. The role of the lock bit group is to extract the bits that produce the collision and to prioritize groups according to the number of consecutive ‘1’. It reduce the number of queries by grouping paging and use backward strategy to reduce the number of queries. BLBO algorithm is proposed on the basis of BS and DBS algorithm [22]. In this algorithm the collision bit is locked by the lock strategy, and then the reader only sends the collision bit information, which reduces the communication complexity. By using the

backward strategy, after each tag is identified, it is returned to the node where the collision occurred, and the recognition efficiency of the BLBO algorithm is close to 50%. In [23], the NBLBO algorithm is proposed on the basis of BS algorithm and BLBO algorithm. The algorithm introduces the idea of adaptive bifurcation, which adjusts the next query prefix by calculating the collision factor after each collision. With the same number of tags, the recognition efficiency of the algorithm is about 3 times of that the BLBO algorithm and it also has a significant reduction in the amount of data transmission and the number of queries.

2.3 QT (Query Tree) Algorithm

The QT Algorithm [2, 24-26] is also a memory less algorithm，the tag only needs to be compared to the query prefix sent by the reader each time, and the tag is sent back to the reader with the prefix. The algorithm is first introduced into the stack to save the query prefix to improve the query efficiency. QT algorithm steps are as follows.

1) In the initial stage of the query, an empty string is pushed onto the stack, and the reader sends an empty string. At this time, all tag responses within the scope of the identification.

2) If there is a collision, the ‘0’ and ‘1’ followed by the last prefix are added to form a new query prefix, and the two new prefixes are pressed into the stack. If there is no collision, a unique tag is identified.

3) If the stack is not empty, popping a query prefix of the stack. After receiving the query command, the tag matching the query prefix returns the code of the remainder. If there is no tag response, an empty cycle will occur, and a query prefix will be popped.

4) Repeat the above 2, 3 steps until the stack is empty and all tags are identified.

QT algorithm is simple and easy. It has no additional storage requirements for the tag, and the hardware cost is low. However, the QT algorithm is greatly affected by the label distribution, it does not prejudge the location of the collision of the label, and the update of the query prefix is more mechanical. It will produce a large number of idle time slots in the process of identification. The following table lists the number of idle time slots in the case where the label length is 12 bits and the number distribution is a random distribution. The number of tags increases from 100 to 600.

Table 2 Slot table for QT algorithm

Number of tags	Query time slot	Idle time slot
100	289	45
200	543	71
300	785	93
400	1031	116
500	1283	142
600	1512	157

It can be seen that as the number of tags increases, the free time slot increases. The query efficiency is reduced, increasing the reader’s energy consumption. But the QT algorithm still inevitably produces a large number of free time slots and collision time slots. In the literature [27], the MBQT algorithm is proposed based on the QT algorithm. The label is changed from binary code to multiple coding, which

reduces the amount of transmission data in the communication process and improves the recognition efficiency. But the algorithm needs to use the reader more storage space, and the performance of the algorithm is also affected by the length of the tag. In [28], a hybrid query tree algorithm is proposed. The algorithm changes the query prefix according to the collision information in each recognition cycle. Compared with the QT algorithm, the algorithm reduces the number of queries and increases the recognition efficiency to about 59%. But the algorithm still does not solve the problem of idle time slot. Zhou Qing proposed the IHQT algorithm based on the QT algorithm [29] which sets a full adder in each tag. This algorithm uses the number of three consecutive "1" after the query prefix to determine the order of the response to the reader. This method avoids the generation of idle time slots and reduces communication complexity.

2.4 CT(Collision Tree) Algorithm

CT algorithm is an improved algorithm in QT algorithm, which was proposed by Dr. Jia Xiaolin in 2012 [12]. Unlike the QT algorithm, the CT algorithm only updates the query prefix for the collision position, reduces the unnecessary query, and eliminates the idle time slot. In the CT algorithm, first, the initial reader sends a query instruction to labels. if there is no label collision, then directly identify, or the reader update the query prefix according to the first collision bit, that is, all the bits before the first collision bit unchanged, Followed by the addition of "0" and "1".Thus, two new query prefix are pushed onto the stack. The reader sends the query prefix at the top of the query stack, and labels compare their own number with the received query prefix. If the same, labels will remove the same part of the prefix sent to the reader, the reader again to judge until the stack is empty so far.

The CT algorithm completely eliminates the idle cycle in the query process, and does not need the information in the process of memory tag recognition. The recognition efficiency is more than 50%. On the basis of CT algorithm, a multi-period identification algorithm (MCT) [30] is proposed, which divides the identification cycle of communication between reader and tag in RFID multi-tag identification into three sub-periods (Q, R0, R1).In the algorithm, labels determines the flag bit according to the query command, and select the response cycle (R0 or R1) according to the value of the flag bit to respond to the reader's query request. But in this way, each time the reader sends the request, the label must judge the flag bit, according to the flag bit to divide the response cycle, so that the communication efficiency of the tag and the reader is greatly reduced. In paper [31], the CT algorithm is improved by using the double prefix and collision bit continuity, and the DPPS algorithm is proposed. Compared with CT algorithm, the average recognition efficiency is improved by 36%, and the average communication complexity is reduced by 35.6%.

In summary, although the research on the anti-collision algorithm has made some achievements in recent years, there are still some problems such as the complexity of the algorithm design and the inability to adapt to the practical application. The algorithm identification efficiency is affected by the large distribution of labels and so on. An efficient and stable anti-collision algorithm is the focus of future research.

3. Comparison of Several Algorithms

At present, most of the references for the improvement of tree based anti-collision algorithm focus on the BS algorithm, BLBO algorithm, QT algorithm and CT algorithm. In this section, we compare the performance of these algorithms with experimental analysis

3.1 Performance Analysis

Table 3 shows the performance parameters of the four algorithms. Where, n is the number of tags to be identified, k is the number length of the tag, x is the number of bits in which the tags collide, l_{pre} is the length of the query prefix sent by the reader, n_{res} is the tag that responds to the reader in each query cycle number.

Table 3 Algorithm performance comparison

Anti-collision algorithm	Time complexity	Communication complexity	Recognition efficiency
BS algorithm [32,33]	$n+\log_2(n!)$	$2k*(n+\log_2(n!)$	$1(1+\log_2(n!)/n)$
QT algorithm [33,34]	$n*(k+2-\lg n)$ (The worst situation)	$(n+1)(2.21k*\log_2 n+4.19k)$	$1(k+2-\lg n)$ (The worst situation)
BLBO algorithm [22]	$2n-1$	$3k-2x-21+(2x+44)*n$	$1(2-1/n)$
CT algorithm[35,36]	$2n-1$	$(2n-1)*[l_{pre}+(k-l_{pre})*n_{res}]$	$1(2-1/n)$

As can be seen from the above table, the time complexity of the BS algorithm is $n+\log_2(n!)$. Due to the existence of $n!$, the time complexity and communication complexity increase rapidly with the increase of the number of labels and the length of the tag number, and the recogniti only the most complicated case, but it can be seen that the QT algorithm is greatly influenced on efficiency will be lower and lower. Obviously, there is still much room for improvement in the BS algorithm. The time complexity of the QT algorithm listed in the above table isby the tag number length. When the tag number is long, the query range of the reader is greatly increased, which increase the number of free time slots. Normally, QT algorithm recognition efficiency is about 34% [12]. The BLBO algorithm and the CT algorithm have the same time complexity, which determines the recognition efficiency of the two algorithms is the same. Because the value of n is greater than or equal to 1, the recognition efficiency is above 50% and the time complexity is only affected by the number of tags, regardless of the length of the label number, so these two algorithms are more stable algorithm for large-scale label recognition occasions.

3.2 Simulation Experiment

The number of queries and the number of bits transmitted are important indicators that reflect the complexity of time and communication complexity. In order to compare the performance of these algorithms more intuitively, the MATLAB simulation tool is used to simulate the query times, communication transmission bits and recognition efficiency of several algorithms. Among them, the number of labels increased from 100 to 600 and the increment is 100.The label number is randomly distributed, and the number is 12 bits. The simulation results are shown in Fig.3 to Fig.5.

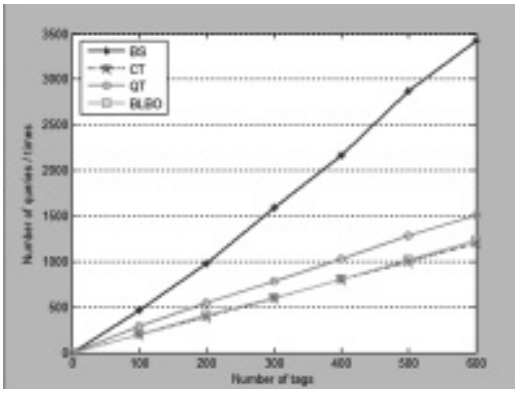

Figure.3 Comparison of query times

It can be seen from Fig.3, BS algorithm in the case of increasing the number of tags, the reader needs to send the most queries, we can see that the BS algorithm is most suitable for use in large-scale label environment, and the number of queries of QT algorithm is about half that of BS algorithm, and the performance of BLBO algorithm is similar to that of CT algorithm, which is better than QT algorithm.

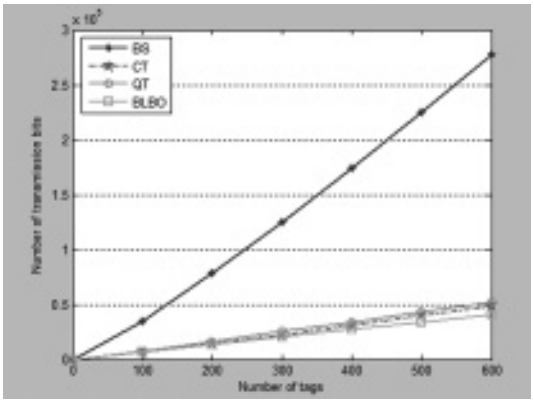

Figure.4 Comparison of transmission bit number

In Fig.4, we can see BLBO algorithm and CT algorithm's recognition efficiency is about 50%, and with the increase of the number of tags, the performance of the algorithm tends to be stable. QT algorithm's recognition efficiency is between 35% and 40%. BS algorithm's recognition efficiency is the lowest and with the increase of the number of tags, the recognition efficiency is gradually reduced.

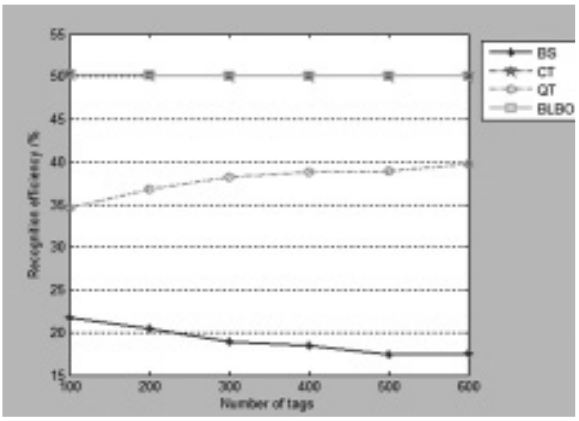

Figure.5 Comparison of recognition efficiency

The number of bits in the transmission between the reader and tags are represented in Fig.5 when use the four algorithms to identify tags. It can be seen from the figure that the BS algorithm the BS algorithm performs the worst, and with the increase in the number of tags, the amount of data needed to grow faster and faster, increasing the cost of the system. QT, CT and BLBO algorithm transmission bits are significantly lower than the BS algorithm. Among them, due to the introduction of the lock back strategy in the BLBO algorithm, it performs the best, followed by CT and QT algorithm.

4. Improvement Strategy of Tree-based Anti-collision Algorithm

In recent years, the research on RFID multi-label anti-collision algorithm has been paid more and more attention by many scholars, and many improvement strategies have been put forward for the anti-collision algorithm of tree, and some research results have been obtained. On the basis of reviewing the relevant literature, this paper summarizes several relatively typical improvement strategies.

4.1 Bit locked

In the tree-based anti-collision algorithm, if the label collides, then only the collision code is not known. In this way, locking the collision bits when collision occurs, and then the reader only sends collision bit information, the tags will only return the collision bit information, which eliminate redundant data. As shown in Figure 6, after the collision, the reader’ s decoding information is 1×0××000.Then the next time, the reader only request the 2, 4, 5 bit to send coded information, so whether the label side or the reader will reduce the information Storage to improve communication efficiency.

In [37], the DBS algorithm is improved by using the method of bit locking, which makes the new algorithm have great improvement in transmission delay and tag energy consumption. In the literature [38], a multi-collision joint lock-bit dynamic adjustment algorithm is proposed. The algorithm uses the highest collision bit and the lowest collision bit to form the lock bit paging instruction. It is preferable to estimate the number of labels in the collision slot, and then to detect the number of collision bits, and dynamically select the algorithm to deal with the collision. The instruction cost of the new algorithm is 12% and 39% lower than that of DBS algorithm and QT algorithm.

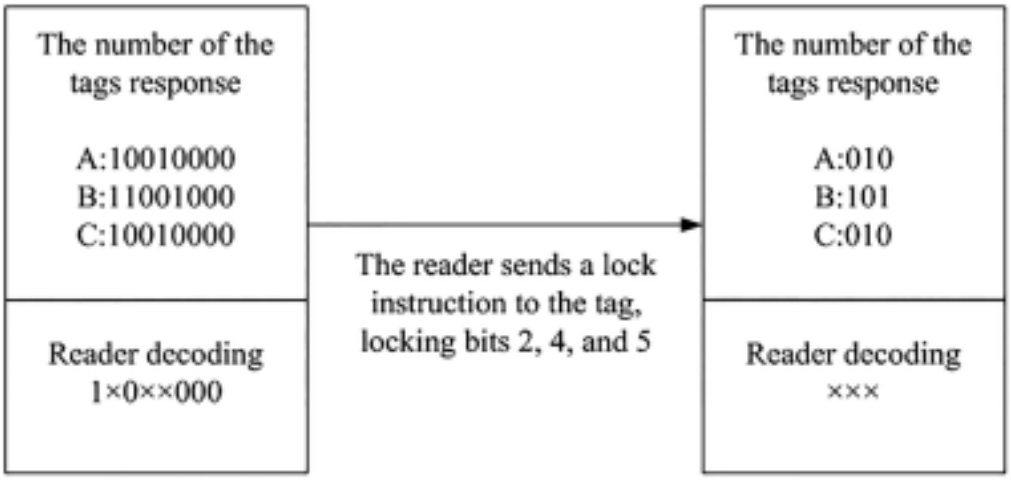

Figure.6 Lock bits strategy diagram

4.2 Adaptive bifurcation

The existing bifurcation of several tree-based anti-collision algorithms is only binary, which leads to the depth

of the tree is too deep and increases the number of queries. If the label set is allocated on a number of sub trees, it can effectively reduce the query tree depth and tag collision probability [22]. Quadtree, octree and other tree bifurcation algorithms are often used to reduce the collision time slot in the tag identification process, accordingly, the number of free time slots increase. Some researchers put forward adaptive bifurcation algorithms to reduce idle time slots. Mr Ding Zhiguo proposes an adaptive anti-collision algorithm. The collision factor is introduced into the algorithm, and the collision factor is the ratio of the collision bit to the label response bit in the collision slot [39]:

$$\mu = \frac{n_c}{n} \tag{1}$$

When the label collides, the collision factor is calculated. When $\mu < 0.3$, it select the binary tree to generate two query prefixes according to the first collision bit; when $\mu \geq 0.3$, it use quadtree to generate four query prefixes according to the first two collision bits. In order to avoid the use of quadtree to generate idle time slots, the literature [40] proposed a method that the reader send detection commands to determine the specific value to optimize the quadruple query prefixes. Instead, Ren [41] proposes a method that uses the XOR operation to eliminate the idle time slot before the determination of the quadruple query prefixes. Wang [42] first use the MLE algorithm to estimate the number of tags, and then use the proposed CBGN (Collision Bit Tracking Tree Algorthm Based on Grouping N-ray) algorithm to deduce the optimal grouping coefficients under different trees. The new algorithm eliminates the idle time slot and reduces the communication complexity significantly.

4.3 Backward

In the traditional BS algorithm, after successful identification of a tag, it is necessary to return to the root node to get the query command. After identifying a label in backward strategy, it will fall back to the label node’s parent node or other non-root node, which can greatly reduce the number of searches, but also can reduce the idle time slot and collision time slot Number of. the most typical algorithm is the intelligent traversal algorithm- STT （Smart Trend-Traversal） [43] proposed by Pan et al. The algorithm takes a preorder traversal node in the collision time slot, and the idle slot takes the mechanism of retreating to the upper layer node, which effectively reduces the number of collisions and the idle time slots. In [44], an enhanced STT algorithm is proposed, which can adaptively adjust the length of the query string according to the last query. Compared with the STT algorithm, the total number of queries is reduced by about 6%. In the paper [45], the backward paging is added to the query instruction of the reader, and the label information is divided into four parts, which reduces the unnecessary backward query path and reduces the amount of communication.

5. Conclusion

The tree-based anti-collision algorithm has the advantages of stability and high recognition efficiency, but there are some shortcomings such as large amount of communication data between reader and tag, high system delay and large influence on the label number distribution. However, the algorithm based on Aloha has strong adaptability and low system overhead, so the hybrid anti-collision algorithm based on tree algorithm and Aloha algorithm will be a hot research topic in the future. In addition, the label recognition for mobile state and capture effect is also the future research direction.

Sponsors or Supporters

This work is partially supported by Science & Technology Program of Weiyang District of Xi’an City with project “201609”.

References

[1]Yuan-Cheng Lai , Ling-Yen Hsiao, Bor-Shen Lin. An RFID anti-collision algorithm with dynamic condensation and ordering binary tree[J].Computer Communications,2013,36:1754-1767

[2] Xin-Qing Yan , Yang Liu , Bin Li, et.al. A memoryless binary query tree based Successive Scheme for passive RFID tag collision resolution[J].Information Fusion,2015,22:26-38

[3] Filippo Gandino,Renato Ferrero,Bartolomeo Montrucchio,et al.Probabilistic DCS:An RFID reader-to-reader anti-collision protocal[J].Journal of Network and Computer Applications,2011,34:821-832.

[4] Wu Nan. Research on RFID anti-collision algorithm based on a tree structure [D]. Changchun: Jilin University, 2014

[5] Yue Keqiang.RFID multi tag anti-collision algorithm research and application [D]. Hangzhou: Zhejiang University, 2014

[6] Overview of multi-tag anti-collision algorithms in RFID[J]. Computer Integrated Manufacturing Systems, 2014,20 (2): 440-451.

[7] Haidar Safa,Wassim El-Hajj,Christine Meguerditchian. A distributed multi-channel reader anti-collision algorithm for RFID environments[J].Computer Communications,2015,64:44-56.

[8] Yuan-Cheng Lai , Ling-Yen Hsiao, Bor-Shen Lin. An RFID anti-collision algorithm with dynamic condensation and ordering binary tree[J].Computer Communications,2013,36:1754-1767.

[9] Journal of Xidian University (Natural Science Edition), 2013,40 (6): 162-167 .Research on Adaptive Anti-collision Algorithm Based on Adaptive Multidimensional Dimensional Isolation [J]. Journal of Xidian University (Natural Science Edition), 2013,40 (6): 162-167.

[10] Klair K,Chin W,Raad R. A survey and tutorial of RFID anti-collision protocols[J].IEEE Communications Surveys and Tutorials,2010,12(3):400-421.

[11] Wang Yu .Research on RFID anti-collision algorithm [D]. Nanjing: Nanjing University of Posts and Telecommunications, 2011.

[12] Jia Xiaolin. Research on Anti-collision Algorithm Based on collision tree for RFID multi label recognition [D]. Chengdu: Southwest Jiao Tong University, 2013.

[13] J.Myung,W.Lee,J,Srivastava,et al.Tag-splitting:adaptive collision arbitration protocols for RFID tag identification[J].IEEE Transactions on Parallel and Distributed System,2007,18(6):763-775.

[14] Mingxing He,Shi-Jinn Horng,Pingzhi Fan,et al.A fast RFID tag identification algorithm based on counter and stack[J].Expert System with Application,2011,38:6829-6838.

[15] Jiang An, WU Jixiong, Huang Shengye, et al. Improved RFID binary search anti-collision algorithm [J]. Computer Engineering and Applications, 2009,45 (5): 229-235.

[16] Chen Feiyu.Improvement of Anti-collision Algorithm Based on Dynamic Binary [D]. Shanghai: Shanghai Jiaotong University, 2013.

[17] Sarkar S, Kak AC, Rama GM. Metrics for measuring the quality of modularization of large-scale object-

oriented software. IEEE Trans. on Software Engineering, 2008,34(5):700-720.

[18] Mustapha Djeddou,Rafik Khelladi,Mustapha Benssalah.Improved RFID anti-collision algorithm[J]. International Journal of Electronics and Communications(AEÜ) ,2013,67:256-262.

[19] Chen Chong, XU Zhi, HE Minghua.Study on a New RFID Anti-collision Algorithm [J]. Journal of Fuzhou University, 2009,37 (3): 367-371.

[20] Li Qingqing.Research on RFID anti-collision algorithm [D]. Nanchang: Nanchang Aviation University, 2012.

[21] Di Chunyu.Research on RFID Anti-collision Algorithm Based on Search Tree [J]; Changchun: Jilin University; 2014.

[22] Wang Xue, Qian Zhi-hong, HU Zhengchao, et al.Study on RFID anti-collision algorithm based on binary tree [J] .Journal of Communications, 2010,31 (6): 49-56.

[23] Liu Xiao-hui.Study on RFID anti-collision algorithm based on binary number [D]. Changchun: Jilin University, 2015.

[24] Shuen -Chih Tsai,Yu-Min Hu,Chen-Hsun Chai et al.Efficient tag reading protocol for large-scale RFID systems with pre-reading[J]. Computer Communications,2016,88:73-83.

[25]Zhang Bo. Research on Anti-collision Technology of CFD [D]. Shanghai: Donghua University, 2010.

[26] Yang,C N,Lin C C.Two couple-resolution blocking protocols on adaptive query splitting for RFID tag identification[J].IEEE Transactions on Mobile Computing,2012,11(10) :1450 — 1463.

[27] Jiao Chuan-hai,Wang Ke-ren.Multi-branch query tree protocol for solving RFID tag collision problem[J].The Journal of China University of Posts and Telecommunications,2008,15(4):51-54.

[28] Jiang Wu, Yang Heng-xin, Zhang Yun.An improved Anti-collision Algorithm for Query Tag RFID Tag [J]. Computer Technology and Development, 2015,25 (2): 86-89.

[29] Zhou Qing, Cai Ming.Improved RFID Hybrid Query Tree Anti-collision Algorithm [J]. Computer Engineering and Design, 2012,33 (1): 209-213.

[30]Jia Xiaolin,Feng Quanyuan,Lei Quanshui.Multi-cycle Collision Tree Algorithm for RFID Tag Identification[J]. Journal of Southwest University of Science and Technology, 2014,29 (1), 39-44.

[31] Jian Su,Zhengguo Sheng,Guangjun Wen.A Time Ffficient Tag Identification Algorithm Using Dual Prefix Probe Scheme(DPPS)[J].IEEE Signal Processing Letters,2016,23(3):386-389.

[32] He Na.Study on anti-collision algorithm in radio frequency identification system and its hardware implementation [D]. Guangzhou: Jinan University, 2007.

[33] Klaus Finkenzeller,RFID Handbook[M].Hanser Verlag,Munich,March 2003.

[34] Shi Hao. A Hybrid RFID Anti-collision Algorithm [D]. Nanjing: Nanjing University of Posts and Telecommunications, 2012.

[35] Jia Xiao-Lin,Feng Quan-yuan,Ma Cheng-zhen.An efficient anti-collision protocal for RFID tag identification[J].IEEE Communication Letters,2010,14(11):1014-1016.

[36] Jia Xiao-Lin,Feng Quan-yuan, Yu Li-shan.Stability analysis of an efficient anti-collision protocol for RFID tag identification[J].IEEE Transactions on Communications.2012,60(8):2285-2294.

[37] Hu Zhenchao.Study on RFID anti-collision algorithm based on binary tree [D]. Changchun: Jilin University, 2009.

[38] Zhang Li, Yuan Meng-Meng, He Xing.Study on Dynamic Adjustable Algorithm for Multi-collision Bit Joint Lock Position [J] .Journal of Electronics Measurement and Instrumentation, 27 (8): 773-779.

[39] Ding Zhi-guo, Zhu Xue-yong, Guo Li, et al.Study on adaptive multi-tree anti-collision algorithm [J] .2010,36 (2): 237-241.

[40] Zhang Xue-jun, Cai Wen-qi, et al.Study on Improved Adaptive Multi-tree Anti-collision Algorithm [J]. Journal of Electronics, 2012,40 (1): 193-198.

[41] Ren Shao-jie, Hao Yong-sheng, et al.A New self-adjusting multi-tree anti-collision algorithm [J]. Computer Measurement and Control, 2015,23 (12): 4180-4183.

[42]Wang Xin,Jia Qing Xuan,Gao Xin, et al.Research on Grouping N-ray Tracking Tree RFID Anti-collision Algorithm[J]. Journal of Electronics,2016,44(2):437-444.

[43] Pan L,Wu H.Smart Trend-Traversal:A Low Delay and Energy Tag Arbitration Protocal for Large RFID System[C].In Proceedings of 28th Annual Joint Conference of the IEEE Computer and Communications. Rio de Janeiro,Brazil,2009:2571-2575.

[44] Shuen-Chih Tsai,Yu-Min Hu,Chen-Hsun Chai,et al.Efficient tag reading protocol for large-scale RFID systems with pre-reading[J].Computer Communications,2016,88:73-83

[45]Tang Zhijun,Yang Yi,Wu Xiaofeng, et al.Novel Back-off Binary Tree Anti-Collision Algorithm for Ultra High Frequency RFID[J]. Computer science and exploration, 2016,10 (5): 612-621.

Model of Ball Mill Based on the CPS

Li Cunfang[1,2], Zhang Taohong[1,2], Zhang Dezheng[1,2], Wang Huan[1,2,3], Zeng Qingfeng[1,2] and Sun Yi[1,2]

[1] School of Computer and Communication Engineering, University of Science and Technology Beijing, China

[2] Beijing Key Laboratory of Knowledge Engineering for Materials Science, Beijing China

[3] The Information Center of AnSteel Groupe mining corporate, Liaoning China, Email: likeword2016@126.com

Abstract. With the development of the new technology of intelligent manufacturing and cyber physical system, a new scheme is proposed for designing of predictive production based on ball mill. First, physical model (PM) and the model based on data (cyber model, CM) are discussed. Then, the combination of physical model and cyber model (CPM) is realized. Physical model is established according to the volume balance formula and the material balance formula. Cyber model uses the algorithm of the extreme learning machine which introduces penalty function. CPM uses the least square method to realize the combination of PM and CM and gets the value of the coefficient. Compare the actual data on ball mill to the data of the model then the result shows that the mean square error of CPM is smaller than the mean square error of PM and CM. The experimental results validate the effectiveness of the proposed method, which can be effectively used in ball mill in our industry.

Keywords: cyber-physical systems, ball mill, cyber model, physical model, cyber-physical model

1. Introduction

Intelligent manufacturing is a core technology of the new industrial revolution. The core technologies converge at cyber-physical system (CPS) [1]. Cyber-physical systems (CPS) is a new type of intelligent system. Governments, academia and the business community attaches great importance to CPS.

CPS is a concentration of computing, communication and control in intelligent technology. CPS has many characteristics such as real-time, safe, reliable, high-powered and so on [2]. Building CPS models is a key technology for intelligent manufacturing. The system usually consists of cognitive layer, equipment layer, sensing layer and control layer. After sensing, collecting, transmitting, storing, mining and analyzing the information about the machine in physical space (PS), a digitalized machine mirroring the physical machine is set up in cyber space (CS) and referred to as the digital model of the physical machine on the CPS cognitive layer [3]. So CPS model need to master the knowledge about computing system and physical system. CPS involves content including the discrete calculating system and the continuous physical process. So it is difficult to establish a unified modeling architecture.

Ball mill is a key equipment which can smash materials. It is suitable for all kinds of ores and other materials and is widely used in mineral processing, building materials and chemical industry, etc. Materials after grinding are aspersed to engine body on the right side under the effect of rotary cylinder

in the overflow ball mill. Finally make products overflow from empty journal. Abrasive machining process is more compact which achieve classification operations and reduce the grinding cycle load effectively. Because ball mills are multi graded and the mechanism is more complex, cyber modeling and physical modeling is very difficult about ball mills.

WANG et al [4] put forward an inverse control strategy based on distributed NN (neural net-work) which used principle of inverse system control and property of the ball mill system. Yuan et all [5] proposed a nonlinear prediction model which used nonlinear partial least squares in the real ball mill pulverizing system. Discrete element method [6] allows modeling of internal steel in ball mill and the motion process of material particles in numerical simulation. Scholars at home and abroad [7] have been studying the fineness prediction model about ball mills. But these models do not reflect the influence directly about operating variables such as the feeding, add water. So these models are unable to real-time dynamically response changeable behavior of circuit operating conditions. This is the reason why these models are not control process models. Graded distribution prediction model is still worthy of further research in industrial ball mill modeling. If you can establish a dynamic model to predict grinding indicators according to water flow, additive amount of grinding ball, characteristics of ore and so on, which will have greater practical value.

Using physical methods establish the continuous physical model. Firstly, establish simple physical equation of a system, and then create a continuous system model based on time according to the property characteristics of the system and the parametric model in continuous system modeling. EA Lee [8] used Newton’ s law analysis to verify physical process and the system model was established. Formal modeling method based on mathematical theory simulates system behaviors. From the perspective of multi-agent systems, a high-confidence software formal model (HCSFM) of CPS based on two complementary formalisms, namely Petri nets and -calculus was proposed by Yu [9]. A quantitative security analysis model based on the combination of Petri net and game theory was proposed by XU [10] to reflect not only the hybrid of cyber and physical world but the behaviors of attackers and defenders. Banerjee [11] proposed a Linear 1 space dimension Spatio-Temporal Hybrid Automata which modeling oriented object was discrete system.

This paper realizes the combination of physical model and cyber model (CPM) based on CPS. According to the volume balance formula and the material balance formula, physical model is established to predict the output of ball mill. Physical model is a dynamic model based on the parameters of water flow, additive amount of grinding ball, characteristics of ore and so on. Use extreme learning machine (one of the neural network algorithm) algorithm to build mathematical modeling of ball mill which can predict the output. Finally use the least squares method to combine physical model and cyber model. Experimental results demonstrate the effectiveness of the proposed method.

2. CPS Model

2.1 Physical Model: PM

Figure 1 is a continuous grinding process of ball mill. Continuous grinding process is the rough ore crushed. When particles have been filtered, the material through belt transmit to ball mill, which is called undressed ore blanking. Overflow ball mills use wet grinding ways. So ball mills need to add a certain amount of water, which is named grinding water flux. A large number of steel ball is a medium. Ball mills

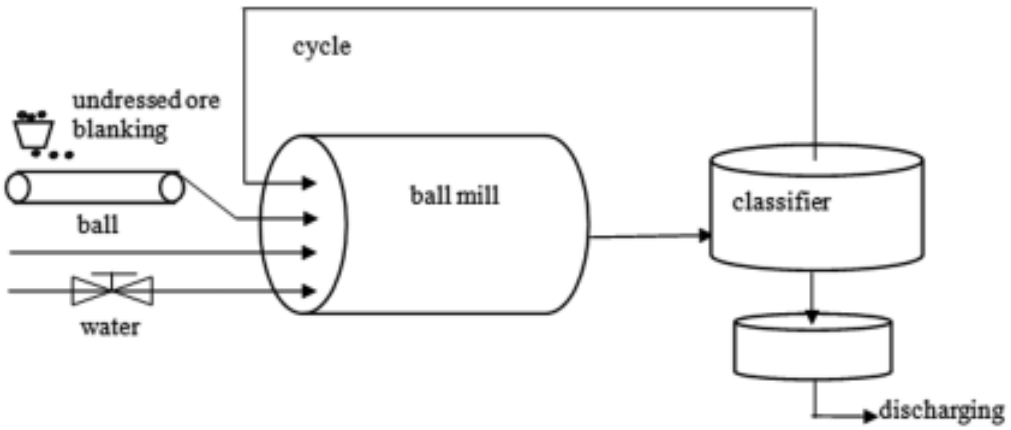

Figure.1 continuous grinding process of ball mill

of rotation grind pulp. After grinding, fine ore which is in the form of pulp overflow from discharging opening of ball mill. Coarse particles enter into the classifier and are recycled into ball mill until in the form of pulp overflow from discharging opening of ball mill. In the process of the experiment, this paper set parameters such as material grindability, cylinder speed, lining structure are invariable.

The input variables in physical model are grinding water flow which is recorded as Rwater_flux(t), undressed ore blanking which is called Rbelt_flux(t), Additive amount of grinding ball that is named Rball_add(t) and swirling flux that is regarded as Rore_flux(t). The output variables are overflow concentration named Covf_con (t) and overflow flux called Rovf_flux(t). According to the overflow concentration and overflow flux, physical model predicts production which is the product of overflow concentration and overflow flux.The volume of pulp V and the length of ball mills L are invariable. Volume balance formula is expressed as:

$$\frac{d(V(t))}{dt} = R_{water\_flux}(t) + R_{belt\_flux}(t) + R_{ball\_add}(t) + R_{ore\_flux}(t) - R_{ovf\_flux}(t). \quad (1)$$

The expression of $R_{ovf\_flux}(t)$ is formulated as follows:

$$R_{ovf\_flux}(t) = k\sqrt{V(t)/L}. \quad (2)$$

k is a adjustive coefficient. Put formula (2) into formula (1) can get formula (3):

$$\frac{V(t+1)-V(t)}{\Delta t} = R_{water\_flux}(t) + R_{belt\_flux}(t) + R_{ball\_flux}(t) + R_{ore\_flux}(t) - k\sqrt{V(t)/L}. \quad (3)$$

Formula 2 can obtained $R_{ovf\_flux}(t)$, Formula 3 can get volume of pulp V. Undressed ore blanking are solid mineral aggregate whose concentration is one. Concentrations of grinding water flux and additive amount of grinding ball are zero. Then the material balance formula is defined as:

$$\frac{d(C_{ovf\_con}(t)V(t))}{dt} = R_{belt\_flux}(t) - C_{ovf\_con}(t)R_{ovf\_flux}(t). \quad (4)$$

Formula (4) is also expressed as follows:

$$\frac{C(t+1)-C(t)}{\Delta t}V + \frac{V(t+1)-V(t)}{\Delta t}C(t) = R_{belt\_flux}(t) - C_{ovf\_con}(t)k\sqrt{V(t)/L}. \quad (5)$$

Formula (5) can get the value of $C_{ovf\_con}(t)$. As such the overflow concentration is:

$$C(t+1) = (R_{belt\_flux}(t) - C_{ovf\_con}(t)k\sqrt{V(t)/L} - \frac{V(t+1)-V(t)}{\Delta t}C(t)) * \Delta t + C(t). \quad (6)$$

Finally, physical model determine the production which is the product of overflow concentration and overflow flux.

2.2 Cyber Model: CM

This paper use cyber model which is extreme learning machine that is called ELM in short [12]. ELM is an algorithm of neural network and generic single-hidden layer feed forward network (SLFN).The input variables of cyber model is the same with the input variables of physical model. The output of the prediction is production.

The SLFN consists of input layer, hidden layer and output layer. Hidden layer has L hidden neuron. The output of output layer is an m-dimension vector. Output function expression is shown as in formula (7).

$$f_L(x) = \sum_{i=1}^{L} \beta_i G(a_i, b_i, x). \quad (7)$$

a_i and b_i are respectively the center of the radial basis function (RBF) node and influencing factor. β_i is weight between neurons of hidden layer and neurons of output layer. β_i is an m-dimension weight vector. G is the output of hidden layer neurons and is also called as activation function. Y is output of prediction. The output function of neural network can be written as:

$$H\beta = Y. \quad (8)$$

$$H = \begin{pmatrix} h(x_1) \\ \dots \\ h(x_N) \end{pmatrix} = \begin{pmatrix} G(a_1, b_1, x_1) \dots G(a_L, b_L, x_L) \\ \dots \\ G(a_1, b_1, x_N) \dots G(a_L, b_L, x_N) \end{pmatrix}_{N \times L}. \quad (9)$$

$$\beta = \begin{pmatrix} \beta_1^T \\ \dots \\ \beta_L^T \end{pmatrix}_{L \times m}. \quad (10)$$

$$Y = \begin{pmatrix} Y_1^T \\ \dots \\ Y_L^T \end{pmatrix}_{N \times m}. \quad (11)$$

This paper uses optimized ELM [13] which is introduced penalty function and is called L_{ELM}. Objective function is shown as follows:

$$Min: \frac{1}{2}(\| \beta \|^2 + C\sum_{i=1}^{N} \| \varepsilon_i \|^2) \quad \text{s.t. } h(x_i)\beta = y_i^T - \varepsilon_i^T. \quad (12)$$

Lagrangian function is expressed as:

$$L_{ELM} = \frac{1}{2}(\| \beta \|^2 + C\sum_{i=1}^{N} \| \varepsilon_i \|^2) - \sum_{i=1}^{N}\sum_{j=1}^{L} \alpha_{i,j}(h(x_i)\beta - y_i^T + \varepsilon_i^T). \quad (13)$$

Solving process is defined as follows:

$$\frac{\partial L_{ELM}}{\partial \beta_j} = 0 \Rightarrow \beta_j = \sum_{i=1}^{N} \alpha_{i,j} h(x_i)^T \Rightarrow \beta = H^T \alpha. \quad (14)$$

$$\frac{\partial L_{ELM}}{\partial \varepsilon_i} = 0 \Rightarrow \alpha_i = C\varepsilon_i. \quad (15)$$

$$\frac{\partial L_{ELM}}{\partial \alpha_i} = 0 \Rightarrow h(x_i)\beta - y_i^T + \varepsilon_i^T = 0. \tag{16}$$

In formula (14), $\alpha = (\alpha_i, ...\alpha_N)^T$.

Put formula (14) and (15) into formula (16), the result is:

$$(\frac{I}{C} + HH^T)\alpha = Y. \tag{17}$$

By formula (14) and (17) , β is (N>>L):

$$\beta = H^T(\frac{I}{C} + HH^T)^{-1}Y.$$

Finally, the output result is:

$$f(x) = H\beta = HH^T(\frac{I}{C} + HH^T)^{-1}Y. \ [13] \tag{18}$$

2.3 Cyber-Physical Model: CPM

The output of physical model is y_p. The expression of y_p is the product of formula (2) and formula (6) at the same time. y_c is the output of cyber model in formula (18). Formula (19) is weighted summation to predict y. w_1 and w_2 are the coefficient values. The relationship between w_1 and w_2 is as shown in formula (20).

$$y = w_1 y_p + w_2 y_c. \tag{19}$$

$$w_2 = 1 - w_1. \tag{20}$$

By formula (19) and (20), (w_1 is expressed by w):

$$y = wy_p + (1-w)y_c. \tag{21}$$

The parameters of y_p is k. The parameters of y_c is ϕ which includes penalty coefficient C and the number of hidden layer nodes L. h is predicted output. This paper uses least square method and regular terms. The purpose of using regular terms is that restraining parameters to make it not too big can reduce the fitting.

$$\frac{1}{2}\min_w \sum_{i=1}^{N}(h_i - y_i)^2 + \lambda_1 \sum_{i=1}^{N} k_i^2 + \lambda_2 \sum_{i=1}^{N} \phi_i^2. \tag{22}$$

The process of solving the coefficient value w is as shown below.

$$J = \frac{1}{2}(\sum_{i=1}^{N}(h_i - y_i)^2 + \lambda_1 \sum_{i=1}^{N} k_i^2 + \lambda_2 \sum_{i=1}^{N} \phi_i^2) \tag{23}$$

$$= \frac{1}{2}(\sum_{i=1}^{N}(w(y_p - y_c) + y_c - y_i)^2 + \lambda_1 \sum_{i=1}^{N} k_i^2 + \lambda_2 \sum_{i=1}^{N} \phi_i^2).$$

Partial derivative of formula (23) is expressed as:

$$\frac{\delta J}{\delta w} = \sum_{i=1}^{N}(w(y_p - y_c) + y_c - y_i)(y_p - y_c) = 0. \tag{24}$$

The value of w is:

$$w = \frac{\sum_{i=1}^{N}(y_c - y_i)(y_c - y_p)}{\sum_{i=1}^{N}(y_p - y_c)^2}. \tag{25}$$

Process of solving the parameters is shown as follows:
solving the parameter k, fixing ϕ , w
Objective function:

$$\frac{1}{2}\min_{w}\sum_{i=1}^{N}(h_i - y_i)^2 + \lambda_1\sum_{i=1}^{N}k_i^2.$$

solving the parameter ϕ , fixing k, w

Objective function:

$$\frac{1}{2}\min_{w}\sum_{i=1}^{N}(h_i - y_i)^2 + +\lambda_2\sum_{i=1}^{N}\phi_i^2.$$

solving the parameter w, fixing k, ϕ

3. Realization and Validation Model

In the process of the experiment, this paper uses 253 data. Experiment selects 80% data as the training set and 20% as the test set. The experiment loops 20 times. The experimental results are average. Do the data cleaning before experiment. Because the magnitude of various parameters is different, data must be disposed. Before modeling normalization processing is carried out for meeting the input requirements of the model. The result of normalization is to make the value of the parameter between -1 and 1.

In the experiment, the value range of parameters: in the physical model, k is from 0.01 to 0.15, in the cyber model, C (punish coefficient) value is from 2^{15} to 2^{20}, L (the number of hidden layer nodes) is 50, 100, 200, 300, 500 or 1000. When the mean square error (mse) of CPM is minimum, the optimum combination parameters is that k is 0.14, C is 2^{19}, L is 300. A parameter is variable and the rest of the two parameters is fixed. Observe effects on the model.

3.1 PM

In physical model, adjust the parameter k which is in formula (2). k is from 0.01 to 0.15. When k is variational, Figure 2 and Figure 3 are the change of the mean square error (mse) in PM and CPM. As can be seen from Figure 3, mse is gradually convergent and the best value of k is 0.14.

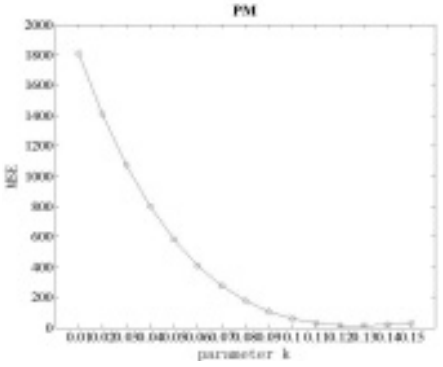

Figure.2 improve parameter k in PM

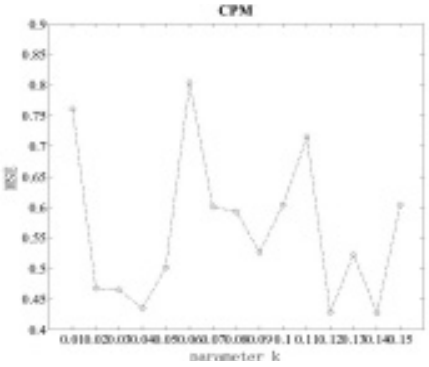

Figure.3 improve parameter k in CPM

3.2 CM

In cyber model, adjust the parameter C (punish coefficient). C is from 2^{15} to 2^{20}. Adjust the parameter L (the number of hidden layer nodes). L is 50, 100, 200, 300, 500 or 1000. When C is variational, Figure 4 and Figure 5 are the change of the mean square error (mse) in CM and CPM.

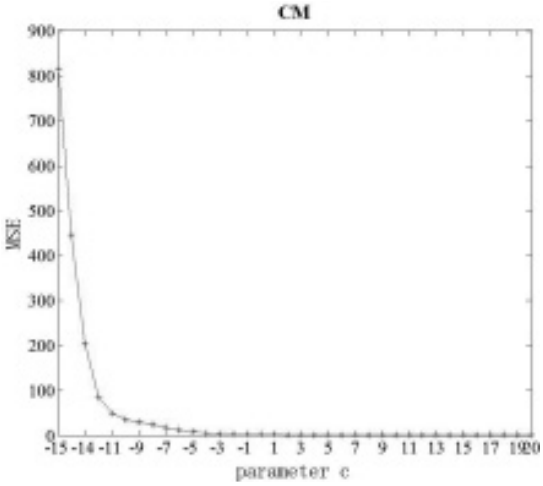

Figure.4 improve parameter C in CM

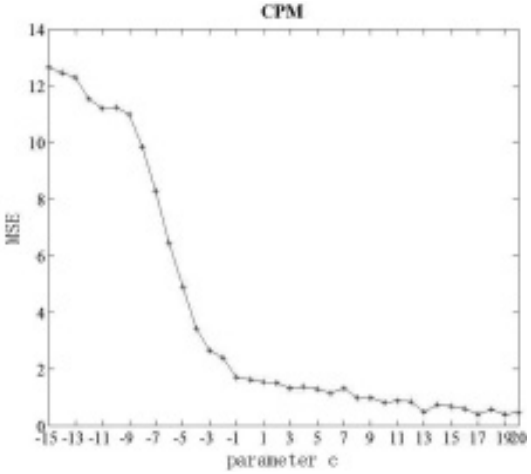

Figure.5 improve the parameter C in CPM

From Figure 4 and Figure 5, mse is gradually convergent in CM and CPM. Table.1 is the partial comparative result of mse between CM and CPM. When C is 2^{19}, mse of CPM is minimum.

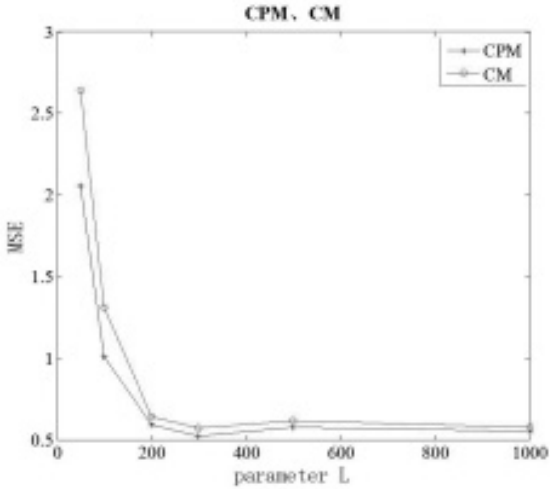

Figure.6 improve parameter L in CPM and CM

The best value of L is 300 from Figure 6. From the result, the conclusion is that mse of CPM is smaller than mse of CM and PM.

Table 1 improve parameter C, contrast mse in CM and CPM

Numbers of experiment	CM	CPM
1	1.8281	1.5291
2	1.7824	1.5032
3	1.4975	1.3073
4	1.5613	1.3616
5	1.4815	1.2907
6	1.3520	1.1646
7	1.5195	1.3138
8	1.1150	0.9884
9	1.1069	0.9908
10	0.9253	0.8316
11	0.9540	0.8650
12	0.9543	0.8602
13	0.5305	0.4948
14	0.8041	0.7353
15	0.7255	0.6851
16	0.6341	0.5924
17	0.4270	0.4087
18	0.5952	0.5628
19	0.4312	0.4083
20	0.4770	0.4577

When adjust parameter L, the change of mse in CM and CPM is shown in Figure 6. The result is stable convergence.

3.3 CPM

Fix optimal parameter and change parameter w. The experiment loops 20 times. In Figure 7, when w is changeable, mse of CPM is also altered.

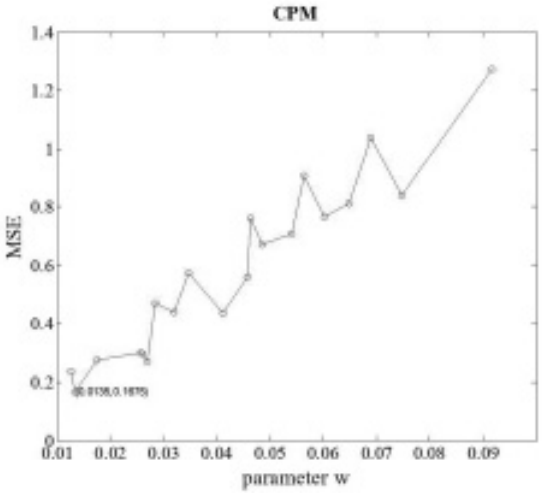

Figure.7 improve parameter w and change of Mean Square Error (mse) in CPM

From Figure 7, the changes of w have bigger influence on the predictive value of CPM. When w is 0.0135, mse of CPM is minimum.

3.4 Model Validation

When parameter is determinate, test data is used to validate model, the predictive mse is shown in Figure 8. From Figure 8, in addition to the individual data points are abnormal, mse of predicted value are smaller. So model is credible.

3.5 Select Data Randomly

This paper uses 253 data. Experiment randomly selects 80% data as the training set and 20% as the test set. The experiment loops 20 times which is same as above. The optimal parameters are fixed. Table.2 shows comparative results of mse in each model and each experiment.

Experimental results show that mse of CPM is smaller than mse of PM when data are selected randomly in each experiment. CPM is mostly smaller than mse of CM. As shown in Table 2, the results demonstrate the feasibility of the model.

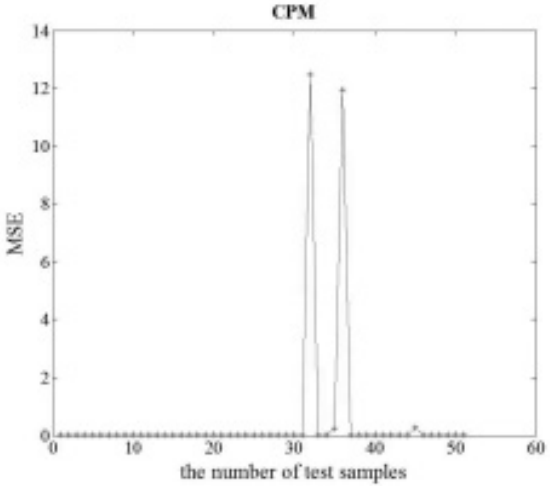

Figure.8 prediction of MSE in CPM

Table 2 comparative mse in CM, PM and CPM

Numbers of experiment	CM	PM	CPM
1	0.0238	21.6516	**0.0344**
2	0.4182	18.2764	0.4081
3	0.0217	19.0294	0.0215
4	0.7217	24.2934	0.6944
5	0.4233	16.2498	0.4064
6	0.00096	17.3997	**0.0036**
7	5.1209	16.5267	4.9692
8	1.0219	17.3815	**1.0059**
9	0.0204	15.7797	0.0200
10	14.9908	16.4463	14.6024
11	0.0015	16.0704	0.0035
12	0.1555	14.5969	**0.1647**
13	0.5444	23.4765	0.5167
14	1.2102	18.8124	1.1645
15	0.4937	17.8530	0.4720
16	0.1140	16.5295	0.1092
17	1.2052	20.4670	1.1643
18	0.2215	22.8540	0.2001
19	0.0976	13.7874	0.0912
20	0.5072	14.6934	0.4980

4. Conclusion

This paper proposes a combining model of cyber model and physical model. The combining model is named CPM. CPM can make that production of ball mill predicts more accurate. At the same time, the experiment demonstrates the combination of computer and physics in CPS modeling. First of all, separate physical model is established. Then the model based on data is separately set up which is named CM. CM uses ELM with penalty function. Furthermore, get coefficients of physical model and cyber model by least square method. In the process of experiment, determine optimal parameters, then regulate various parameters respectively and compare the effects of various parameters on the model. In section 2.4, through the test figure can be seen that CPM model predicts accurate. Experimental results demonstrate effectiveness of the proposed method. Finally, Select data randomly and compare mean square error of the model. The experimental results show the feasibility of the model. So this method can be effectively applied in industrial ball mill.

References

[1] Lee J, Bagheri B, Kao H A. A cyber-physical systems architecture for industry 4.0-based

manufacturing systems[J]. Manufacturing Letters, 2015, 3: 18-23.

[2] ZHOU Xing-she, YANG Ya-lei, YANG Gang. Modeling methods for dynamic behaviors of cyber-physical system[J]. Chinese Journal of Computers,2014, 37(3): 1

[3] Chen J, Yang J, Zhou H, et al. CPS Modeling of CNC Machine Tool Work Processes Using an Instruction-Domain Based Approach[J]. Engineering, 2015, 1(2): 247-260.

[4] WANG Dong-feng, YU Xi-ning, SONG Zhi-ping. Dynamic mathematical model of ball mill pulverizing system and its inverse control based on distributed neural networks[J]. Proceeding of the CSEE, 2002, 22(1): 97

[5] Yuan Y, Zhang Y, Cao H, et al. Nonlinear prediction model for ventilation of ball mill pulverizing system[C]//Control Conference (CCC), 2016 35th Chinese. TCCT, 2016: 2025

[6] Mishra B K. A review of computer simulation of tumbling mills by the discrete element method: part I—contact mechanics[J]. International journal of mineral processing, 2003, 71(1): 73-93

[7] MA Tian-yu, GUI Wei-hua. Optimal control for continuous bauxite grinding process in ball-mill[J]. Control Theory & Applications, 2012, 29(010): 1339-1347

[8] LEE E A. Introduction to embedded systems-a cyber-physical systems approach[M]. UC Berkeley, 2014: 79

[9] YU Zhen-hua, CAI Yuan-li, FU Xiao, et al. Formal modeling and analyzing high-confidence software of cyber-physical systems[J]. Systems Engineering theory and practice, 2014, 34(7): 1857

[10] XU Xin, YU Hui-qun, HUANG Jun-hu. Petri net based security quantitative analysis model for cyber-physical system[J] . Computer Engineering and Applications, 2014, 50(3): 82

[11] BANERJEE A, GUPTA S K S. Spatio-temporal hybrid automata for safe cyber-physical systems: a medical case study[C]//2013 ACM/IEEE International Conference on Cyber-Physical Systems (ICCPS). Philadelphia,USA, c2013: 71

[12] Huang G B, Zhu Q Y, Siew C K. Extreme learning machine: a new learning scheme of feedforward neural networks[C]//Neural Networks, 2004. Proceedings. 2004 IEEE International Joint Conference on. IEEE, 2004, 2: 985

[13] Huang G B, Zhou H, Ding X, et al. Extreme learning machine for regression and multiclass classification[J]. IEEE Transactions on Systems, Man, and Cybernetics, Part B (Cybernetics), 2012, 42(2): 513

Author Brief and Sponsors

About the Author: Li Cunfang (1990-), female, Shandong people, Current M.S. student, research direction: machine learning and modeling. E-mail: likeword2016@126.com.

This paper is supported by the Fundamental Research Funds for the Central Universities, China (No. FRF-BR-15-059A), and the 48th Scientific Research Foundation for the Returned Overseas Chinese Scholars (48).

BIM-technologies for Buildings Operation Experiment in MGSU

Andrey Volkov[1,a], Pavel Chelyshkov[1,b]

[1]Moscow state university of civil engineering, 129337, Russia, Moscow,

Yaroslavskoe shosse 26

Email: [a]rector@mgsu.ru, [b]chelyshkovpd@gmail.com,

Abstract. This article describes the approach of experts of the National Research Moscow State University of Civil Engineering (MGSU) to the construction of modern operating systems in buildings using BIM-technology. This article was performed within the Russian State tasks MGSU project "Methodology of ideas, design and verification of energy-efficient engineering systems conventionally abstract objects (on formal models of buildings)" .

Keywords: energy-efficient control, software for automated building management systems, operational control, life-support systems, information modelling of construction projects, engineering simulation, control of engineering systems, automated monitoring.

1. Introduction

Since 2008, in National Research Moscow State University of Civil Engineering (MGSU) exist Situational Energy Efficiency Centre of MGSU (SEC MGSU).

Today SEC MGSU provides energy-efficient control of the operation of two buildings with a total area of the University for more than 18 000 sq. m. Infrastructure SEC MGSU enables operational control of the operation of engineering systems, archiving and analysis of data, verification of the technical and technological solutions and software for automated building management systems (ABMS).

2. Discussion

SEC MGSU is the epitome of an experimental platform and a new approach to building - view of the construction of the object throughout the life cycle - from conception to the time of the disposal. This approach involves the development of the concept and design of construction projects according to the conditions and terms of further operation. It allows - for capital construction projects - to achieve substantial savings in operating costs (payment of resources - heat, water, electricity, maintenance costs operation service; the cost of sudden failure of hardware engineering systems due to lack of timely diagnosis, to eliminate the consequences of accidents costs because of lack of engineering safety systems).

Implemented in SEC MGSU system performs the operational management and analytical data processing of all engineering objects of life-support systems: electricity, lighting, heating, heating, ventilation, water supply and sewerage. The quality of the power supply is controlled by 110 points,

heat parameters - flow rate and coolant temperature - controlled at 40 points, at 10 points controlled the water flow, traffic control is carried out in 100 points and in 100 points is carried out ambient light control, noise is monitored in 90 points, in 95 points internal air temperature is controlled and at 10 points relative humidity of internal air is controlled. In addition, SEC MGSU is equipped with a weather station, transmitting in the system environmental conditions (ambient air temperature, relative humidity of the outside air, wind speed and direction, the presence of rain).

Figure.1 Educational Laboratory Building, equipped with energy-efficient automated control system.

3. Method

The system is based on the main-modular principle. The data from the end devices are transmitted to the control device modules (one module consists of up to 5 rooms), then the information is transferred to the storey controller, then to a central server SEC MGSU. The central server is physically consists of two servers - the first is subject to problems of operational management, the second is subordinate to the tasks of archiving and analytical processing data. It is controlled in real time. Access to the information management system is carried out on a local network of university, when you enter of appropriate access data. Through the information system interface available information on all the parameters controlled by the SEC MGSU, available setting values of the parameters of engineering systems and the assignment of rooms' microclimate parameters.

In addition to the above-described infrastructures in SEC MGSU also established laboratory facilities to carry out research projects activities with students and graduate students. Here are created 5 unique laboratories in various fields of building automation and energy saving. Laboratory equipment - proprietary research stands its own design. A wide range of features and options scaling of developed scientific equipment allows to use them in the work since the educational process of 3rd year Baccalaureate and ending with the preparation of doctoral theses.

Special attention in SEC MGSU is pad to practical application and promotion of energy-efficient solutions for the construction. Conducted in SEC MGSU experiments show payback of used improved energy efficiency technologies within 3-5 years. Thus, the undeniable is attraction of investment for the owner of real estate such technology introduction [4-12].

In 2015 began a new stage of development MGSU SEC associated with the use of BIM-technologies.

Information modelling of construction projects for today is one of the most effective tools to reduce the cost of design, construction, operation and disposal of buildings and structures. A look at the life cycle of construction projects as a continuous process makes it possible at the stage of concept development and design to take the necessary decisions to improve the efficiency of their operation, and recycling. At the same time the use of BIM-technology in the design process significantly speeds, reduces the cost and improves the quality of design process itself, contributing to the avoidance of errors, collisions and making it easier to verify compliance with regulatory requirements [1-3,13].

Above applies primarily to construction projects, information model of which began to form in the early stages of the life cycle and "lived" with the object through all processes: the adjustment of design decisions, changes in design solutions in the construction, repair and overhaul, alterations, replacement of systems engineering equipment and so on. However, significantly improve the

efficiency of existing buildings and structures is also possible through the creation of an information model of the object directly at the operation stage.

Creation of such a model in the first place, increases the efficiency of repair work, in large building complexes allows administering maintenance service work taking into account the current state of the elements of buildings, optimize engineering systems equipment.

An example of such an information model is implemented today in SEC MGSU. The model is based on three main blocks - architecture 3-d model, engineering simulation model systems and system of automated monitoring and control of engineering systems.

4. Conclusion

Merging into a single building information model allows these components to achieve the results described above and, in addition, harnessing simulation model of engineering systems, analyze the effectiveness of the use of new types of equipment before carrying out maintenance work associated with its replacement. Also, integration of a simulation model of engineering systems with a system of automated monitoring and control of engineering systems makes it possible to verify the modules of simulation model corresponding to the different types of equipment, including undergoing testing.

Thus, for today in the Moscow State University of Civil Engineering building has created a unique scientific and practical platform for development and testing of advanced technologies for construction and housing. To date, close to completing work on the creation of an information model of the operated building, designed to ensure the transition to a new level of maintenance of building.

Acknowledgements

This work was financially supported by the Ministry of Russian Education (state task #2014/107)

References

[1] Volk, R., Stengel, J., Schultmann, F. Building Information Modeling (BIM) for existing buildings - Literature review and future needs (2014) Automation in Construction, 38, pp. 109-127.

[2] Wang, X., Chong, H.-Y. Setting new trends of integrated Building Information Modelling (BIM) for construction industry (2015) Construction Innovation, 15 (1), pp. 2-6.

[3] Shanmuganathan, S. BIM - A global consultant ‘s perspective (2013) Structural Engineer, 91 (11), pp. 102-104.

[4] A.A.Volkov, D.E. Namiot, M.A. Shneps-Shneppe, On the tasks of creating an effective infrastructure for habitat. // International journal of open information technologies. - 2013. - V7 (1). - pp. 1-10.

[5] J Duffy,W Beckman, Thermal processes using solar energy. - M .: Mir, 1977.

[6] M.M. Brodach, Heat Energy optimization orientation and size of the building. // Proceedings of the Research Institute for Building Physics. M., 1987. The heat treatment and durability of buildings.

[7] P.P.Denisov, Influence index space-planning solutions building on the heat consumption. - „Housing “ 1981, № 1.

[8] B.I. Giyasov, The impact of infrastructure development on the urban living environment // Vestnik MGSU. - 2012 - V4

[9] Volkov, A. General information models of intelligent building control systems: Scientific problem and hypothesis (2014) Advanced Materials Research, 838-841, pp. 2969-2972.

[10] Volkov, A. General information models of intelligent building control systems: Basic concepts, determination and the reasoning (2014) Advanced Materials Research, 838-841, pp. 2973-2976.

[11] Volkov, A.A., Sedov, A.V., Chelyshkov, P.D. Modelling the thermal comfort of internal building spaces in social buildings (2014) Procedia Engineering, 91, pp. 362-367.

[12] Volkov, A., Chelyshkov, P., Sedov, A. Application of computer simulation to ensure comprehensive security of buildings (2013) Applied Mechanics and Materials, 409-410, pp. 1620-1623.

[13] Volkov, A., Sedov, A., Chelyshkov, P. Usage of building information modelling for evaluation of energy efficiency (2013) Applied Mechanics and Materials, 409-410, pp. 630-633.

UAV Dynamic Simulation Model Establishment Method Based on Simulink/ Aerosim

Chen GuoShao[1], Yang Sen[2,3]

[1]School of Computer Science and Engineering, Xi'an Technological University,

Xi'an 710021, China, Email:59483672@qq.com

[2] Department of UAV Engineering, Ordance Engineering College, Shijiazhuang, China

[3] School of Automation Science and Electrical Engineering, Beihang University, Beijing, China, Email: 568657132@qq.com

Abstract. Aiming at the problem of UAV dynamic modeling with high difficulty and poor timeliness, a UAV dynamic model based on Simulink/Aerosim rapid method is established in this paper. Based on the analysis of UAV system internal structure, using Simulink/Aerosim toolbox to build six degrees of freedom dynamic simulation model of unmanned aerial vehicle and the setting of relevant parameters and RTW environment configuration process is analyzed, finally, by analyzing the typical flight parameters of a certain type UAV in ideal environment and wind interference environment, the feasibility and validity of the method is illustrated.

Keywords: Simulink/Aerosim, dynamic model, flight parameters

1. Introduction

In the process of establishing the dynamic model of UAV, timeliness is a factor that cannot be ignored. Therefore, it is of great practical value to study the rapid and effective method of UAV dynamic model. Foreign Rapid Prototype Technology has been applied to flight simulation experiments. For flight dynamics models in training simulators, the accuracy of modeling is not as accurate as a research-based simulator, but is modeled difficulty and timeliness is the need to focus on solving the problem. Therefore, this paper proposes a rapid establishment method of UAV dynamic model based on Simulink / Aerosim for the problem of poor performance of training unmanned aerial vehicle, which provides technical support for the rapid establishment of aircraft system models in UAV simulation training systems [1-2].

2. UAV Dynamic Simulation Model Development Method Based on Simulink/Aerosim

2.1 Dynamic simulation model development

UAS internal structure is as shown in Fig.1.

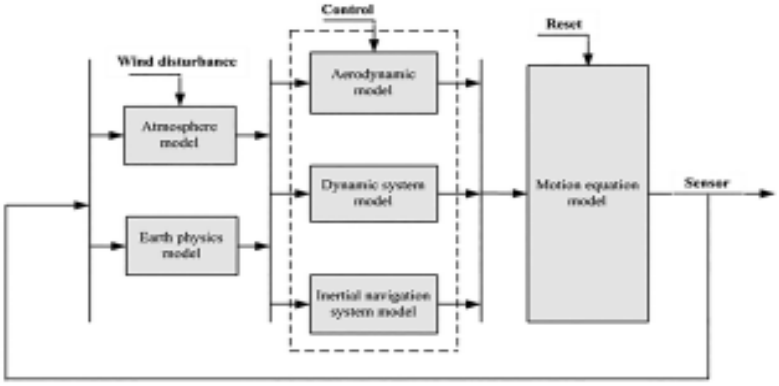

Figure.1 UAS internal structure

The system uses the Simulink / Aerosim toolbox provided by Unmanned Dynamics to build a 6-DOF unmanned aerial vehicle dynamic simulation model[3]. UAV module and the initial value of the process shown in Fig.2.

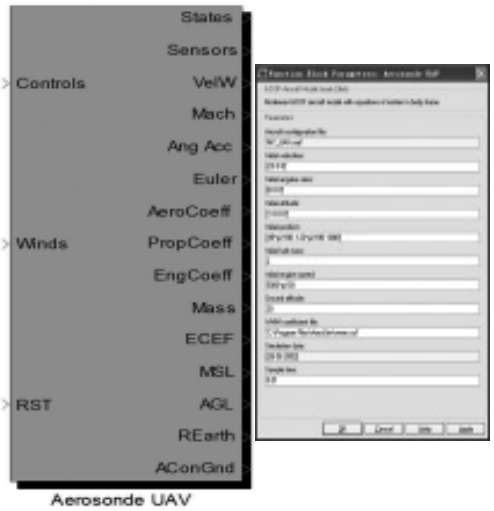

Figure.2 UAV module and its initial value set diagram

The relevant parameters that need to be configured in the modeling process include [4]:

①UAV parameter configuration file. Aerosim in this file default file name is template_cfg.m, this default file name to MY_UAV, in the command window to run the file MY_UAV can generate MY_UAV.mat file directly, as shown in Fig.3.

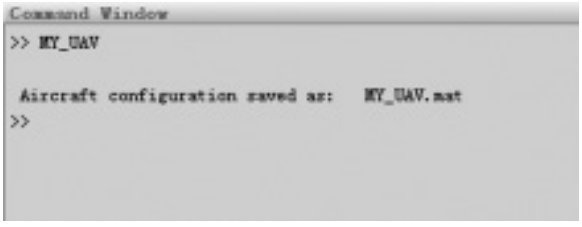

Figure.3 UAV parameter configuration file (.mat) generated schematic

② The center of gravity of the aircraft. The default aircraft center of gravity position can be considered

at the origin, for example: rAC =[0 0 0].

③ Aerodynamic parameters range. In order to ensure that the aerodynamic model output is within the linear range, the range of aerodynamics must be defined. The module used here is a module in the Aerosim toolbox. To ensure the reliability of the simulation, the module must be provided under linear conditions. Accepted range of parameters (usually small angle range), mainly including airspeed, angle of attack and side slip angle.

④ Aircraft related pneumatic parameters. Including the mean aerodynamic chord-MAC, the wing span-b and the wing area-S.

⑤ Used to calculate the relevant parameters of aerodynamic coefficient and aerodynamic moment coefficient. The aerodynamic coefficients include the drag coefficient, the pitch moment coefficient and the yaw moment coefficient. The drag coefficient includes the drag coefficient, the side force coefficient and the lift coefficient.

⑥ Propulsion system related parameters. The propeller mounting position rHub, the reference position relative to the origin, the propeller range Rprop, and the moment of inertia Jprop.

⑦ Engine parameters. For example: Engine speed vector RPM=[1500 2100 2800 3500 4500 5100 5500 6000 6400], the pressure MAP=[60 70 80 90 92 94 96 98 100].

⑧ Characteristic height of the atmospheric data.

⑨ Aircraft inertia parameters and full-load moment of inertia when loading at full load, and so on, including the maximum load weight,

no-load center of gravity, full load center of gravity.

Through the related parameter setting and the parameter configuration file generation, we can carry out the development of the dynamic simulation model of the specific model.

2.2 RTW development environment configuration [5-9]

RTW as Matlab/Simulink expansion tool, it can be built by the user Simulink model to generate real-time operating system running on the executable program Shorten the UAV simulation training system development cycle[8].The RTW program automatically creates the following four steps:

1) Model analysis;

2) Target language compiler generates code;

3) Custom binding file generation;

4) Executable program generation.

RTW program creation is from the Simulink module analysis and establishment of the beginning, set the compiler environment, you can use the Tool | Real-Time Workshop | Build model menu to compile and connect the model, and ultimately generate executable files[9]. The parameter setting dialog box is shown in Fig.4.

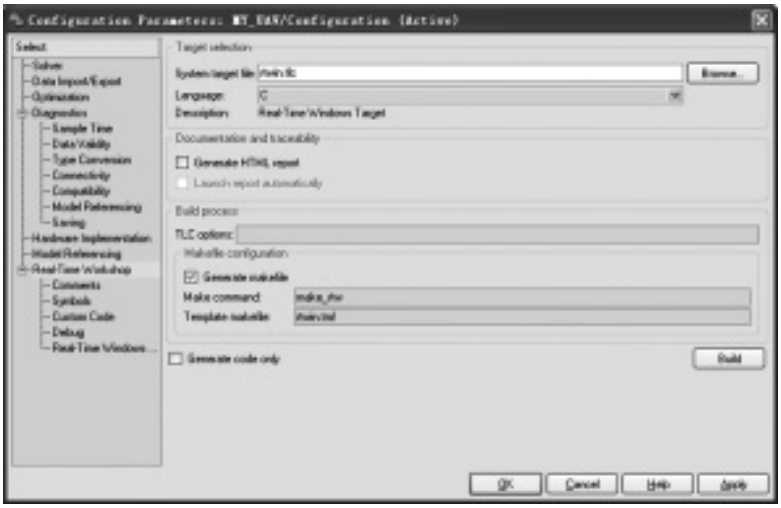

Figure.4 Parameter Settings dialog box

Click the „Browse " option corresponding to the System target file in the parameter dialog box of Figure 4; the real-time tool target selection dialog box shown in Fig.5 will be displayed. The desired target file type can be selected, Here for the rtwin.tlc, that is, Real-Time Windows Target type.

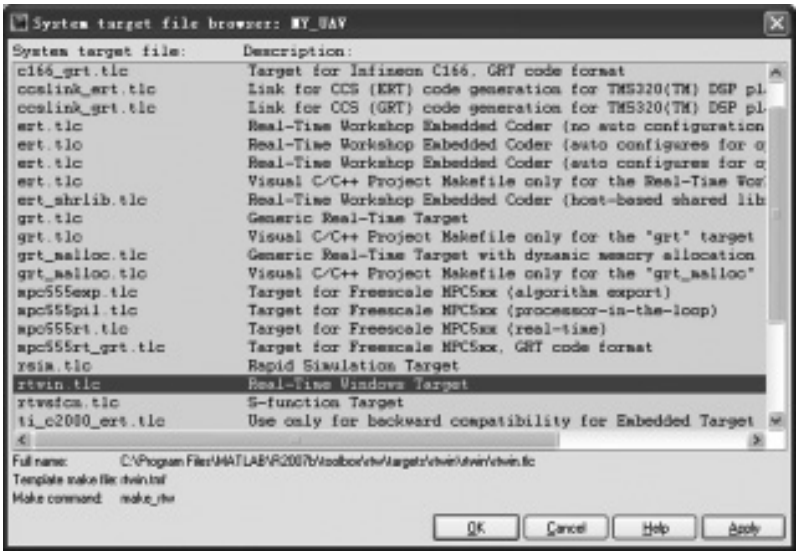

Figure.5 Real-time tool target selection dialog box

3. Typical Examples

3.1 Dynamic simulation model of typical unmanned aerial vehicle based on Simulink/Aerosim

Modify the file named Config_template.m in the Sample folder under the Aerosim installation directory. You can set the UAV model for the specific aerodynamic layout required by the user by modifying the relevant parameter values in this file. UAV initialization needs to configure the relevant parameters include:

① Aircraft configuration file

② Initial position

③ Initial velocities

④ Initial altitude

⑤ Initial angular rates

⑥ Initial fuel mass

⑦ Initial engine speed

⑧ Ground altitude

⑨ Sample time

Through the above parameters configuration file modification and flight simulation initial value settings, you can customize a specific model (that is, a specific pneumatic layout) of the UAV, and can set the initial value of the simulation operation.

3.2 Example simulation analysis

The structure model of the UAV flight simulation system shown in Fig.6 is constructed and simulated in Simulink/Aerosim environment for a certain type of unmanned aerial vehicle. The feasibility and effectiveness of the simulation system are illustrated by studying the typical parameters of the UAV (airspeed and 3 Euler angles) in the ideal environment (Wind[0 0 0]) and the wind disturbance environment (Wind[xyz]) The UAV parameter settings file name UAV.m, in the Matlab command window run this file UAV, and then you can generate UAV.mat file. The UAV.mat configuration file is filled in the parameter configuration file option in MY_UAV, then the parameters of the UAV will be set according to the parameters in the configuration file. The relevant parameters are set as follows:

1) UAV center of gravity range: rAC=[0 0 0].

2) Aerodynamic parameters Range: Airlift range VaBnd=[33 50] m / s, (aircraft flight speed range 120 ~ 180km / h) Attack angle range=[- 0.1 0.5] rad, side slip angle range=0.5 0.5] rad.

3) UAV related pneumatic parameters: the average pneumatic chord length MAC = 0.54148m, wing expansion b = 7.5m, wing area S = 3.965m2.

4) Propeller installation position:rHub=[2.1875 0 0]m, propeller range Rprop=0.94m, propeller inertia moment Jprop=0.29264kg • m2.

5) take-off and no-load parameters: take the no-load the maximum quality mempty=240kg, full load maximum mass mgross=320kg, no load when the center of gravity Cgempty = [0.156 0 0.079] m, full load center of gravity Cggross=[0.159 0 0.090]m.Momentary moment of inertia Jempty=[0.7795 1.122 1.752 0.1211] kg • m2, moment of inertia at full load Jgross= [0.8244 1.135 1.759 0.1204] kg · m2

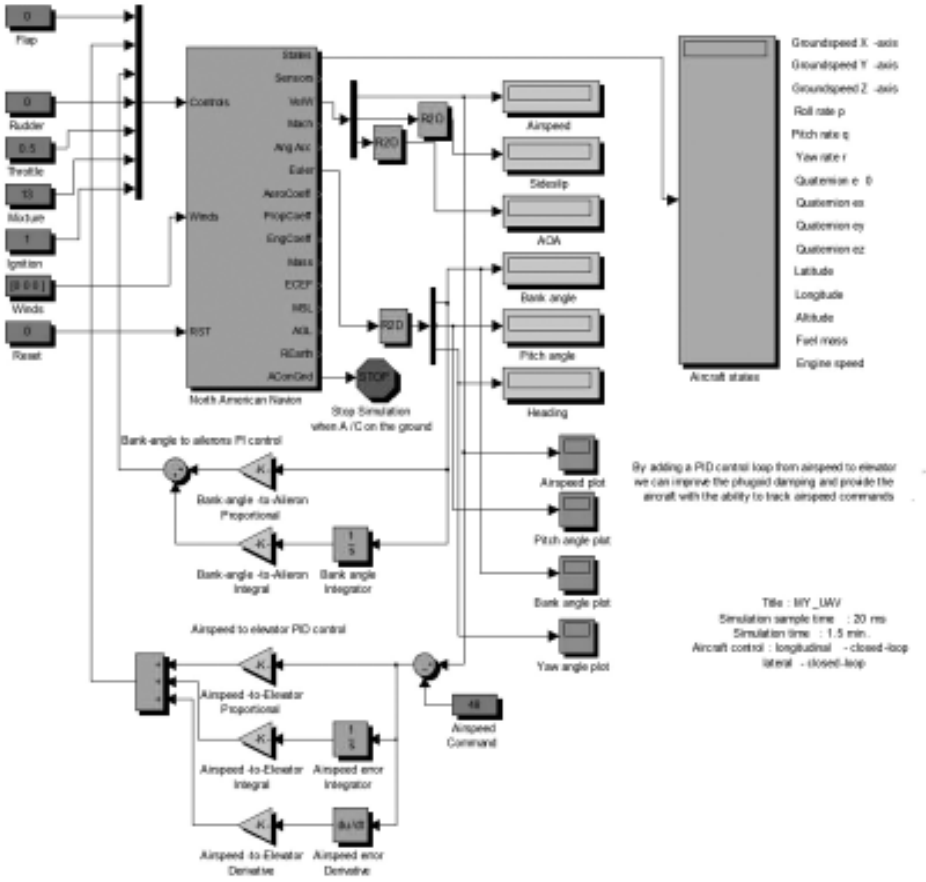

Figure.6 UAV model structure diagram

According to Fig. 6 shows the UAV model structure set the initial parameters shown in table 2.

Table 1 UAV model initial parameter value setting

label	initial value setting	parameter value
1	Initial velocity	50m/s
2	Initial angle velocity	[0 0 0]
3	Initial altitude	1000m
4	Initial position	[pi/4 -0.677/pi 1000]
5	Initial fule mass	60.5kg
6	Initial engine speed	5596 r/m
7	Initial altitude	20m
8	Sample time	50ms

To enhance the stability of the control, airspeed, tilt angle added to the PID control loop. In Winds=[0 0

0] and Winds=[5 -3 0] in two flight environments,UAV typical parameters, namely, airspeed, tilt, pitch and The output value of the flight angle is shown in Fig.7 to Fig.10.

Set the airspeed initial value of 50 m/s, the stability value of 35m/s, it can be seen from Fig.7 that the velocity value of the UAV is gradually stabilized to 35m/s after 20s or so, with the ideal environment (Wind = [0 0 0]) and the wind disturbance environment Wind = [5 -3 0]). In the wind-disturbing environment, the velocity fluctuates above the steady value (35 m/s), which is closer to the actual airborne; It can be seen from Fig.8, after 20s or so, UAV tilt angle from -0.8 ° gradually become 0 ° , that is, unmanned aerial vehicles from the tilt state to the horizontal state; It can be seen from Fig.9, after 20s or so, the aircraft' s pitch angle stabilized to about 13 ° , that is, the aircraft is doing climbing movement; It can be seen from Fig.10, after 20s or so, the aircraft yaw stability 0 ° (ie 360 °) or so, that is, the plane is doing direct flight.

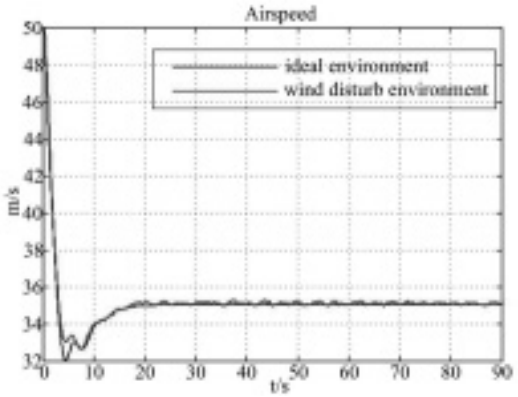

Figure.7 Airborne output of UAV in two flight environments

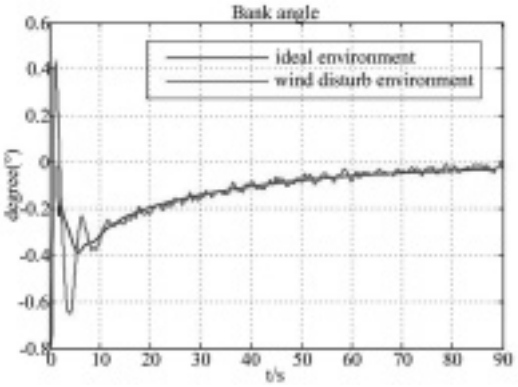

Figure.8 Unmanned aircraft tilt angle output in both flight environments

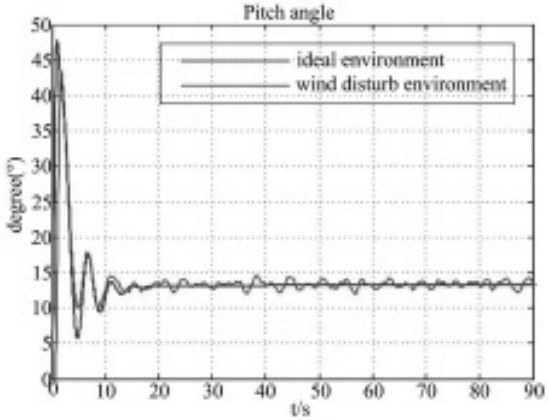

Figure.9 UAV pitching output in both flight environments

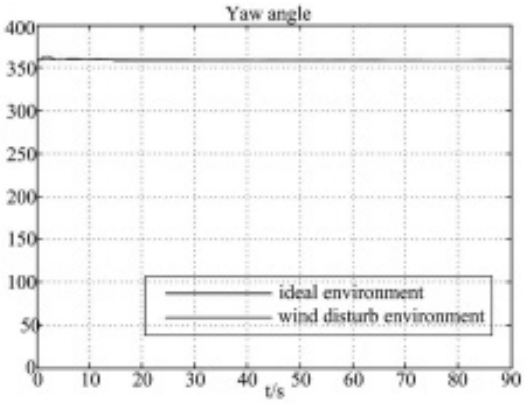

Figure.10 UAV yaw angle output in both flight environments

The simulation results show that the output of UAV typical flight parameters can not only meet the demand of UAV dynamic modeling, but also improve the efficiency of the whole system. The method is based on the dynamic model of UAV To the unmanned aerial vehicle flight simulation system engineering has important application value.

4. Conclusion

In this paper, aiming at the actual modeling requirements of UAV dynamic model, a fast integration model of UAV simulation model based on Simulink/Aerosim is proposed. Based on the analysis of the internal structure of the UAV system, the relevant parameters and the development environment configuration method of the modeling process are analyzed, and the simulation analysis is carried out with a specific aerodynamic layout of the UAV as an example. This method can meet the demand of UAV dynamic modeling, and can effectively improve the development efficiency of the whole flight system, and has certain application value.

Acknowledgment

No. 23(2013) Special fund of Shaanxi Provincial Department of Education

References

[1] Xiao Weiguo, Er Lianjie. Research on Time Delay and Compensation for Hardware-in-loop Simulation System on Dual-computer[J]. Aerospace Control, 2004, 34(8): 24-29.

[2] Feng Liang，Rapid Development of UAV Autopilot Using MATLAB/Simulink，American Institute of Aeronautics and Astronautics，AIAA Modeling and Simulation Technologies Conference and Exhibit 5-8 August, 2002.

[3] Information on AeroSim block user’s Guide. http//: www.u-dynamics.com.

[4] Qi Zhen-heng, Hu Dewen. Airborne IMU simulation based on Simulink and FlightGear[J]. Journal of Chinese Inertial Technology, 2008, 16(4): 400-404.

[5] The Math Works Inc. Real-Time Workshop for Use with Simulink (version6) [M] USA: The Math Works Inc 2004.

[6] Fan Xiaodan, Sun Yingfei. Rapid development of real-time control systems in C++ Based on RTW[J]. J Tsinghua Univ(Sci & Tech), 2003, 28(9): 62-67.

[7] Kong Fan-e, Chen Zong-ji. Real-time Simulation of Flight Control System Based on RTW and VxWorks[J]. Journal of System Simulation, 2007, 43(7): 895-898.

[8] Zhang Yi, Wang Shixing. SIMULATION SYSTEMS ANALYSIS AND DESIGN[M]. Beijing: National Defense Industry Press, 2010.

[9] Li Qiang, Wang Mingang. Code generation of simulink models in the hardware-in-loop simulation[J]. ELECTRONIC MEASUREMENT TECHNOLOGY, 2009, 32(2): 28-30.

The Research of Information Delay in the Neural Network Forecast Remote Control System

Xu Shuping[1], Chen Yiwei[1] ,Cheng Xinhua[2] and Su Xiaohui[1]

[1] School of Computer Science and Engineering, Xi'an Technological University , 710032

[2] Department of Electromagnetic Engineering, Hanzhong Vocational And Technical College 723002, China

Email: 563937848@qq.com; xusp686@163.com

Abstract. Aiming at the issues of random delay and delay uncertainty in both the before channel and feedback channel for network control system, the root causes of random delay influence closed-loop control system by case is analysis, and the predictive control method based on neural network to solve the feasibility of existence network random delay in control system closed-loop control has provided. Simulation results show that the method can reflect and predict the delay characteristics of between measurement data represents the network path, and can effectively substitute for the actual network in the design of closed-loop control system based on Internet to research; the method used fast and accurate can be used for online learning network model and forecast the network delay value, provides a new way to remote closed-loop control based on Internet.

Keywords: Model predictive control, Network time-delay, Simulation, Networked remote control system, Closed-loop control.

1. Introduction

Network control system based on Internet broke through the many limitations on control system based on field bus and become the new development direction of the network control system, stable, fast, and accurate still the ultimate goal of network control systems pursued [1]. Introduction network easy for the organization and deployment of the control system but the transmission delay and data drops inevitably exist in network communication, these will give control system adverse effects even cause instability. Therefore, in recent years, the network control system design and analysis has aroused widespread concern in both academia and industry. Literature [2] proposed a new method to improve the network latency problem. First, feedback information of the server sends the client is no longer the traditional image information while status information with the robot movement, contained less byte code. Secondly, on the server side, we set reasonable threshold for the parameters of the dynamic packet to effectively control the time of sending the packet. Only when any one parameter value in the packet exceeds its threshold, the dynamic information was only package and send to the client, data transmission in such networks is greatly reduced. These two aspects, due to reduce the data volume, network congestion reduced and delay and packet loss are greatly improved. Literature [3] describes

the network programs and topology of achieve the common CNC machine tools Internet access and remote monitoring by communication controller; given network transmission delay calculation by such a network structure; proposed the method to improve CNC machine tools real-time remote monitoring by establish data buffer in communication controller, use high-speed MCU and zero-copy technology, emergency data processing technology. Literature [4] simplified the block diagram of remote control system based on Internet, the former delay and feedback delay combined total delay so that the system only needs to design a compensator, the system design is simplified and uses the smith compensator to compensate control to improve system quality. To the uncertainty of network delay, use buffering techniques in the site control computer to convert the uncertain time delay into a fixed delay, even without network delay prediction can also to achieve better control effect. Literature [5] uses the hydraulic system as the controlled object; there are challenging researches on the remote control system in the Internet environment. The experimental results show that, when according to the principle of Smith compensator design dynamic compensation and appropriate delay prediction algorithm can make the Stability original system before not join the network latency links to restore stability after joining the network, so that the remote control of the mechanical movement using the Internet possible. However, due to the uncertainty delay in network transmission links and the data use policies of sampling information processor the control signal distortion after the transmission so that the system steady state error.

See from the current study, analysis and design network controller gradually development by a single variable to multivariate, determine to random, classical control theory to intelligent control theory and advanced control algorithm. But this is only the beginning, so far does not have a systematic approach for analysis, modeling, design whole network control system, and the architecture of the network control system continues to change, the current method is largely concentrated in the condition of network delay is no more than one sampling period, and other cases have yet to be depth.

Self-learning and adaptive capacity of neural network made the neural network model predictive control applications and research gaining increasing attention in the control system, and the prediction control based on neural network has strong robustness can adapt to the changing of system status and network latency links. This paper applied the neural network model predictive control to the network closed-loop system to reduce the impact of random delay to the system, and verified validity of the method by simulation, the method is an effective way to solve the network latency closed-loop control.

2. Network Control Research Background Based on Internet

In order to study the impact of network latency on the remote closed-loop control system, set up remote motor control system platform based on Internet , a brushless DC motor as charged object, developed DSP as core and motor drive modules with serial communication functions which directly connected the server serial port in order to facilitate the research on motor network control technology and control network functions embedded in the information networks, for the development of the control network search a more portable way, that is though the method of control functions embedded in the information network to build control information network. Remote motor control based on Internet shown in Fig. 1, this paper used a DSP controller as inner ring, PC server as outer ring dual-loop control structure. The inner ring composed by DSP to complete real-time, general motor closed-loop control; the outer ring of PC server as core to complete the remote closed-loop control. Such a structure ensured more reliable and efficient control effect under the condition of network delay.

This double-loop control system based on improve the performance of the remote controller can achieve safe, reliable and real-time closed-loop control under the conditions of network latency. The inner ring of DSP controller as core complete conventional closed-loop controls of the brushless DC motor, such as complete the speed closed-loop control of brushless DC motor based on DSP. The outer ring constituted by the client-server, DSP controller and brushless DC motor to complete the macroscopic closed-loop control of the client. For example, the client issued the directive forward 2cm and server sent the directive to the DSP controller, the DSP controller on their own to complete the instruction and maintain communication with the client. During the directive implementation, even if it is disconnected from the network, the DSP controller also on their own to complete the control task regardless of the impact of network performance.

3. The Impact of Network Transmission Delay on the System Real-Time

The remote control of such a complex computer network based on Internet, information transmission and processing on the network takes time, the sender and receiver of information can be viewed as a network transmission delay, the transmission delay existence made network real-time restrict, which is response time determined by the inherent properties of the network system and is inevitable. The presence of network delay and its uncertainty is not conducive to achieve closed-loop control based on network, because in such a system, the network transmission delay not only appears in the before control channel the system, but also appear in the information feedback channel shown in Fig. 1. The delay in the feedback channel makes the controller can not found the controlled variable changes; the delay in the before channel makes the control signal unable to work on the controlled object. These factors not only affect the system dynamic quality, but also affect the system stability.

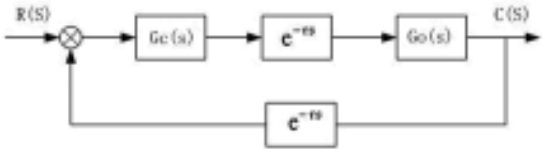

Figure.1 NetworkRemote Control Systems

The closed loop transfer function of network closed-loop control system can be drawn from Fig. 1:

$$\frac{C(S)}{R(S)} = \frac{Gc(S)Go(S)e^{-2\tau}}{1+Gc(S)Go(S)e^{-2\tau}} \quad (1)$$

The characteristic equation is:

$$1+Gc(S)Go(S)e^{-2\tau} = 0 \quad (2)$$

Visible, characteristic equation of transfer function of closed-loop control system with the network transmission delay links is a transcendental function of complex variable s, the root of the characteristic equation is no longer finitely but an unlimited number. This is also an important feature of time-delay systems, from the point of information transmission; network delay closed-loop system is a time-delay systems of transmission delay included in the forward channel and feedback channel on the time. Delays

caused a negative effect for most of the linear control system and the system changes from stable to unstable. Visible the presence of network delay links not only affect the dynamic quality, but also affect the system stability. Therefore, analysis the time-delay system stability and controller design is a very difficult subject.

4. The Root Causes Research on the Impact of Network Transmission Delay Links on the Closed-Loop Control Systems

In order to study the impact of network delay on the closed-loop control system, the typical second-order system in a remote control, a simple single-link robot arm as control objects to study the network closed-loop control problems. The system dynamics equation [6]:

$$\frac{d^2\phi}{dt^2} = -10\sin\phi - 2\frac{d\phi}{dt} + \mu \tag{3}$$

Among them, ϕ represent the angle of robot arm; μ represent the behalf of DC motor torque. The simulink block diagram of mechanical arm can draw on the type shown in Fig. 2

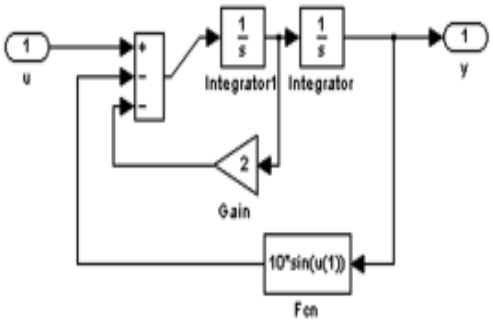

Figure.2 Simulink Block Diagram of Mechanical Arm

According to actual situation of the network closed-loop control let a delay link connected between the system controller and the controlled object, another delay link connected to the feedback channel. In the network control system, the forward channel and feedback channel is generally the same physical link, and sent in both directions at the same time, that these two values of delay links are the same, so this paper set the two delay value in delay link set to the same to study. First, delay time in the delay links adjust to 0, that is not including delay link, repeatedly adjust the PID parameters to obtain the satisfied response curve. Then, keeping the PID parameters unchanged, increase the network delay value gradually starting from 0.02 seconds obtain the response curve shown in Fig. 3, seen from Fig. 3 with network delay value increasing, the system performance gradually deteriorate, when the delay increased to 0.05 seconds the system become the oscillating system, continue to increase delay to 0.06 seconds system response divergence, that is the system becomes unstable.

Realing the PID parameters of the of increase 0.06 seconds delay link instability control system obtain the response curve shown in Fig. 3 (d). Visible, by adjusting the controller parameters really can make the original unstable closed-loop control systems becomes stable and meet the remote closed-loop control requirements of system which not high request about fast like robot arm. System control parameter adjustment is a bit trickier, as the delay size and system parameters change constantly adjusted to limit its scope of application, especially not for interstellar adventure, the work environment unknown

controlled object, therefore, intelligent control links with adaptive require introduction.

The manipulator control system in Figure 3 as for example analysis, assume that the sampling period of 0.05 seconds in Figure 3, set the delay value to 0.05s, the control information in time k transmitted to the controller after 0.05s, as opposed to the system sampling time 0.05s, the controller receives status information at the moment of k has pass a sampling point, the state of the system has become the state in time k +1, that is state of the k time fed back to the PID controller at

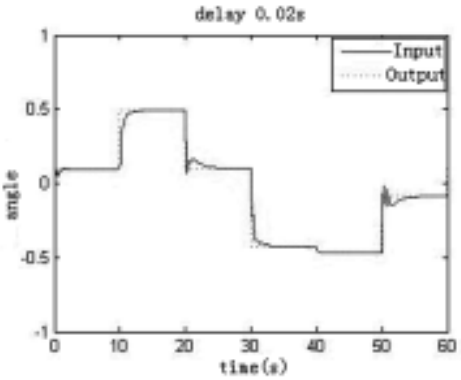

(a) response after adding 0.02 seconds time delay

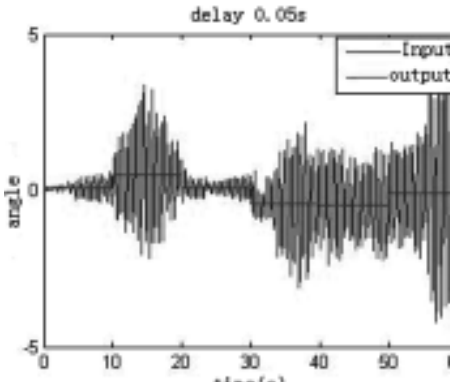

(b) response after adding 0.05 seconds time delay

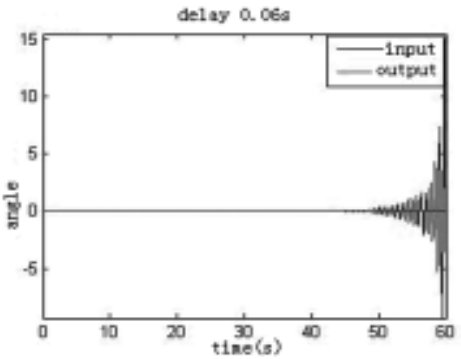

(c) response after adding 0.06 seconds time delay

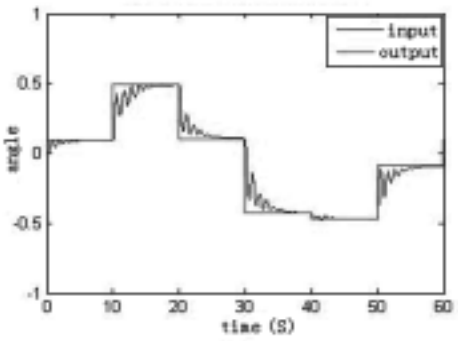

(d) response after regulate PID parameters at 0.06seconds time delay

Figure.3 response after increase network latency

time k +1, the PID controller for time k, the state at time k+1 has not yet come, but this time system status values at k-1 after a sample time delay before it is passed controller, therefore, the controller can only decision at time k should be imposed control value u (k) based on the state of the k-1 times, and this control value can be a real work on the system after a time delay, while at the time k +1 and the state of the system has been turned into a time k+1 the state of X(k+1), while u (k) produce at the state time k-1, so u (k-1)grieved and u (k +1) required difference two sampling cycles. In these two sampling cycle, the state of the system state transition, that is x (k-1) transfer to the x (k+1), x (k-1) and x (k+1) often is different lead to u (k-1) and u (k +1) is different. In other word, the system control value produced offset and the greater delay the greater offset, which is the root source of result in deterioration of the system closed-loop control performance and even instability.

The above analysis shows that the system performance deterioration caused by the remote network delay because of can not correctly calculate the amount of control exerted by the controller to the system ,if the system model is known and the size of delay is known, then forecast the state of system in accordance with the principle of the system predict compensation, and calculate the size of control value need to be added the control system in accordance with the predicted state, that is time k applications to predict the state $\hat{\chi}$ (k+1) at time k+1 yet not the state of x(k-1) at time k-1 calculation to be applied to the system state at time k, then the control value u (k +1) at actual time k +1, the u (k +1) after a delay transmission in the time k +1 transfer to the system just after a sampling period, the state of the system change into x (k +1) ,

So, if the predicted state $\hat{\chi}$ (k+1) is infinitely close to the actual state x (k +1), the performance of control network delay closed-loop control system can be infinitely close the performance of the closed-loop control system without delay links, which is the basic idea of the predictive control model. However, the delay of the control network is time-varying and controlled objects are often immediately confounding factors, it is can not use an inconvenience model to predict the state of system and can not use a specific delay time to do the fixed step predictive control, neural network has the advantages of online learning the state of the system, predictive control based on neural network has strong robustness to be adaptive to the change of system status and network delay aspects ,it is a way to solve the network latency closed-loop control.

5. Model Predictive Control

Model predictive control is according to the running state of the system over the past time and present moment, more accurate forecasting system desired output value in the future moment, calculated control value of the system should be added according to output value desired depending on certain optimization algorithm adaptive computer control of online solving control value [7-10]. Visible, model predictive control algorithm is an adaptive control method based on the future state of controlled object or dynamic predictive value of output and online solving current control [8-13]. Model predictive control is a newer computer control algorithm developed in the late 1970s; the algorithm actually encompasses three steps: prediction model, rolling optimization and feedback correction [9-16].

5.1 Prediction Model

For a module description of the alleged object behavior in the predictive control based on neural network belong to forward model of system, there use the training methods as shown in Fig.4, where dashed box picture shows the actual controlled object, here is the simulink block diagram of the robotic arm, at random input signal u to produce output y. Selected BP neural network with one hidden layer as training model of a controlled object , set the number of hidden layer neurons is 10, using the Levenberg-Marquartdt learning rules, with the group [u, y] data training neural network model of the charged object, the results shown in Fig.5, where Fig.5 (a) is the data used for training, Fig. 5 (b) is convergence diagram for training.

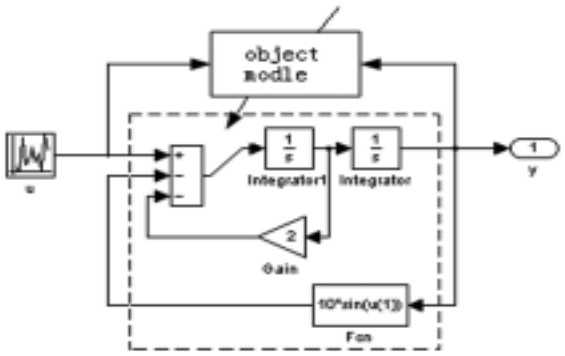

Figure.4 Neural Network Training Block Diagram of the Manipulator

5.2 Rolling Optimization

Rolling optimization is an optimal control algorithm, which uses the output of the rolling finite domain optimization that is the goal of optimization over time. Predictive control proposes optimization index based on the moment in every time instead of using global optimization indexes. Rolling optimization index locality through make it can only get the global optimal solution in the ideal case, but when the model mismatch or time-varying and non-linear or confounding factors can take into account this uncertainty in a timely manner compensate, reducing the deviation, keeping the actual optimal control ,and it is also easy to use input/output value of finite difference time domain to identify rapidly the state of controlled object so as to implement the online adjustment to the control law and need for repeated optimization .

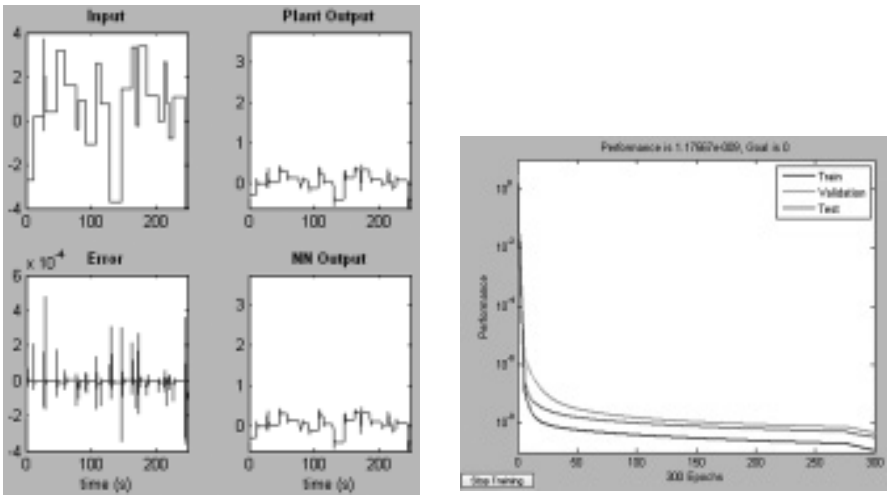

(a) (b)

Figure.5 Neural Network Model Training Results of Manipulator

Optimization algorithm in this article also uses neural network to achieve, set the time-domain involved in the optimization value of 2, using the BP network neural of hidden layer neuron number 7, the same learning rule Levenberg-Marquartdt do the online training to achieve the control signal to the continuous optimization. Training block diagram is shown in the dashed box in Fig.4. Neural network optimization device in accordance with a given input signal u produce predictable output u1, u1 is imposed to the neural network model of the controlled object to produce predictable output y1, y1

compare with the desired output u of the system, and both the difference to train the neural network optimization. Then, the output u2 of the e2 enough litter as the actual amount of control applied to the actual controlled object. Visible, the optimizer in the regulation system is the inverse model of the charged object. Y1 can also be compared with actual output y2, and the error e1 and the actual input u2 of charged object, output y2 as the data of training charged object neural network model.

5.3 Feedback Correction

Feedback correction is forecast control to keep the dynamic correction forecasting model to ensure that the prediction model with infinitely close to the actual controlled object, and make optimization algorithm establish on the basis of the correct prediction of the system state then the new optimization. Error e1 is the amendment process of the neural network model of the controlled object. Neural network prediction model is built on the basis of the past run data in system, the new operating environment and the actual system has the nonlinear, time-varying, interference and other factors make prediction model based on neural networks need to constantly learn to modify their weights and even structure to ensure that it can well represent the actual controlled object to a control signal prediction.

6. Simulation Analyses

Build the Simulation block diagram shown in Fig. 6 under robotic arm Smulink environment, network training based on neural network predictive control by the steps in Fig. 4-Fig. 5, and at the role of the same random input signal gradually adjust the value of delay to simulation. The results in Fig.7. show that the prediction control based on neural network has a good control performance to the fixed delay network. Further used random delay module shown in Fig. 8 (a) instead of fixed delay module in Fig.6 immediately delay module for delay characteristics of input shown in Fig. 8(b), where In.mat file stored random input signal in Fig. 6. There are used random input signal stored in this file in order to compare the simulation results in the simulation. Finally, simulation under the random delay conditions and results shows in Fig.8(c). Whether a fixed delay or random delay neural network predictive controller can satisfy the closed-loop control requirements in the network delay conditions.

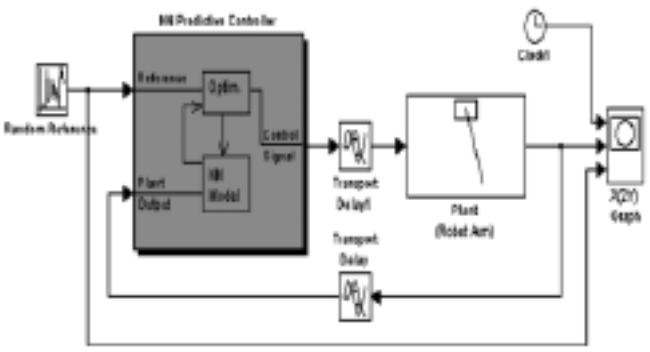

Figure.6 Simulation of Network Closed-Loop Control System based on Predictive Neural

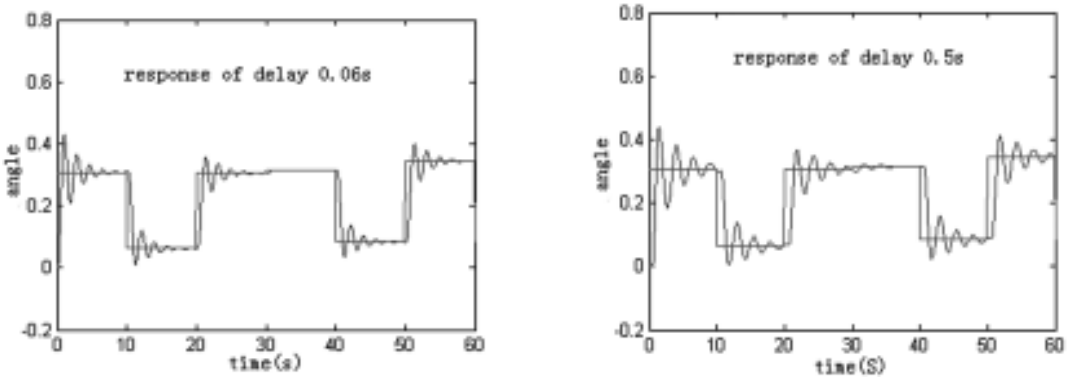

(a)Response of delay 0.06s (b)Response of delay 0.5s

Figure.7 Predictive Control Random Responses Curve based on Neural Network

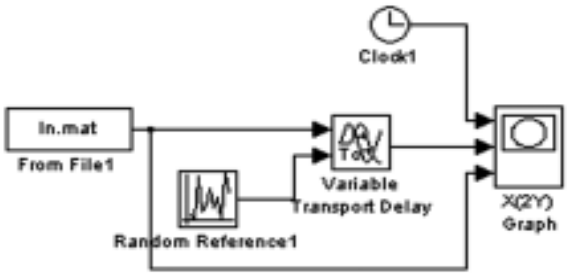

(a)fixed delay module figure

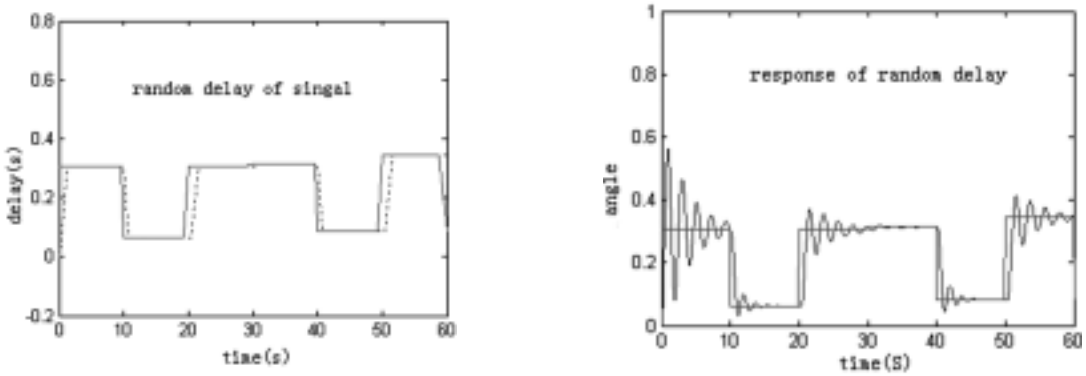

(b) Delay Curve under Random Delay (c)Response Curve under Random Delay

Figure.8 Responses under Random Delay

7. Conclusion

This article discusses the difficulties of remote closed-loop control, that is the difficulty different from the general control system lies in the uncertain network delay exist in system channel and feedback channel and which greatly reduced the system stability and improved control system design difficulty. This paper described problems on the network closed-loop control from uncertain network delay to includes network delay controller design method, and studied the impact of network transmission delay on the

network closed-loop control system, proposed by predictive control based on neural network to solve feasibility of the network control system which existence random delay closed-loop control, and verified the validity of the method by simulation.

Acknowledgment

The authors wish to thank the cooperators. This research is partially funded by the Project funds in Shaanxi province department of education (15JF019) and the Project funds in shanxi province department of science industrial projects(2015GY067).

References

[1] Xi Yu-geng, Li De-wei, Lin Shu, "Model predictive-status and challenges," Acta Automatica Sinica, vol.39 no.3, pp.713-717 , March, 2013.

[2] Edlund K,Bendtsen J D, Jorgensen J B, "Hieratachical model-based predictive control of a power plant portfolio," Control Engineering Practice, vol.19, no.10, pp.1126-1136, 2011.

[3] Zheng Y, Li S Y, LiN, "Distributed model predictive control over network information exchange for large-scale systems", Control Engineering Practice, vol.19, no.7, pp.757-769, 2011.

[4] Lin S, De Schutter B, Xi Y G, Hellendoorn H, "Fast model predictive control for urban road networks via MILP," IEEE Transactions on Intelligent Transportation Systems, vol.2, no.3, pp.846-856, 2011.

[5] Ghods A H, Fu L P, Rahimi-Kian A, "An efficient optimization approach to real-time coordinated and integrated freeway traffic control," IEEE Transactions on Intelligent Transportation Systems, vol.11, no.4, pp.873-884, 2010.

[6] Zu-de, Z. and C. Ben-yuan, "Research of Networked control system time delay distribution," Control and decision, vol .25, no .4,pp.592-597,2010

[7] Shou-ping, G. and Y. Ting, "Network control system predictive control based on pole placement and time delay error compensation," Information and control, vol .38, no .1,pp.37-42,2009

[8] Yah, Z., W. Wei and Y. Wei-Ming,. "The research and development of network based robot control technology," Robot, vol .24, no .3,pp.276-282,2007

[9] Huang, J.Q., F.L. Lew and K.A. Liu, "Neural predictive control for telerobot swith time delay," Journal of Intelligent and Robotic Systems, vol .29,pp.1- 25,2009.

[10] Chen, S., C.F.N. Cowan and P.M. Grant, "Orthogonal Least Squares Learning Algorithm for Radial Basis Function Networks," IEEE Transactions on Neural Networks, vol. 2,no.5,pp. 302-309 ,2010.

[11] Lian Fengli, "Network design consideration for distributed control systems," Control Systems Technology, vol.10, no.2, pp.297-307 , March 2012.

[12] ZHUANG Yah, WANG Wei, YUN Wei-ming. „The research and development of network based

robot control technology," Robot, vol.24,no.3,pp.276-282 ,2011.

[13] Y. Kanayama, N. Miyake, "Trajectov Generation for Mobile Robots," Robotics Research, the MIT Press, vol.3,no.6, pp.333-340, 2006.

[14] Guoping Zhang, Wentao Gong, "The Research of Access Control Based on UCON inthe Internet of Things," Journal of Software, vol.6, no.4, pp.724-731, 2011.

[15] Jingyang Wang, Min Huang, "Research on Detectable and Indicative Forward Active Network Congestion Control Algorithm," Journal of Software, vol. 7, no.6, pp.1195-1202,2012.

[16] Yuan Gao, Peng-yu Liu and Ke-bin Jia, "A Fast Motion Estimation Algorithm Based on Motion Vector Distribution Prediction," Journal of Software, vol. 8, no.11, pp.2863-2870,2013.

About the Author:

Biography: Xu shuping, (1974-05-07), female (the Han nationality), Shaanxi Province, Working in Xi'an technological university, professor, the research area is computer control.

Seven-spot Ladybird Optimization Algorithm Based on Bionics Principle

Wei Feng-tao, Lu Feng-yi and Zheng Jian-ming

School of Mechanical & Instrumental Engineering, Xi'an University of Technology,

Xi'an 710048, China.

Email: weifengtao@xaut.edu.cn, lufengyi_123@126.com, zjm@xaut.edu.cn

Abstract. For solving the problems of modern intelligence algorithms such as slow convergence and low precision, a new algorithm based on bionics principle has been proposed which is inspired by the foraging behavior of seven-spot ladybirds in the nature. By analyzing the bionic principle of Seven-spot ladybird Optimization(SLO), we simulate the region search pattern of predation of seven-spot ladybirds ,combining fast extensive search with careful and slow intensive search of the ladybirds,meanwhile we use three kinds of evaluation information to evaluate the solutions one by one ,then the exploration and local approximation in the SLO are balanced. Next,in this paper we analyze the SLO theoretically by mathematics, presenting its specific process and proving the feasibility of SLO. The results based on a set of widely used benchmark functions show that Seven-spot ladybird can converge fast and yield distributed solutions with higher precision.

Keywords: bionics principle,Seven-spot Ladybird Optimization,region search pattern,feasibility analysis ,function optimization

1. Introduction

In the mid-1950s, people founded bionics inspired by the mechanism of biological evolution, and explored a class of heuristic algorithmwhich called intelligent bionic algorithmwith the help of bionic principles.The basic idea of this algorithm is derived from a natural phenomenon or a biological behavior of the simulation.In the existing bionics algorithms, the literature [1] proposed a particle swarm optimization algorithm by simulating the foraging behavior of the birds in the nature(Particle Swarm Optimization, PSO); In the literature [2] , Artificial Bee Colony (ABC) is proposed by simulating the breeding of bees and taking honey. In [3] , the Harmony Search (HS) algorithm is proposed by simulating the principle of a musical performance.There are also some algorithms proposed by some scholarsbased on some animal habits boldlysuch as Chicken Swarm Optimization [4] , Cockroach Swarm Optimization [5] and Mosquito Host-Seeking algorithm [6].Compared with the traditional optimization algorithms, this kind of algorithms does not rely on the nature of the objective function and the limitation of the search space which is easy to realize by programming. Moreover,it is suitable for solving nonlinear problems that traditional methods can not solve and have been widely used in engineering [7-8] . When dealing with the complex problems with multi-dimensions and high-peaks, some of the bionics algorithms usually

have a number of problems such as easy to fall into local optimum, poor solution quality and premature convergence and so on .

In this paper, a new intelligent algorithm named Seven-spot Ladybird Optimization (SLO) is proposed based on the predation habit of seven-spot ladybirds. This algorithm makes full use of the group wisdom of the ladybirds. Moreover , the SLO uses a wide area search method with fast positioning when ladybrids are looking for prey and a slow circuitous local search method when ladybirds have found preies .The two methods are combined in order to enhance the search ability and convergence of the SLO.The validity of the algorithm is analyzed by using testing functions.

2. Bionic Principles of the SLO

In the process of searching for preies also known as aphids, the predation method of seven-spots ladybirds has a great breadth and depth, while they often use their visual and olfactory cues to locate prey. To find prey, this kind of insects often turns its head to the left and right alternately,rarely crawling in line and its motion trajectory is staggered. The above-mentioned behavior is called wide-area search. Once preying on their aphids, the ladybirds will reduce search speed while in order to enhance the efficiency of the search,they will increase detour of the route that is around the prey. This behavior is called a geographically centralized search, also known as local search[9].If the predation rate in a certain region is lower than a threshold value or the time between two predation intervals exceeds the giving-up time, the ladybirds will move themselves from the local search to the wide-area search, flying away to a new area, this process is called migration. The giving-up time is defined as the longest time that the ladybids can wait for after the last time predation to leave the area [10].The specific predation process of the ladybirds is shown in Fig1. As the aphids are distributed in groups and they almost have no ability to escape, so behaviors of seven-spot ladybirds which combine local with wide-search method can greatly improve the predation efficiency.

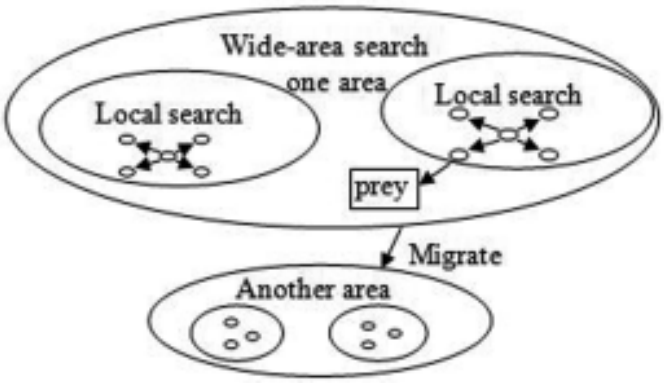

Figure.1 A predation process of Seven-spots ladybirds

Seven-spot Ladybird Optimization is a kind of intelligent optimization algorithm which is constructed by simulating the predation behavior of seven-spot ladybirds, where the specific bionic principle is: seven-spot ladybirds are simulated as feasible solutions in search space; the search method of the partition search mechanism with the combination of local and wide area in the predation process of the ladybirds is simulated into the search process of the algorithm; the location of the ladybirds during foraging is simulated as the objective function of solving the problem; the ladybirds individual survival

of the fittest in the nature is simulated into a process of a better solution instead of poor solution in the algorithm, so as to achieve the purpose of searching for optimal solution from space.

3. Seven-Spot Ladybird Optimization Algorithm

3.1 Specific introduction of SLO algorithm

Searching optimization of the algorithm is composed of two methods: local search method and wide area search methods while each search space is divided into sub-spaces at the beginning of the search;the ladybirds are always close to the global optimal solution noted as g_{best} in the solution space and each ladybird will produce its own optimal solution noted as p_{best} in the search process at the same time; since the search space is divided into several subspaces, each subspace will produce a subspace historical optimal solution noted as l_{best} when the subspace is searched by the ladybird. Through the comparison of its current position noted as $present$、l_{best}、p_{best} and g_{best}, the individual updates the next step and finally achieves the purpose of optimization.

For a ladybird in a D-dimensional space, suppose t represents number of current iterations, position of the ladybird is marked as $X_i^t \Rightarrow (X_{i1}^t, X_{i2}^t, X_{i3}^t, \ldots, X_{iD}^t)$; its speed is marked as $V_i \Rightarrow (V_{i1}, V_{i2}, V_{i3}, \ldots, V_{iD})$ .The updating formula of the location for ladybird i is,

$$X_i(t+1) = X_i(t) + V_i(t) \tag{1}$$

Where, $V_i(t)$ represents the current speed, $X_i(t)$ represents the current position.

The search methods are divided into local search and wide area search, if the ladybird made a wide area search before, then it will make a local search in this cycle.When the local search is completed, the ladybird will convert itself into a wide area search, so the updating formula of the ladyird in the local search speed is,

$$V_i(t) = c \times r_1 \times (pbest_i(t) - X_i(t)) + \varepsilon_1 \tag{2}$$

The updating formula of the ladyird in the wide area search speed is,

$$V_i(t) = c \times r_2 \times (lbest_i(t) - X_i(t)) + \varepsilon_2 \tag{3}$$

Where, r_1、r_2 are random numbers in the [0,1] which obey the uniform distribution so as to increase the randomness of the search; c is a learning coefficient so as to adjust the step length and direction; ε_1、ε_2 are two relatively small random numbers.

If the position has not been improved after a certain cycle, a new solution is substituted for the position near the global optimal solution according to Eq. 4.

$$x'_{i,j} = x_{gbest,j} + \phi\omega \tag{4}$$

Where, ω is the neighborhood of the global optimal solution g_{best}, ϕ is a correction value which is the random number of the interval [-1,1].

The basic flow of the SLO is shown in Fig.2.

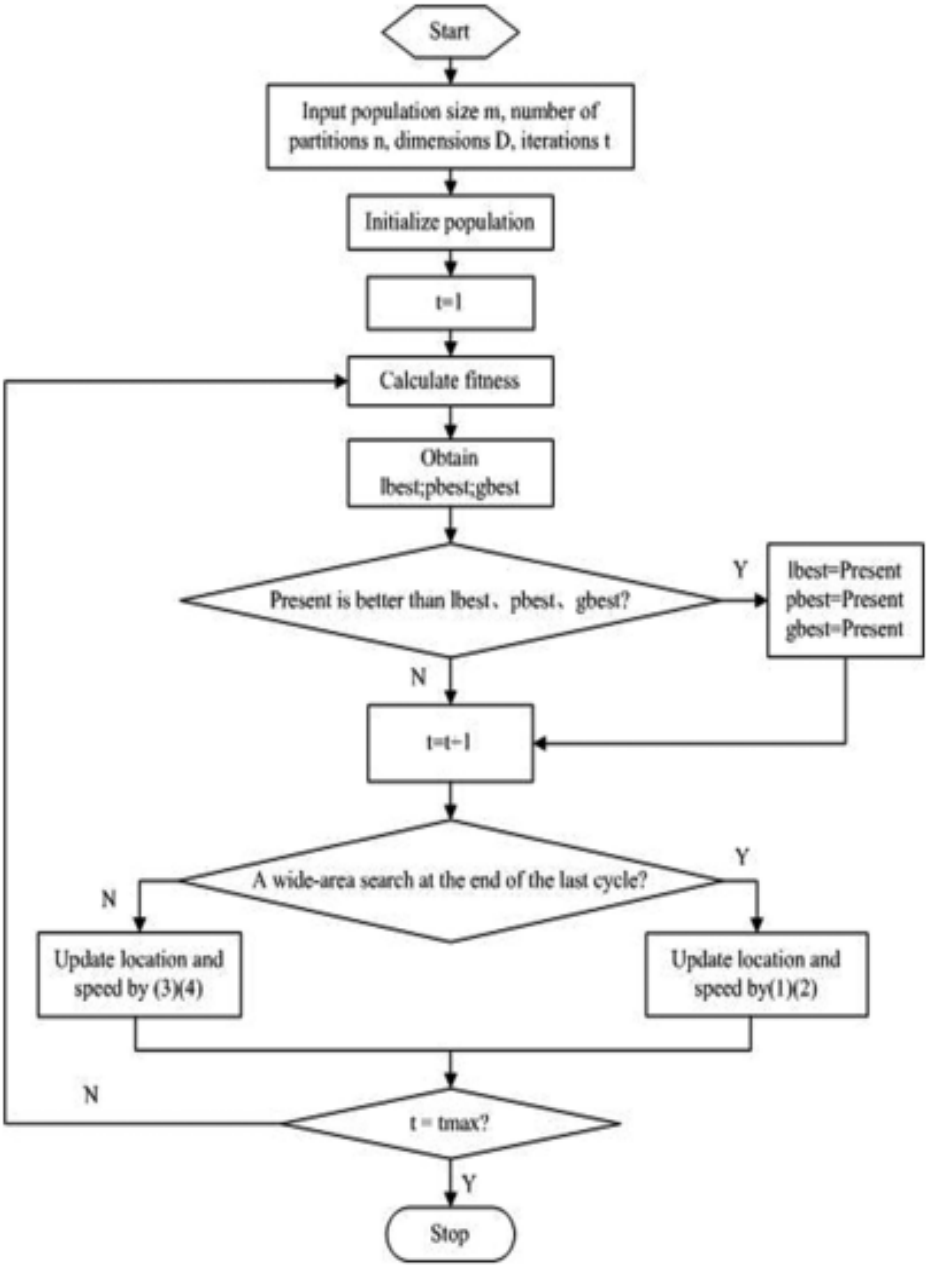

Figure.2 Flow chart of the SLO

3.2 The feasibility analysis of SLO algorithm

In order to analyze feasibility and observe the optimal effect of the algorithm intuitively, this paper selected *Rastrigin* function to compare its position at the initial and the end after 500 cycles in 2-dimensions where the specific operating principle is: the initial individual position of the algorithm marked as $X_i^t \Rightarrow (X_{i1}^t, X_{i2}^t, X_{i3}^t, \ldots, X_{iD}^t$ is a random number between [0,1]. As the number of iterations increases, the individual positions in the population move in the direction of the optimization of the function values according to the SLO steps. The results of the comparison are shown in Figure 4 where 4 (a) and 4(b) show the initial and final positions respectively of the individual of each search space.

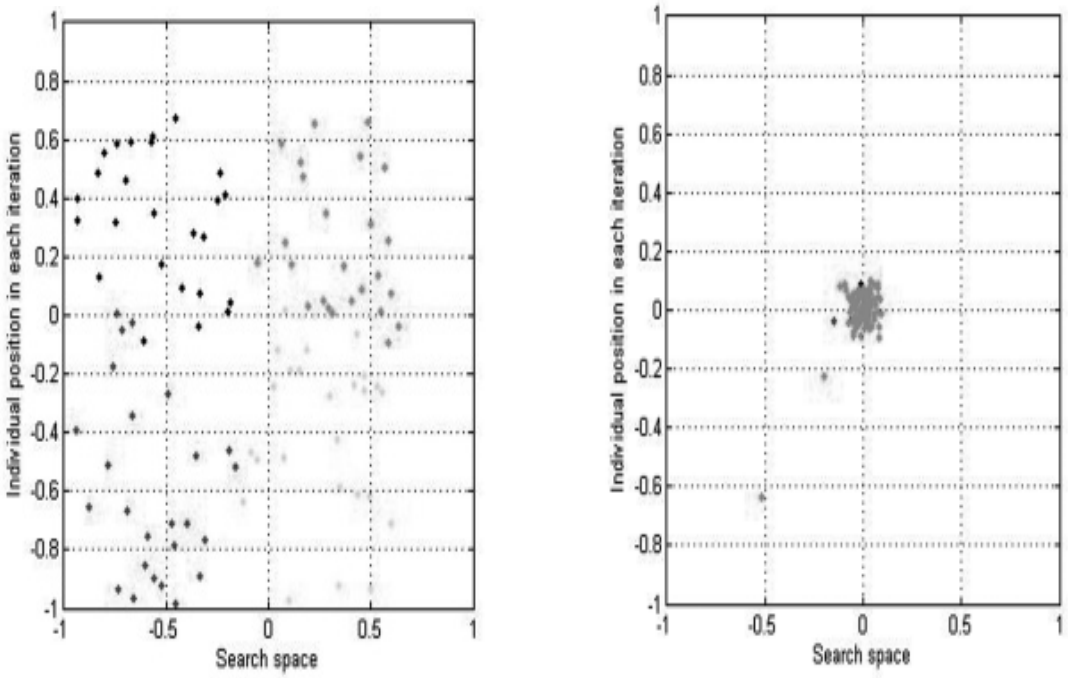

(a)Initial distribution of individual positions (b) Final distribution of individual positions

Figure.3 Comparison of the operation results of SLO

It can be seen from Fig.3 that the individual distribution of the search space at the initial time of the optimization is a mess,while it obeys some rules:seven-spot ladybirds are clustered,individuals are closely linked but they are not in collision,which indicates that the algorithm is parallel and easy to share with the population information.Since the test function has a global optrimal value of 0 near($0,0,\cdots,0$),the vast majority of members of the ladybirds are distributed near $(0,0)$ as the algorithm stops which indicates the feasibility of the SLO.

4. Simulation Experiment and Analysis

Six typical testing functions as shown in Table 1 are used to analyze the performance of SLO while compared with PSO, ABC and HS , the basic parameters those algorithms used are set as shown in Table 2. The simulation platform is Windows XP, and the simulation software is Matlab2014 (a).

Table 1 Typical testing functions

Name	Expression	Type	Range	Minimum
Griewank	$f_1(x)=\frac{1}{4000}\sum_{i=1}^{n}(x_i)^2-\prod_{i=1}^{n}\cos(\frac{x_i}{\sqrt{i}})+1$	Multi-modal	[-600,600]	0
Ackley	$f_2(x)=-20e^{-0.2\sqrt{\frac{1}{n}\sum_{i=1}^{n}x_i^2}}-e^{\frac{1}{n}\sum_{i=1}^{n}\cos(2\pi x_i)}+20+e$	Multi-modal	[-32,32]	0

Rastrigin	$f_3(x)=\sum_{i=1}^{n} x_i^2-10\cos(2\pi x_i)+10$	Multi-modal	[-10,10]	0
Salomon	$f_4(x)=-\cos 2\pi\sqrt{\sum_{i=1}^{n} x_i^2}+0.1\sqrt{\sum_{i=1}^{n} x_i^2}+1$	Multi-modal	[-5,5]	0
Schwefel's	$f_5(x)=\sum_{i=1}^{n}\lvert x_i\rvert+\prod_{i=1}^{n}\lvert x_i\rvert$	unimodal	[-10,10]	0
Sphere	$f_6(x)=\sum_{i=1}^{n} x_i^2$	unimodal	[-100,100]	0

Table 2 Testing parameters of each algorithm

Algorithm	PopulationSize(N)	Maxium Iterations (M)	Dimension(D)
SLO	25	500	D=10;30;50
PSO	50	500	
ABC	50	500	
HS	50	500	

To fully reflect the performance of the algorithm, four algorithms are run for 30 times in D=10, 30, 50. And the indices of mean value, optimal value and variance of the algorithm are used to evaluate the optimization properties of the algorithm. The simulation results are shown in table 3-5. In order to observe the convergence of SLO algorithm intuitively, figure 4 shows fitness evolution curves obtained on 6 functions in D =50 that tested by four algorithms to optimize,where the number of iterations is set to the abscissa, the fitness value (base – 10 logarithm) is set to the ordinate.

Table 3 Simulation testing results in 10-D

Name	Dimensio	Indice	SLO	PSO	HS	ABC
f_1	10	*Best*	2.1440e-9	5.2795e-2	3.0476e-3	4.6420e-5
		Mean	1.6659e-3	8.2021e-3	2.9927e-2	4.3921e-3
		Std	4.3248e-4	3.2789e-4	2.2576e-3	3.9486e-3
f_2	10	*Best*	-5.3363e-3	7.8205e-1	1.9480e-1	9.5212e-1
		Mean	2.2968e-2	9.5397e-1	8.4129e-1	9.5234e-1
		Std	2.5353e-2	9.9953e-2	7.8991e-1	1.7728e-4

f_3	10	*Best*	1.0106e-6	7.6108	3.5556	1.4492e-8
		Mean	6.3989e-2	9.1032	1.4079e+1	1.4255
		Std	3.0174e+1	3.8023e+1	2.5889e+2	9.3210e+3
f_4	10	*Best*	1.0610e-5	1.4987e-1	1.7989e-1	1.9042e-2
		Mean	2.8664e-3	1.5268e-1	1.8293e-1	4.5964e-2
		Std	5.8336e-4	2.9980e-4	1.0474e-3	4.8746e-2
f_5	10	*Best*	1.0513e-8	5.4643e-2	2.1235e-2	4.5642e-4
		Mean	1.1560e-2	7.9289e-2	2.3097e-1	1.0244e-2
		Std	1.9061e-2	1.8648e-2	1.7274e-1	2.1923e-2
f_6	10	*Best*	1.1317e-8	3.3975e-2	1.8063e-2	1.0975e-14
		Mean	1.7325e-2	6.4460e-2	2.6815e-1	5.2047e-2
		Std	4.2551e-2	4.2218e-2	2.1377e-1	6.1868

Table 4 Simulation testing results in 30-D

Name	Dimensio	Indice	SLO	PSO	HS	ABC
f_1	30	*Best*	3.2145e-9	5.1580e-2	2.5236e-2	8.3693e-4
		Mean	3.0745e-3	5.7688e-3	9.8092e-2	1.9574e-2
		Std	1.2382e-4	1.2240e-3	5.6659e-3	1.0006e-1
f_2	30	*Best*	-5.2700e-3	1.3903	5.1606e-1	9.5212e-1
		Mean	3.0349e-2	1.4547	1.2872e-1	9.5239e-1
		Std	1.1078e-1	8.0031e-2	8.0880e-1	1.2064e-4
f_3	30	*Best*	1.2925e-6	1.3288e+2	4.4681e+1	4.1044e-1
		Mean	2.2453e-3	1.3780e+2	9.6527e+1	6.1215e+1
		Std	4.4413e+2	3.0818e+2	3.2336e+3	2.6165e+6
f_4	30	*Best*	2.6855e-5	3.0987e-1	2.9991e-1	1.3817e-1
		Mean	4.9253e-3	3.1226e-1	3.0286e-1	2.4424e-2
		Std	1.5897e-3	3.5566e-4	8.9552e-4	7.5598e-1
f_5	30	*Best*	6.3100e-8	1.2141	7.9248e-1	2.2403e-2
		Mean	5.2142e-2	1.3213	1.8964	1.0684e-1
		Std	3.3865e-1	3.2974e-1	1.8693	3.6342e-1
f_6	30	*Best*	6.5532e-8	1.4428	8.4510e-1	2.5147e-7
		Mean	9.6317e-2	1.5879	2.1980	3.9218e-1
		Std	1.1237	8.0026e-1	2.7285	1.6467e+2

Table 5 Simulation testing results in50-D

Name	Dimension	Indice	SLO	PSO	HS	ABC
f_1	50	*Best*	4.2234e-9	1.0877e-1	7.2478e-2	8.6653e-4
		Mean	3.3346e-3	1.1647e-1	1.4481e-1	1.4424e-2
		Std	1.7208e-3	1.6674e-3	6.6099e-3	6.3858e-3
f_2	50	*Best*	-5.2503e-3	2.3162	1.7489	1.2566e-1
		Mean	3.0943e-2	2.3602	2.4828	1.7553e-1
		Std	1.2542e-2	4.1347e-2	2.9499e-1	2.9604e-1
f_3	50	*Best*	1.6812e-5	2.8364e+2	1.1483e-2	4.7141
		Mean	2.5915e-1	2.8867e+2	2.1223e-2	1.2258e+1
		Std	4.2107e+2	3.8855e+2	9.0867e-3	4.2271e+3
f_4	50	*Best*	4.0342e-5	3.7987e-1	3.9133e-1	1.6191e-1
		Mean	5.4999e-3	3.8255e-1	3.9196e-1	1.6731e-1
		Std	2.8011e-3	4.8918e-4	2.8373e-4	3.0765e-2
f_5	50	*Best*	1.3577e-7	2.9843	2.5168	1.2382e-1
		Mean	1.0479e-1	3.6012	4.7555	1.6924e-1
		Std	1.3230	1.2198	5.7054	3.6047e-1
f_6	50	*Best*	1.3321e-7	3.3803	2.7070	4.6932e-2
		Mean	1.7205e-1	3.6575	5.3044	3.7246
		Std	3.8914	2.6320	9.2624	2.2524e+3

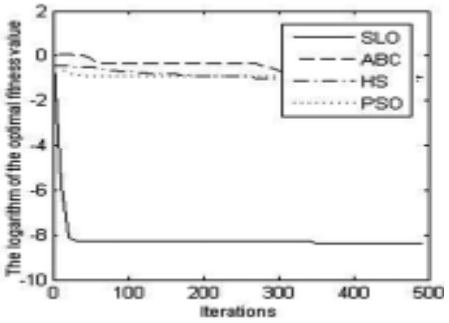

(a)Griewank function

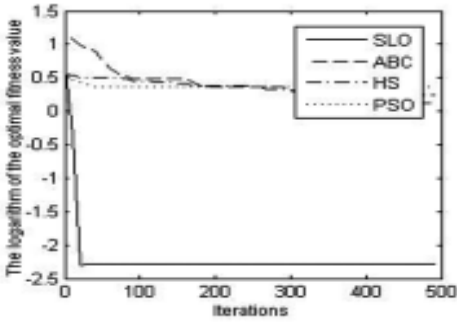

(b) Ackley function

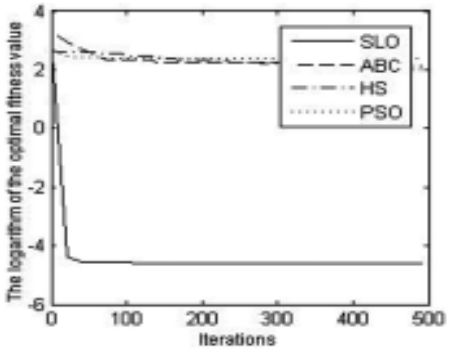

(c) Rastrigin function

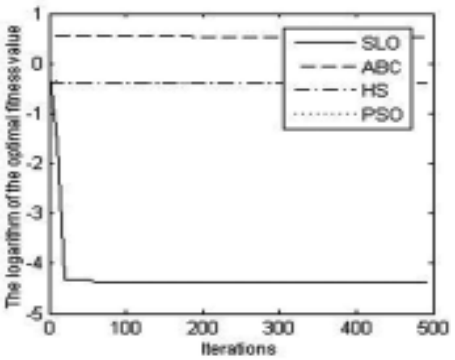

(d) Salomon function

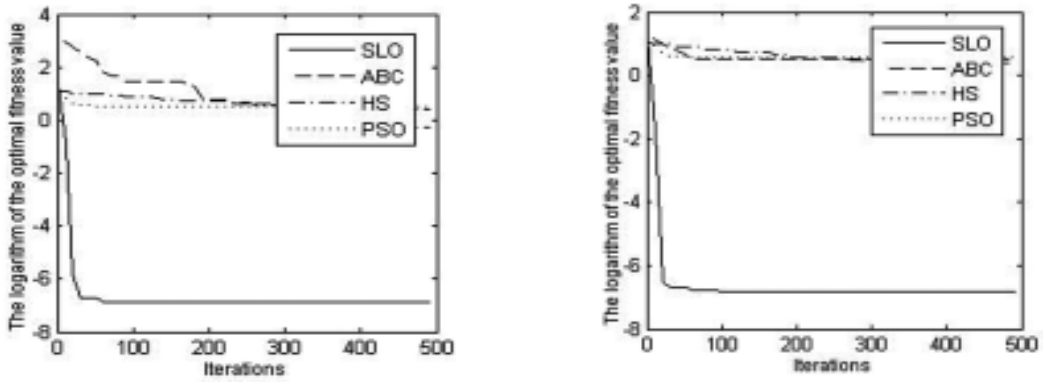

(e) Schwefel’s function (f) Sphere function

Figure.4. Optimization iterative curves of test functions of the SLO

The optimal value marked as $Best$, mean value marked as $Mean$ in table 3 ~ 5 can reflect the convergence precision and optimization ability of the algorithm while variance marked as Std which can reflect the stability of the algorithm.From table 3 we can see that SLO is better than the other three algorithms for functions f_1, f_2, f_4, f_5 in low-dimension (D = 10).Especially, the accuracy of SLO is more than e-9 for multi-modal function f_1. Although accuracy of the SLO is not as high as that of ABC in terms of f_3 and f_6, stability of the SLO is much higher than the latter and SLO also performed well. As the dimension increases, the search space becomes more complex, and it is more challenging referred to the search ability of algorithm.When the dimension increases to 30 and 50, the optimal accuracy and mean optimal value of SLO are better than the other three algorithms for all functions as shown in table 4~5 . It is worth noting that convergence accuracy of f_1、f_5、f_6 in the SLO is more than e-7 which is obviously better than that of the other three algorithms.

The optimization iteration curves of the testing functions can directly reflect the convergence speed and accuracy of the algorithm. It can be seen from fig. 4 that SLO has high convergence speed and high precision for the functions f_4 and f_6 , which shows that SLO has good searching ability;SLO can smoothly pass through a large number of local optimal points in f_1 and f_3 ; SLO can cross the traps of local optimal almost effortlessly in f_2 and f_5 . All of the above can show that SLO is not easy to fall into local optimum.Generally, the convergence performance of SLO is better than that of PSO 、 HS and ABC under the same number of iterations.

5. Conclusions

As to the problems of falling into local optimum and low solution precision in exsiting algorithms, this paper proposed a new bionic algorithm by simulating the predatory process of seven-spot ladybirds. The SLO makes full use of the characteristics of the partition search mechanism and combination of the local and wide area search of the ladybirds when searching for preies which achieves a good balance between global exploration and local exploitation. Compared with the three representative biomimetic intelligent algorithms, the results show that the SLO has good convergence precision ,high stability and fast convergence speed in dealing with low - dimensional and high - dimensional problems.

Acknowledgment

This work is partially supported by the National Natural Science Foundation of China (51575443, 51475365),and the Ph.D Programs Foundation of Xi'an University of Technology (102-451115002).

References

[1] J. Kennedy, R. Eberhart. Particle swarm optimization. Proceedings of the IEEE International Conference on Neural Networks, Perth: IEEE, 1995: 1942-1948.

[2] Karaboga D.An idea based on honey bee swarm for numerical optimization,Technical Report-TR06[R].Kayseri:Erciyes University,Engineering Faculty,Computer Engineering Department,2005.

[3] Geem ZW,Kim JH,Loganatham GV. A new heuristic optimization algorithm: harmony search[J]. Simulation,2001,76(2):60-68.

[4] MENG X B,LIU Y,Gao X Z,et al. A new bio-inspired algorithm: chicken swarm optimization [C]//5th International Conference on Swarm Intelligence .Hefei: Springer International Publishing,2014:86-94.

[5] CHENG L. New bionic algorithm： cockroach swarm optimization[J].Computer Engineering and Applications, 2008,44(34):44-46.

[6] Feng X, Zhang J W, Yu H Q. Mosquito Host-Seeking Algorithm for TSP problem[J].Chinese Journal of computers,2014,37(8):1794-1808.

[7] Cheng X B.Multi-target Tracking Based on Improved Simlified Particle Swarm Optimization[J]. Computer Engineering,2016,42(08):282-288.

[8] Yang X H,Xue Jian,Wang Y L.Deployment Optimization of Intergrated Network Node Based on Improved Artificial Bee colony Algorithm[J].Computer Engineering, 2016,42(03):116-120.

[9] Wang G. Foraging behavior of predatory ladybugs [J]. Entomological Knowledge,1991,28(5):316-319.

[10] J.L.Hemptinne,M Gaudin,et al.Social Feeding in ladybird beetles:adaptive significance and mechanism[J].Chemoecology.2000(10):149-152.

DSM Modelling for Digital Design Using Verilog HDL

Xing Xue[1], Yao Chen[2], and Junchao Wei[3]

[1] Faculty of economics and management, ShangLuo University, 726000 ShangLuo, China, chenyao3505@gmail.com

[2] Electronic information and electrical engineering college, ShangLuo University, 726000 ShangLuo, China, 16563961@qq.com

[3] School of Mechanical Engineering, Northwestern Polytechnical University, Xi'an 710072, China, weijunchao@mail.nwpu.edu.cn

Abstract. In the practice of product design, the efficient control of complexity has increasingly gained importance. The Dependency Structure Matrix (DSM) has proved to be a useful tool for analysing system structure and managing structural complexity. In order to provide a deep insight of system structure in designing Verilog HDL source code artefacts for digital system designers and project managers, the paper proposes a DSM modelling method based on the characteristics of the digital system structural modelling with Verilog and the component dependencies relationship. A DSM modelling example is presented. Result shows that with the DSM model, the source code artefacts can be efficiently analyzed.

Keywords: design structure matrix, modeling, Verilog HDL, digital design

1. Introduction

Verilog-HDL can be used to model and design a digital system in a form of software programming. How to manage the complexity of source code artefacts is an issue for digital designers. Structural considerations are an established approach to manage complexity [1,2]. A digital system can be decomposed into many sub-systems or modules. Relationships between these modules exist. So system analysis is needed.

The DSM[3,4] is a square matrix to identify the dependencies or relationships between components of a system. Components of a system can be parts in a product, tasks of a project, and departments within an organization to be modelled. An n×n DSM has n elements with identical row and column labels and each entry of the DSM represents a particular kind of relationship, such as information flow, force flow, and so on.

In the example DSM in Fig. 1, elements are represented by the shaded elements along the diagonal. An off-diagonal mark signifies the dependency of one element on another. If element clk sends information to or influences the behaviour of element M2, then the (Row clk, ColumnM2) entry of the DSM contains a mark. Of course, we can also use the binary relations 1 and 0 to represent the relationships between DSM elements. Furthermore, other numerical values can present more detailed information,

such as the assessment of importance, rework probabilities, impact of changes, probability of changes, etc.[5]. When a DSM is modelled, it is usually analyzed with clustering algorithms or other algorithms. Through DSMs, valuable insights from the system structure can be derived after examining the interactions within and among the subsystems.

The DSM has been used in many fields, including the software field [5-9]; however, no paper is found to use Dependency Structure Matrices (DSMs) for digital design using Verilog. This paper attempts to introduce the DSM to this field. The focus of the paper is how to model DSMs for Verilog HDL programs from a structural viewpoint without considering technical constraints. A simple analysis of system structure using DSMs is illustrated.

The rest of this paper is structured as follows. Section 2 reviews digital design using Verilog. Section 3 sets up some rules to model the DSM. Section 4 presents an example model. Finally, the paper proposes a conclusion.

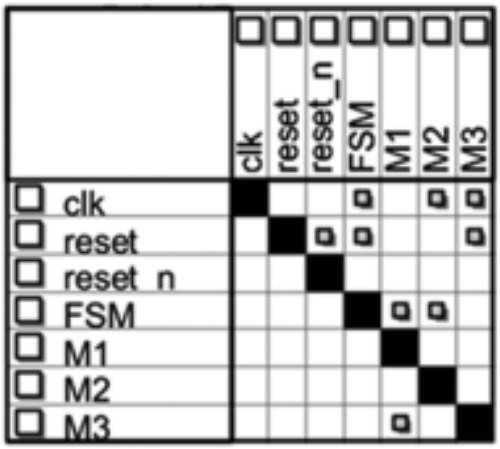

Figure.1 Example DSM

2. Structural Modelling Using Verilog HDL

Digital circuits are composed of interconnected components, such as logic gates and triggers. In most cases of the digital designs, models are used to express the digital circuits and the design work is done using CAD tools. The design using Verilog HDL embodies hierarchical and modular methodology. At every level of a hierarchical design, the efforts focus on the related level, and details of lower hierarchical levels are hidden, thus facilitating the complex design. This methodology helps to reuse the available modules or purchase IP modules. Furthermore, this hierarchical composition makes functional verification easier.

A structural model is composed of 3 kinds of object instances [11]: 1) built-in primitives(and, or, xor, etc); 2) user defined primitives (UDP, such as mux4); and 3) designed modules.

Instantiation refers to the formation of a high-level Verilog module by connecting low-level logic primitives or modules. The instantiated object is called as instance. The structural modelling process is done using instantiation.

A module is a basic unit in Verilog HDL. It describes the function of a logic entity. The function of a module can be described separately, or through other instances of other modules. That is, a structural

module can include behaviour statements (such as always), continuous assignment statements (assign), build-in primitives, UDPs and other modules, or a combination of these objects. In this sense, a module describes a structure and behaviour of a hardware block in the form of software. A module includes ports as interfaces to exchange information with external environment. From a systematic and structural viewpoint, ports of a module can stand for this module.

3. DSM Modelling for Digital Designs Using Verilog

For a digital system design using Verilog, the source code is a kind of design artefacts. Components of this artefact can be module instances described above or other objects of interest, such as reg variables, wire variables, or always blocks. These components can be considered as elements of a DSM and relationships between these elements are defined by signal interaction or logical dependency.

The DSM modelling procedure consists of three major steps:

Step 1: choose components of digital system according to the hierarchy level.

Step 2: represent these components in a DSM. For a Verilog module instance, its port signal set stands for the module itself as a "macro" DSM element; for a block, a set of variables interacting with the outside of the block represent the block itself as a DSM element; a variable can be directly placed in the DSM.

Step 3: build up relationships between these elements in the DSM. These relationships depend on interface signal interactions or logical dependencies.For example, a variable on the left-hand side of an assignment statement depends on variables on the right-hand side.

4. Example

Fig. 2 shows a portion of FPGA-based functions of a certain control card. There are several instantiated modules:

1) SDAC

M1(.StartDAC(StartSDAC), .DAC_Addr(SDAC_addr), .DAC_Data(SDAC_data), .DAC_Clk(clk_20M), .DAC_SCK(SDAC_sclk), .DAC_SDO(SDAC_sdo),

.DAC_CSn(SDAC_cs)); // serial DAC module

2) M_PWM M2(.Clk(clk),.PWM_En(PWM_en),.count1(count1),

.Count2(count2),.Q_PWM(pwm)); // PWM module

3) Generator20M M3.clkin(clk), .clkout(clk_20M), .reset(reset));

And there is a finite state machine as a block:

```
always @(negedgeclkor posedgereset )
begin
        ……
End
```

In addition, there is an assignment statement about nets reset_n and reset:

assign reset_n = !reset;

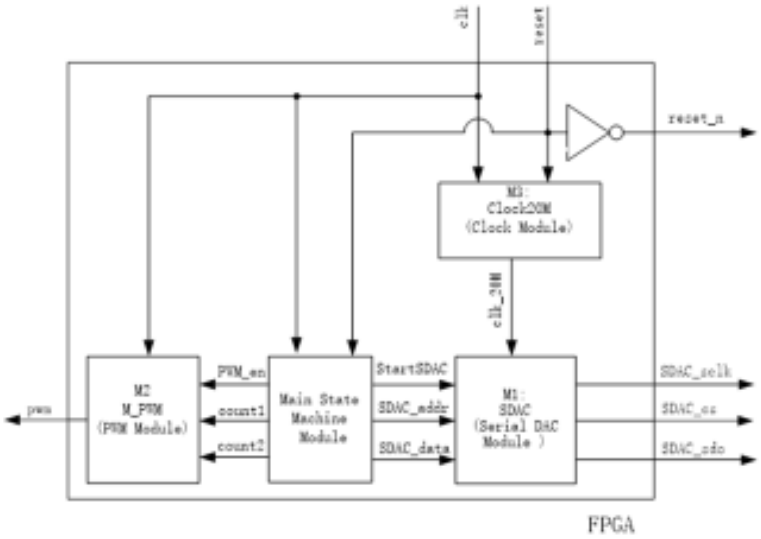

Figure.2 System Composition and Module dependency in the example

These three instantiated modules, the finite state machine block and variables reset_n and reset are chosen as elements for DSM elements. The DSM for these digital system can be obtained, as shown in Fig. 3. From this model, it is shown that the net reset_n depends on the net reset. The behaviour of the finite state machine is dependent on the net clk and reset. All these relationships between elements are obviously signified by marks. If a condensed model is needed, interface signals for modules or the block can be hidden and only element names and relationships between these elements are preserved (see Fig. 1). However, many details are lost in this condensed version.

A simple analysis of artefact architecture is degree analysis of elements [12]. For example, clk and reset have high out-degrees, so these two elements have more impacts on others while M1 and M2 have no impact on others.

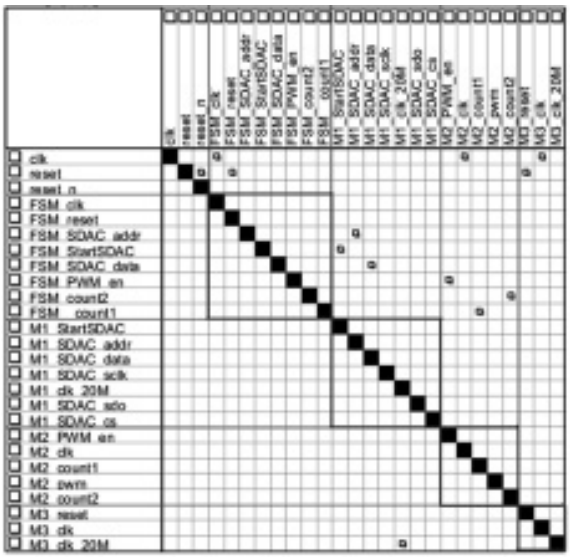

Figure.3 DSM modeling for the system in Fig. 2

5. Conclusion

DSMs can reveal the relationships between components in a system in a concise way and provide designers with insight into the system. This paper set up some rules about building up DSMs for digital design usingVerilog-HDL. With the DSM model, the source code artefacts can be efficiently analyzed.

References

[1] Lindemann U., Maurer M. & Braun T., Structural Complexity Management - An Approach for the Field of Product Design.Berlin :Springer, 2009.

[2] Biedermann,W.&Lindemann,U., On the applicability of structural criteria in complexity management.18th International Conference on Engineering Design, ICED 11, Copenhagen, Denmark, pp.11-20, 2011.

[3] Steward,D. V., The design structure system: A method for managing the design of complex systems. IEEE Transactions on Engineering Management, 28(3).pp.71 – 74, 1981.

[4]Browning,T.R., Applyingthedesignstructurematrixtosystemdecompositionandintegrationproblems:a reviewandnewdirections. IEEETransactionsonEngineeringManagement,48(3),pp.292 – 306,2001.

[5] Lee, W.-T.,Hsu, K.-H.&Lee, J., Designing Software Architecture with Use Case Blocks using the design structure matrix,2012 International Symposium on Computer, Consumer and Control,Taichung, Taiwan.pp.654-657, 2012.

[6]Sangal, N., Jordan, E., Sinha, V. &Jackson, D.,Using Dependency Models to Manage Complex Software Architecture. 20th Annual ACM Conference on Object-Oriented Programming, Systems, Languages, and Applications, San Diego, CA, United states. pp. 167-176, 2005.

[7]Sosa, M. E., Browning, T.&Mihm, J., Studying the dynamics of the architecture of software products.2007 Proceedings of the ASME International Design Engineering Technical Conferences and Computers and Information in Engineering Conference, Las Vegas, NV, United states.pp. 329-342,2007.

[8]LaMantia, M. J.,Cai, Y.,MacCormack,A.D.&Rusnak, J.,Analyzing the Evolution of Large-Scale Software Systems using Design structure matrices and design rule theory, 7th IEEE/IFIP Working Conference on Software Architecture, WICSA 2008 , Vancouver, BC, Canada .pp. 83-92 ,2008.

[9]Mirson, A.,Skrypnyuk, O.,Elezi, F.&Lindemann, U.,MDM-based software modularization by analysing inter-project dependencies, 13th International Dependency and Structure Modelling Conference, Cambridge, MA, United states.pp.143-157, 2011.

[10] Ashenden,P. J. ,Digital Design: an embedded systems approach using verilog. Morgan Kaufmann Publishers,2007.

[11] Cavanagh, J., Verilog HDL: Digital Design and Modelling.CRC Press,2007.

[12] Sosa, M. E., Eppinger, S. D., and Rowles, C. M., 2007, "A Network Approach to Define Modularity of Components in Complex Products," ASME J. Mech. Des., 129(11), pp.1118 – 1129.

Author Brief and Sponsors

Xing Xue, She received Master degree in School of Management from Xi'an University Of Architecture And Technology, Xi'an, China, in 2009. Now she works at ShangLuo University. Her current research interests include information management and information process.

This work was supported by Natural Science Foundation of Shangluo City of Shaanxi Province of China and ShangLuo University (project no.sk2014-01-21, sk2014-01-16)

An Improved Universal Evidence Combination Method

Yongchao Wei

Department of Research of Civil Aviation Flight University of China

Guanghan 618307, China, email:mylife001@126.com

Abstract. The Dempster-Shafer evidence combination method will appear inconsistent conclusions for the conflict evidence. One new universal evidence combination method was proposed. According to the concept of the Pearson correlation coefficient. Evidence distances which represent the conflict degree were calculated, and then the weight coefficient were further converted. The evidences probability were redistributed by using the weight coefficient. Finally, the improved synthesis rule was used to the evidence combination. The examples results show that the algorithm has strong versatility and stability in the evidences combination, can be applied to information fusion, uncertain information decision-making and other fields.

Keywords: Evidence combination, conflict , weight , evidence pretreatment

1. Introductiong

DS evidence theory is first proposed by Dempster in the 1960s and further developed by Shafer, and is a theory of reasoning belonging to artificial intelligence areas. As a method of uncertainty reasoning, DS evidence theory provide a natural and powerful way for the expression and synthesis of uncertain information, within the framework of the basic assumptions for the power set of the collection, it can make full use of the probability distribution function, likelihood function and other functions to describe and deal with uncertain information, so get a wide range of applications in information fusion and uncertain reasoning [1-3].

When a large inconsistency or conflict between the evidences, DS evidence combination method can not be used or the results obtained from which may be odds with reality. How to achieve effective multi-source information fusion on high degree of conflicting evidences is the current hot research, a variety of conflicting evidences combination methods are proposed [4-9]. By studying them, the overall synthesis rules can be divided into two broad categories: modified the rules of synthesis methods and the ways to modify the original evidences.

Single conflict evidence synthesis method has its limitations, so, this paper presents one evidence combination method by the fusion of pre-integration rules and synthetic methods modified. First, by converting the Pearson coefficient into weights of evidence, and thus be used to modify the source; and then the modified rules are further used for combination. Experimental results show that the new method can quickly get the proper results of the normal or conflict evidences, and has good adaptability, reliability and fast convergence rate.

2. Ds Theory

In the DS evidence theory [9,10], the identification framework Θ of fusion system contain N complete incompatible assumption propositions, its power set P(Θ)=2Θ={A1, A2, A3⋯A2N}.. Evidences E1, E2, E3。。。En. The basic probability distribution functions respectively are m1, m2, m3⋯mn.

$$\sum_{A\in P(\Theta)} m(A)=1\ ,\quad m(\Phi)=0\ ,\quad m(A)\geq 0 \tag{1}$$

The corresponding Dempster combination rule is:

$$\begin{cases} m(A)=\dfrac{1}{1-k}\sum\limits_{\bigcap A_j=A}\prod\limits_{1\leq i\leq N} m_i(A_i) \quad for\ A\neq\Phi \\ m(\Phi)=0 \end{cases} \tag{2}$$

Where, k is the conflict factor, which reflects the conflict degree between the evidences.

$$k=\sum_{\bigcap A_j=\Phi}\prod_{1\leq i\leq N} m_i(A_i) \tag{3}$$

In the Dempster combination rule, k is a coefficient measuring the conflict level between the evidences. If k = 1, we can not use the Dempster combination rule for information fusion; and when k $\rightarrow$ 1, the combination results of a high degree conflict evidences is inconsistent with the actual processing. Conflict is also a kind of information, the extraction and analysis of them, and being added into the combination rules, one new combination method can be got.

3. New Combination Method

New method fuses evidence pre-processed and synthetic rules modified. According to the principles of conflict information available, weights of evidences can be obtained from the Pearson coefficient, the more collision with other evidences, the smaller its weight. Then the modified combination rules are used to fuse weighted evidences.

3.1 Pearson Correlation Coefficient

Pearson correlation, also known as product-moment correlation (or product-moment correlation) is a linear correlation proposed by Pearson of British statistician in the 20th century [11]. Suppose there are two variables X, Y, and then the Pearson correlation coefficient of the two variables can be calculated by the following formula:

$$\rho_{X,Y}=\frac{\mathrm{cov}(X,Y)}{\sigma_X\sigma_Y}=\frac{E((X-\mu_X)(Y-\mu_Y))}{\sigma_X\sigma_Y} \tag{4}$$

Where E is the mathematical expectation, cov is the covariance.

$$\mu_X=E(X) \tag{5}$$

$$\sigma_X^2=E(X^2)-E^2(X) \tag{6}$$

Pearson correlation coefficient is one measurement of the degree between two variables. Its value is in a range from -1 to 1, where 1 indicates perfect positive correlation, 0 independent, and -1 indicates a

perfect negative correlation.

3.2 Weight

Step1: According to (4), calculate the Pearson coefficient p(E1, E2) between the evidence E1, E2;

Step2: The sum of the Pearson coefficient of the evidence Ei is defined as:

$$\delta(E_i) = \sum_{j=1, j\neq i}^{n} p(E_{i,} E_j) \tag{7}$$

Step3: Ec is the center evidence, if it is satisfy with the (8):

$$\delta(E_c) = \max_{1\leq i\leq n}(\delta(E_i)) \tag{8}$$

Step4: The weight wi of evidence is defined as:

$$w_i = \delta(E_i) / \delta(E_C) \tag{9}$$

3.3 Modified Combination Rules

The weight of the evidence source is wi, wi $\in$ [0,1], the combination rules of the weighted basic probability assignment are inheritance from [12], following steps below.

Step1: Calculating all the weights based on algorithm above, the weight vector W = (w1 , w2 , ⋯, wn)

Step2: According to (10), the probability of the evidence will be re-allocated.

$$m_k^{'}(A_i) = \begin{cases} w_k * m_k(A_i) & A \neq \Theta \\ 1 - \sum_{A_i \neq \phi} w_k * m_k(A_i) & A = \Theta \end{cases} \tag{10}$$

Step3: Calculate the conflicting value k and the average level supporting proposition q(A), which are defined as below.

$$k = \sum_{i,j:A_i \cap A_j = \Phi} m_1^{'}(A_i) m_2^{'}(A_j) \tag{11}$$

$$q(A) = \frac{1}{n} \sum_{i=1}^{n} m_1^{'}(A_i) \tag{12}$$

Step4: Substituting the new probability distribution into the following formula to calculate the synthesis results.

$$\begin{cases} \tilde{m}(A) = \sum_{i,j:A_i \cap A_j = A} m_1^{'}(A_i) m_2^{'}(A_j) + k \bullet q(A) & A \neq \Phi, \Theta \\ \tilde{m}(\Phi) = 0 \\ \tilde{m}(\Theta) = 1 - \sum_{A \in \Theta} \tilde{m}(A) \end{cases} \tag{13}$$

4. Experiments Results and Analysis

Through the analysis results of normal and conflict evidences situations, this section will verify the validity of the new method. Suppose $\Theta = \{ a , b , c\}$.

4.1 Normal Data

Table 1 Focal Elements Distribution

Evidence	Propositions		
	a	b	c
m1	0.90	0	0.10
m2	0.88	0.01	0.11
m3	0.5	0.20	0.30
m4	0.98	0.01	0.01
m5	0.90	0.05	0.05

Table 1 is the source of evidence for the normal data, there is 5 groups. Seen from Table 1, the artificial reasoning synthesis results should be a.

Table 2 Combination Results

Algorithm	Evidences			
	m_1, m_2 K=0.1970000	m_1, m_2, m_3 K=0.6007000	m_1, m_2, m_3, m_4 K=0.6118870	$m_1, m_2, m_3, m_4 m_5$ K=0.6507264
Dempster	$m(a)$=0.9863014 $m(b)$=0 $m(c)$ = 0.0136986 $m(\Theta)$ = 0	$m(a)$=0.9917355 $m(b)$=0 $m(c)$ = 0.0082645 $m(\Theta)$ = 0	$m(a)$=0.9999150 $m(b)$=0 $m(c)$ = 0.0000850 $m(\Theta)$ = 0	$m(a)$=0.9999953 $m(b)$=0 $m(c)$ = 0.0000047 $m(\Theta)$ = 0
Yager[13]	$m(a)$=0.7920000 $m(b)$=0 $m(c)$ = 0.0110000 $m(\Theta)$ = 0.1970000	$m(a)$=0.3960000 $m(b)$=0 $m(c)$ = 0.0033000 $m(\Theta)$ = 0.6007000	$m(a)$=0.3880800 $m(b)$=0 $m(c)$ = 0.0000330 $m(\Theta)$ = 0.6118870	$m(a)$=0.3492720 $m(b)$=0 $m(c)$ = 0.0000017 $m(\Theta)$ = 0.6507264
SUN[14]	$m(a)$=0.8930454 $m(b)$=0.0005677 $m(c)$ = 0.0229211 $m(\Theta)$ = 0.0834658	$m(a)$=0.6591065 $m(b)$=0.0242335 $m(c)$ = 0.0621528 $m(\Theta)$ = 0.2545073	$m(a)$=0.6754816 $m(b)$=0.0193952 $m(c)$ = 0.0458762 $m(\Theta)$ = 0.2592470	$m(a)$=0.6612917 $m(b)$=0.0202513 $m(c)$ = 0.0427544 $m(\Theta)$ = 0.2757027
WEI[15]	$m(a)$=0. 96733 $m(b)$=0. 0009850002 $m(c)$ = 0. 031685 $m(\Theta)$ = 0	$m(a)$=0. 8215649 $m(b)$=0. 01044716 $m(c)$ = 0. 06840459 $m(\Theta)$ = 0. 0995834	$m(a)$=0. 8478351 $m(b)$=0. 006129951 $m(c)$ = 0. 03761158 $m(\Theta)$ = 0. 1084234	$m(a)$=0. 8511387 $m(b)$=0. 007711634 $m(c)$ = 0. 02205105 $m(\Theta)$ = 0. 1190986

PAPER	*K=0.197* *m(a)=0. 96733* *m(b)=0. 000985* *m(c) = 0.031685* *m(Θ) = 0*	*K=0.5970444* *m(a)=0. 8523845* *m(b)=0. 04143542* *m(c) = 0.1043324* *m(Θ) = 0.00184768*	*K=0.60431695* *m(a)=0. 8853891* *m(b)=0. 03264323* *m(c) = 0. 0777387* *m(Θ) = 0. 0042289*	*K=0.641591966* *m(a)=0. 889182* *m(b)=0. 03395038* *m(c) = 0. 07212327* *m(Θ) = 0. 0047443*

From table 2, the supporting degree of evidence a increase with the increase of data in normal circumstances, Dempster, Wei[15] and the algorithm are faster speed convergence to a, and get the correct integration results. As evidence increasing, the unknown results of Yager [13], Sun [14] and Wei [15] increase, the uncertain results of the algorithm are far less than the above three algorithms, and close to zero. The overall analysis being seen in the data source of evidence under normal circumstances, Dempster, Wei [15] and the algorithm can get the correct the synthesis results, but our algorithm has the highest reliability.

4.2 Conflicting Data

Table 3 Conflicting Data

Evidence	**Propositions**		
	a	*b*	*c*
m_1	0.98	0.01	0.01
m_2	0	0.01	0.99
m_3	0.90	0	0.10
m_4	0.90	0.01	0.10

Tables 3 are the conflicting evidences of 4 groups, from the artificial reasoning, when there are only two groups evidences, the synthesis results should be c, but as the number of evidences increases, the end result should be a. evidence 2 is highly conflicts with other evidences.

Table 4 Combination Results

Algorithm	**Evidences**		
	m1, m2	*m1, m2, m3*	*m1, m2, m3, m4*
Dempster	*k=0.99* *m(a)=0* *m(b)=0.01* *m(c) = 0.99* *m(Θ) = 0*	*k = 0.99901* *m(a)= 0* *m(b)=0* *m(c) = 1* *m(Θ) = 0*	*k = 0.999901* *m(a) = 0* *m(b)=0* *m(c) = 1* *m(Θ) = 0*
Yager[13]	*k=0.99* *m(a)=0* *m(b)=0.0001* *m(c) = 0.0099* *m(Θ) = 0.99*	*k = 0.99901* *m(a)= 0* *m(b)=0* *m(c) = 0.00099* *m(Θ) = 0.99901*	*k = 0.999901* *m(a) = 0* *m(b)=0* *m(c) = 0.000099* *m(Θ) = 0.999901*

SUN[14]	*ε= 0.3716* *m(a) = 0.18* *m(b) = 0.004* *m(c) = 0.194* *m(Θ) = 0.622*	*ε= 0.512* *m(a) = 0.321* *m(b) = 0.003* *m(c) = 0.188* *m(Θ) = 0.488*	*ε= 0.604* *m(a) = 0.42* *m(b) = 0.003* *m(b) = 0.181* *m(Θ) = 0.396*
WEI[15]	*k = 0.99 ,* *m(a) =0.4851,* *m(b) = 0.01* *m(c) =0.5049* *m(Θ) = 0*	*k=0.48251* *m(a)=0.7589* *m(b)= 0.0019* *m(c)=0.1119* *m(Θ) = 0.1272*	*k = 0.44651* *m(a) =0.8341* *m(b) = 0.0012* *m(c) =0.0599* *m(Θ) = 0.1048*
PAPER	*k = 0.99* *m(a) =0.4851,* *m(b) = 0.01* *m(c) =0.5049 ,* *m(Θ) = 0*	*k = 0.152* *m(a) =0.9337065* *m(b) = 0.0005023976* *m(c)= 0.0145743* *m(Θ) =0.0512168*	*k = 0.099* *m(a) =0.9683049* *m(b) =0.000206358* *m(c) =0.002402914* *m(Θ) =0.02908585*

From the combination results of tables 4 for the conflict evidences, we can see that Dempster and Yager [13] algorithms do not apply to conflicting evidences combination; Sun [14] algorithm although can be used for the conflict evidences combination, the distribution of precision is not enough, the convergence is slow , the value of uncertain results are high, and as the evidences increasing, the uncertainty value did not significantly reduce, and can not get the recognition results; Wei [15] and our algorithm can get the correct results, and both have reduced the level of conflict, our algorithm fully consider the credibility of evidence and other global information, which greatly reduces the level of conflict between the evidences, and thus minimize the interference of conflicting evidences on the combination results, with a strong anti-interference ability. From Table 4, we can see that the algorithm can have a good decision with three evidences. From the test results, we can also see that, as evidence of supporting a increases, the value of m (a) steadily improves, the uncertainty recognition results are almost zero, and which indicate that our algorithm has high reliability. So, our algorithm can solve the conflict problems in the evidence synthesis, and has the best advantage compared to other algorithms.

5. Conclusion

For the combination of conflict evidences, with the combined advantages of evidence pre-processing and modified combination rule, one new algorithm was proposed. By firstly using the Pearson coefficient for the pretreatment the source evidences, and then the modified rules for the combination. Algorithm not only solves the conflict problem of evidence synthesis, but also has high versatility and robustness, and will have some practical value in engineering applications.

Acknowledgment

This work was supported by the Specialized Research Fund for National Natural Science Foundation of China (Grant No. U1633127).

References

[1] Dempster A P.Upper and Lower Probabilities Induced by a Multi-valued Mapping[J].Annual Mach Statist,1967,38(4):325-339.

[2] Yang J B.Singh M G.An evidential reasoning approach for Multiple-attributed decision making with uncertainty[J].IEEE Transaction on System,Man and Gybernetics,1994,24(1):1-18.

[3] Yang J, Sen P. A general multi level evaluation process for hybrid MADM with uncertainty [J]. IEEE Trans. on System, Man and Cybernetics, 2006, 36 (10) :1458-1473.

[4] Guo Huawei,Shi Wenkang, Deng Yong, etal. Evidential conflict and its 3D strategy: discard, discover and disassemble[J].Systems Engineering and Electronics,2007,29(6):890-898

[5] Guo Hua-wei, Shi Wen-kang,Liu Qinf-kun etal. A New Combination Rule of Evidence[J].Journal of Shanghai Jiaotong University. 2006,40(11):1895-1900

[6] Li jia Xu, Yangzhou Chen, Pingyuan Cui. Improvement of D-S evidential theory in multi-sensor data fusion system[C] // Proc. of the 6th World Congress on Intelligent Control and Automation , 2004 :580-589.

[7] Smet P.The combination of evidence in the transferable belief model[J].IEEE Trans.On Pattern Analysis and Machine Intelligence,1990,12(5):447-458.

[8] Chen Yi-leng, Wang Jun-jie. An improved method of DS evidential reasoning[J].Acta Simulata Systematica Sinica. 2004,16(1):28-30

[9] Liu W. Analyzing t he degree of conflict among belief functions[J] . Artificial Intelligence, 2006 ,170 (11) :909-924.

[10] Liu Tong-ming, Xia Zu-xun, Xie Hong-cheng.Data Fusion and its Application[M].BeiJing. National Defense Industry Press. 1998, 20-160.

[11] J. L. Rodgers and W. A. Nicewander. Thirteen ways to look at the correlation coefficient[J]. The American Statistician, 1988.42(1):59 – 66.

[12] Li Bi cheng, Wang Bo, Wei Jun etal. An efficient combination rule of evidence theory[J]. 2002,17 (1):33-36

[13] Yager R R. On the dempster-shafer framework and new combination rules [J] . Information Sciences ,1987 , 41 :93-137.

[14] Sun Quan, Ye Xiu qing, Gu Wei kang. A new combination rules of evidence theory[J].Chinese Journal of Electronics 2000, (8):117-119.

[15] WEI Yong-chao. An Improved DS evidence combination method baded on KL distance[J]. Telecommunication Engineering.2011,51(1)27-30.

Review on RFID Identity Authentication Protocols Based on Hash Function

Yang Bing[1,a], Liu Baolong[2,b] and Chen Hua[3,c]

[1,2,3] School of Computer Science and Engineering, Xi'an Technological University,

Xi'an 710021, China,

Email:[a]1769579475@qq.com,[b] 24503148@qq.com

Abstract. Radio frequency identification (RFID) is one of the key technologies of Internet of Things, which have many security issues in an open environment. In order to solve the communication problem between RFID tags and readers, security protocols has been improved constantly as the first choice. But the form of attack is also changing constantly with the development of technology. In this paper we classify the security protocols and introduce some problems in the recent security protocols.

Keywords: RFID, protocol, Hash, authentication, attack

1. RFID System Introduction

Radio Frequency Identification (RFID) is a non-contact automatic identification technology, it uses Radio Frequency signal to complete the automatic identification to obtain relevant information of target acquisition, at the same time complete the exchange of information among the target objects, having a wide range of applications among Internet of things. RFID is widely used in the fields of access control, logistics, monitoring, tracking, anti-counterfeiting, identification, security, military, and medical treatment because of its non-contact, fast identification of moving objects, high identification efficiency, can work in harsh environment and convenient operation and so on, But at the same time caused a lot of security issues.

A typical radio frequency identification system consists of a reader (Reader), a tag (Tag), and an antenna (antenna), as shown in Fig.1. In the physical configuration, the tag consist of the RFID front end, the antenna, identity information, the digital baseband for storing information and processing protocols, As a result, the tag can store identity information, usually placed on objects that require authentication. Reader and tag communicate through the radio interface with the background database connection. In the RFID system, the implementation of the label data is the key to information retrieval, we can obtain the label information in the back-end database to understand the special information of the product. The product information needs certification, logistics records and key information management can be saved in the end database.

There are two main defense methods in the face of RFID system security issues: passive detection (physical methods) and active defense (security protocol). As passive detection reduces the utilization

of tags, there are some difficulties to implement, so some active security mechanisms (security authentication protocols) are preferred. The second part introduces the attack model and security requirements of the RFID system. The third part introduces the classical security protocol of the RFID system. The fourth part introduces the research status of the classic protocol. The last part is the summary.

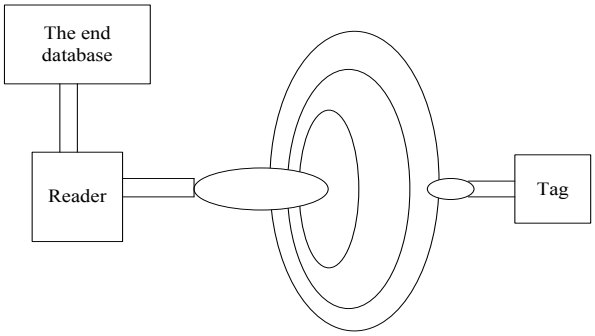

Figure.1 RFID system

2. RFID Attack Model and Security Requirements

2.1 Attack Model Introduction.

RFID systems are vulnerable to suffer attack of various forms, because RFID readers and tags transmit information by wirelessly. RFID security protocols as a solution to security threats, the various forms of attack will be introduced firstly.

● ***Personate Attack.*** A clone tag attack that allows the reader to believe that the received data is from a legitimate tag. An attacker can create an authenticated tag through entering the appropriate format data in a blank tag.

● ***Replay Attacks.*** An effective data transfer is recorded by the attacker and maliciously repeated or sent back between the tag and the reader in an insecure channel between the tag and the reader. Such as a device (not necessarily a tag), masquerading as a trusted entity, and playing back a tag response message to the reader. Another way is to maliciously replay legitimate readers' requery to the tag, aims to retrieve the tag' s private information, in order to avoid this happening, the response of each tag and the reader must be unique in every round.

● ***Tracking Attacks.*** This attack is considered the most important prevention attack which can cause a significant loss of privacy to the label holder. It is easily to be tracked if any information can be connected to a given tag. Thus updating information can prevent such attacks after each successful authentication.

● ***Man-in-the-Middle Attack and Information Disclosure.*** The attacker controls the flow of information by replaying or modifying information between the tag and the reader, at the same time the reader and tag do not detect any anomalies in this attack.

● ***DOS Attacks.*** Similar to tracking attacks, this attack is a major concern in RFID systems. These attacks are easy to achieve, but difficult to prevent. One method is that an attacker maliciously collides with a tag, causing the reader to load more data than they can handle; the other is an attacker blocks

messages that are transmitted between the tag and the reader. The attack could cause desynchronize messages between the tag and the reader.

● ***Forward Attack.*** A system is belong to forward security means the current label response message eavesdropped by the attacker is not linked the previous response message.

2.2 Introduction to security requirements.

In an RFID system, the reader sends a response message received from the tag to the backend database. The database would compare feedback information received from the label, while the database needs to send the news to the label passed the authentication, the label also must carry on the authentication to the database' s identity. In the mutual authentication process, the forgery data must be prohibited from being authenticated. However we must find an effective way to prevent the attacker from modifying the authentication information because the wireless channel between the tag and the reader. In the design of RFID authentication protocol, we must consider the following aspects of the security requirements:

● ***Confidentiality.*** Electronic tags can only send messages to valid readers and can not reveal any valuable information to attackers during system operations. Once the attacker has access to valuable information, the identity of the label information may be leaked. Therefore, a complete RFID security solution must be able to ensure that the information contained in the label can only authorize the reader to access.

● ***Indistinguishability.*** The output value of the tag is required for each authentication is not the same and not directly linked the tag ID value. If an attacker can distinguish a specific output from a target tag, thus the tag can be tracked, that is so-called the anonymity of the tag.

● ***Authenticity.*** It refers to the prohibition of false electronic tags to deceive the reader or server.

● ***Forward Security.*** If an attacker obtains the privacy information of the tag, the tag cannot be tracked. That is, although the adversary obtains the tag' s output information but couldn' t contact the previous round of information.

● ***Efficiency.*** Though efficiency is not included in the security requirements, passive tags in the protocol need to operate hash function XOR operation and so on. Thus efficiency is a necessary factor to consider in the design of security protocols.

3. Introduction to Classic Security Protocols

3.1 Hash—lock protocol.

Hash-lock protocol [2] is proposed by Sarma et al. in order to avoid information disclosure and tracking, in which use meta ID to replace the real tag ID, the protocol flow shown in Figure.2. In this protocol, the tag does not have a dynamic refresh mechanism and the meta ID remains unchanged during the authentication process, further more the tag ID is transmitted in plain text over an unsecured channel. Thus Hash-lock protocol is vulnerable to fake attacks, replay attacks and tracking -positioning attacks.

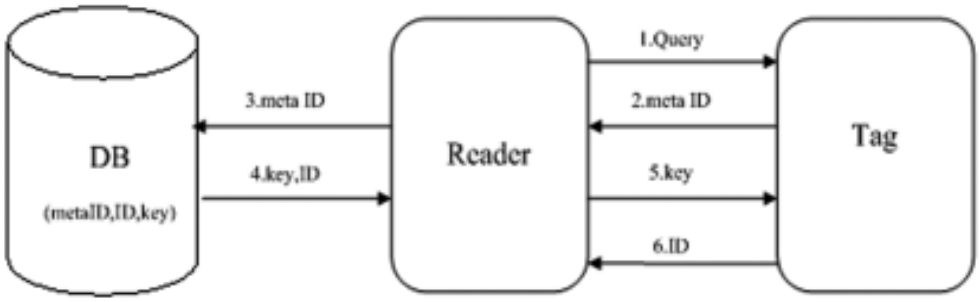

Figure.2 Hash—lock protocol

3.2 Randomized Hash—lock protocol.

In order to solve the problem of position tracking in Hash-lock protocol, Weis et al proposed Randomized Hash-lock protocol [3], using query-reply mechanism of the random number, the protocol flow shown in Figure.3. In this protocol, a pseudo-random number generator is used to increase the amount of label operation within the allowable range of label cost. Tag ID remains unchanged, and the plaintext is still sent between the tag and the reader, causing this protocol is vulnerable to counterfeit attacks, replay attacks, were tracking attacks. In order to validate each tag, the reader must effectively compute the hash value of the each tag ID stored in the back-end database, the resources consumed by the whole authentication process are huge, it is easy to cause DOS attack, and does not apply to a large number of label attestation.

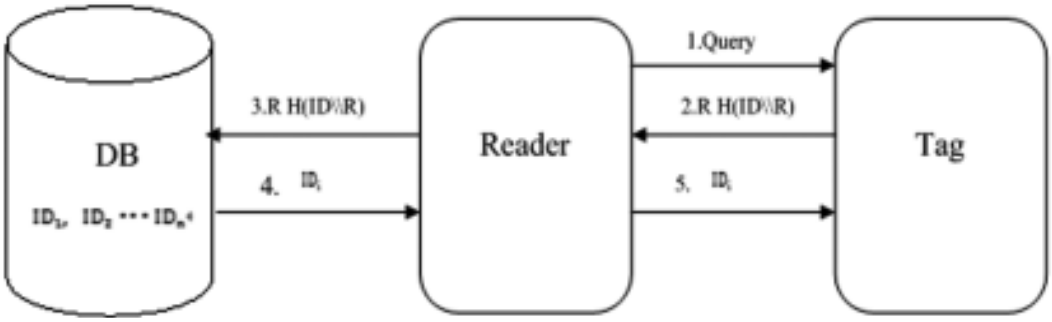

Figure.3 Randomized Hash—lock protocol

3.3 Hash—chain protocol.

Hash-chain protocol [1] is proposed by Ohkubo et al., which is also based on the challenge-response mechanism, the protocol flow shown in Figure.4. Tag and the back-end database share an initial secret value. The protocol resolves the forward security problem when the reader sends an authentication request to the tag, and the tag sends a different response. But in the protocol only reader authenticate the identity of the tag, the tag does not authenticate the identity of the reader, so it is vulnerable to personate attacks and replay attacks. Meanwhile Back-end database' s search work is huge, for each round needs to look up $m \times n$ times, where m is the chain length, n is the number of ID. And ID space is large under normal circumstances, such as up to 128 bits. To ensure randomness, where m should be large enough, as a result it is easily to lead DOS attacks.

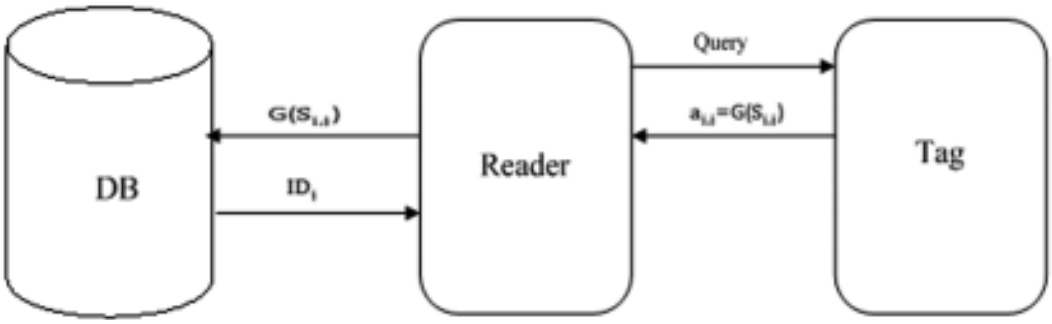

Figure.4 Hash—chain protocol

4. Research Status of Security Protocols

The existing security protocols are divided into four categories, the first type proposed improved protocol respectively security protocol based on the shortcomings of Hash-lock protocol for the study, which also divided into four specific cases, the first section summarized respectively; next type proposed protocol based on the shortcomings of the Randomized Hash-lock protocol; the third type proposed improvement protocol based on Hash-chain protocol; the last type is based on the above three basis protocol, taking into account the safety and efficiency and cost of the label factors fully, proposed comprehensive protocol. The following will be introduced respectively.

4.1 Security protocols based on Hash - lock protocol.

For the shortcoming of the Hash-lock protocol, Lee [15] proposed protocol keep using meta ID instead of the real tag ID value in the original protocol, meanwhile using semi-random access control (SRAC), which provides mutual authentication and good security to prevent tracking attacks, fake attacks, DOS attacks, but in the case that the attacker eavesdropped and playback Meta ID, tags can also be successfully authenticated by legitimate readers, thus the protocol does not have anti-replay attacks. Subsequently, a low-cost RFID authentication protocol (LCAP protocol) was proposed in [14], which uses the challenge-response scheme to ensure the positional privacy of the tag holders. However, if the attacker eavesdropped the current label response, message could be inferred the previous message tags responded and sent, and the protocol cannot provide forward security. Choi et al. [17] proposed an improvement scheme based on the protocol [14] in which the labels are grouped and the back-end database is assigned to each group index also saved in the tag. The shared key and an initialization value and the like are stored in the tags and database.

This protocol does not reveal the tag’s privacy information, using random numbers and counter variables to ensure location privacy, anti-trace attack and impersonation attack, but it is not completely safe. The attacker can derive the previous response information by tapping the response message of the current label, so it doesn’t provide forward security. In [18], an improved scheme is proposed by Choi et al. Taking account into forward security and synchronization attacks, it provides forward security but doesn’t authenticate the reader identity regretful.

One improvement protocol is a serverless system and the two entities involved in authentication are tags and readers. Tan et al. [8] pointed that if the reader and the back-end database couldn’t create a secure and continuous network connection, RFID systems would not be used, if that will limit the application

of RFID systems in remote areas. Thus a server-free security authentication protocol is proposed. In which the back-end database is used as the certification authority (CA) to write the label's secret value into the tag and initialize it, and the reader must obtain authorization from the CA to access a specific set of tags. As well each legitimate reader downloads the authenticated access table from the CA. This protocol is not a strict authentication protocol and cannot guarantee the anonymity of the tag ID, because the communication between the reader and the CA is considered to be secure.

In the references [10,11,12] proposed some protocols based on the Tan et al. Protocol and successfully resist major attack models, including tracking, eavesdropping, and clone attacks. In the scheme [10, 11] achieved mutual authentication and symmetric key setting are implemented, but symmetric key may cause other problems. In scheme [11], the reader and the tag share the key in other states, and the reader identifies the tag with a random number, meanwhile dynamic information must be synchronized between the reader and the tag in order to successfully operate the system. In this case, an attacker can initiate a asynchronous attack to break the synchronization and face the problem of asynchronization.

At the same time, Ha et al. [19] also proposed a serverless security authentication protocol, each tag needs to maintain a state parameter SYNC, that is, the state protocol, but it is well known that the security protocol in RFID is stateless, , each tag and reader does not need to maintain any status information, and the management of the status values in the tags is cumbersome in the communication session. For example, the attacker will be very easy to get the label to protect privacy information after the label's calculation error will change the SYNC value. In this case, the attacker can re-set the state value to 0 when the tag in the session does not successfully end the communication, causing the tag to not work properly. The protocol has a forward privacy threat, and the protocol's security depends on the tag ID during the update session to provide the forward privacy service. Two kinds of attack means are listed in the reference [20] aimed at protocol [19], can destroy its forward privacy, an improved stateless value is proposed in addition, but it is also a serverless security protocol.

One kind of improved scheme is just to consider the forward security. In reference [9], the back-end database and the label share the shared key. The reader only transmits the tag and the back-end database. The tag ID value is not updated, but the key value is updated after each successful authentication.

Other improved scheme does not consider the synchronization problem. In reference [4, 5, 6], some improved methods based on Hash-lock protocol are proposed. The new protocols avoid the tracking attack when the reader accesses the tag receive different response message every round. There are still security flaws. For example, the label ensures the cost and security, but it is not a good solution to the synchronization problem of the label and database in reference [6].

4.2 Security protocols based on Randomized Hash—Lock protocol.

Because of its practicality, there are rarely improved protocols based on Randomized Hash-Lock protocol. The practicality is that the mutual authentication process is completed by only two exchanges of information. Compared other security protocols, mutual authentication cannot be completed by two exchanges of information, at least three to four steps are required to exchange information, and just only one-sided authentication is required such as Tan et al. [8]. Compared to reference [16] maintains the previous authentication step, only transmits the tag ID value to the original protocol in the last step. The improved protocol adds a hash function to the reader and the transmitted message is a hash function consisting of random number and tag ID value, this improved security significantly but at the

same time have high memory consumption, just for only for small networks. Future research may look for a scheme that keeps authenticating each other during the communication process, not just at the beginning of the session, since the authenticated tag is unlocked and its risk of being deceived by the reader can be significantly reduced.

4.3 Security protocols based on Hash—chain protocol.

ID tag in the Hash-chain protocol is dynamically updated, also known as dynamic ID authentication protocol. For it does not authentication the identity of the reader, so this is vulnerable to personate attacks and replay attacks and its back-end database search work is huge and other shortcomings. Thus reference [24] combined with three-way handshake agreement, proposed to create a two-way authentication method serial number in the communication time to encrypt information, but the agreement belongs to the serverless system.

Reference [13] pointed out that Luo et al.' s protocol used two hash functions to update the key value. The reader only communicated the communication between the tag and the back-end server, and almost omitted the reader in the protocol. The counter will also increment the tag value after each round of authentication. When the server sends a request for authentication to the tag, the tag responds to the counter, the counter hashes and the shared key, after the backend server verifies that the random number of sessions is used as the encryption key. However if the count value of one tag is significantly different from the count value of the surrounding tag, the attacker can track the tag according to the count value of the tag in this protocol. In addition if the attacker sends a query request to the tag and the count and key values of the tag are not changed by a valid server, the tag would respond to the same value and attacker can track this tag. Or if an attacker listens to a second session and changes the response value, it is considered to be valid by the tag, and then the tag responds with a message sent by the attacker to the reader. The reader surely cannot decrypt the message. If a lot of tags are attacked, the protocol would suffer DOS attack. At the same time it also analyzed the protocol of Lee et al. specific about the attacker' s personate tag to send a message to the reader, eavesdrops the random number s sent by the reader to the tag, and changes the value to 0, eavesdrops the tag' s return value, and modifies the sending reader, so the agreement is vulnerable to personate attacks.

There are improved protocol based on Hash Chain protocol In reference [21, 22], for example, reference [22] uses a hash function to approximate the randomness, the protocol does not change the secret value in the hash chain, only a hash function to achieve the dynamic update of the label to reduces the huge amount of queries in the backend database in the original protocol meanwhile its time complexity decreases from $O(m \times n)$ to $O(m+n)$. However, the two protocols only improve the security flaws of the original protocol, but the back-end database has exhaustive search and large number of hash operations in verifying the identity of the tags and readers and the efficiency is not obviously improved, so it is not suitable for large tags to be widely used.

4.4 Comprehensive improvement protocols.

In the design of the protocol, the tag only could bears a lower calculation cost, just including the hash function and the random number operation. so the authentication server part of the protocol undertakes a lot of computation and low efficiency. After studying these protocols, in order to overcome this shortcoming, the researchers have done a lot of work can be divided into three general types.

The first type is about the hash value of the ID and other information sent by the tag [3] and the server can pre-calculate and store the hash value to the backend database. Upon receiving the label response message, the server can find the tag ID stored in itself. In general a protocol requires O (1) computational efficiency to validate a tag, using an efficient hash map instead of traversing all tag ID operations. These protocols have a good reliability and anti-traceability, however an attacker can intercept messages sent from the server and then replay the messages to the tag. By comparing the response messages of the tags, the attacker can track the target tag because the response message is fixed before the successful authentication.

The second type of the improved protocols based on tree, packet and shared key idea in order to overcome the deficiency of tag tracking attacks in the first class, hence these protocols improve the key search efficiency of the server and reduce complexity from linear to logarithm, but these agreements are vulnerable to compromise attacks. Based on the tree protocol, such as reference [24], using the tag as a leaf node in the tree, and the key assigned to the internal node. The server stores all the keys and each tag also stores its own key and the associated key $O(\log N)$ from the leaf node to the root node.

During the authentication process, the tag would respond with a hash of the $O(\log N)$ key and a random number, and the server can verify the root key value of the tag. However, tree-based protocols are vulnerable to compromise attacks because each tag shares a set of keys with other tags in the tree structure. Similarly Group-based protocols are also vulnerable to compromise attacks since each group’ s labels share a single key. For example, in reference [25], the tag shares a protection key with the server, and the tag sends the hash value of the protection key to the server that can calculate the hash value during the authentication process. However the protection key in the protocol is shared in the label is known so it is vulnerable to compromise attacks.

Reference [27] proposed a protocol for passive tags but only consider the forward security, and the label of the agreement is too large, which does not meet the low-cost requirements.

Table 1 Security of different protocols

Security attributes	Personate attacks	Replay attacks	Tracking attacks	DOS attacks	Forward security
literature[1]	✓	✓	×	○	✓
literature[2]	✓	✓	✓	×	○
literature[3]	✓	✓	✓	○	✓
literature[14]	×	×	×	○	×
literature[15]	×	✓	×	×	✓
literature[17]	×	×	×	○	×
literature[18]	✓	○	○	○	✓
literature[19]	○	○	○	✓	×
literature[8]	○	✓	○	✓	✓

×: does not exist ○: partially exist ✓: exist

5. Conclusion

This paper first introduces the attack types and security requirements of RFID system recently, and the three classical protocols including Hash-lock protocol, Randomized Hash—lock protocol and Hash-chain protocol based on Hash function, as well as the problems of these protocols including improved protocol based on classical protocols would be illustrated in Table 1. For these shortcomings, the existing security protocols are divided into four categories, of which the first three are based on the improvement of three classic protocols, the last one is based on three classic protocol solutions moreover considering the safety and Efficiency and the cost of tag. However there are a variety of problems in security protocols, including security flaws, efficiency issues, and non-compliance with large-scale tags. At present, there is no good security protocol is recognized as safe, feasible, efficient and so on, the future work is still gathered in how to design a reliable, safe and efficient RFID security protocol.

Sponsors or Supporters

This work is partially supported by Science & Technology Program of Weiyang District of Xi'an City with project "201609", the Science & Technology Program of Department of Shaanxi Education with project "15JK1350".

References

[1] Ohkubo M, Suzuki K, Kinoshta S, "Hash-chain based for-ward-secure privacy protection scheme for low-cost RFID" Proceedings of the 2004 Symposium on Cryptogra-phy and Information Security. Berlin: Springer-Verlag,2004,pp.719-724.

[2] Sarma S, Weis S, Engels D, "RFID systems and security and privacy implications," Proc of the 4th Int Work-shop on Cryptographic Hardware and Embedded Systems. Berlin: Springer, 2002,pp. 454-469.

[3] Weis S A, Sarma S E, Rivest R L, "et al.Security and privacy aspects of low-cost radio frequency identification systems," Proc of the 1st Security in Pervasive Com-putting.Berlin: Springer, 2003,pp.201-212.

[4] Taoyuan, Zhou Xideng, "Mobile mutual authentication protocol based on hash function," Journal of Computer Applications, 2016, 36 (3),pp.657 - 660.

[5] Hou Jinhuan, Ding Fuqiang, "New things RFID security protocol analysis and design of," electronic technology and software engineering, 2015.

[6] Zhao Ting, Wang Jian, "Dynamic RFID authentication protocol," 2010 Hash function of the National Communications Security Conference on.

[7] Guo Wei, "Improvement of HASH Chain Protocol in RFID," second national information security protection technology conference proceedings, 2013, 6, 21.

[8] C. Tan, B. Sheng, and Q. Li, "Secure and serverless rfid authentication and search protocols," vol. 7, no. 4, april 2008, pp. 1400 - 1407.

[9] Minghui Wang, Yongzheng Tang, Fang Shi, Junhua Pan, "An effective RFID authentication protocol," 2012 2nd International Conference on Consumer Electronics, Communications and Networks (CECNet), pp.141 – 144.

[10] Tan C., Sheng B., and Li Q., "Severless search and authentication protocols for RFID," In Proceedings of the Fifth Annual IEEE International Conference on Pervasive Computing and Communications(PerCom '07), New York, USA. pp. 3-12 .
[11] Ahamed, S. I., Rahman, F., and Hoque, M., Kawsar, E, and Nakajima,T, "YA-SRAP: Yet another serverless RFID authentication protocol," In Proceedings of the 4th IET International Conference on Intelligent Environment (IE08). Seattle, USA. pp. 1-8,2008.

[12] Feng Zebo, Wu Xiaoping, Liu Haohan, "RFID security authentication protocol a new free end database," Journal of Naval University of engineering, 2015,02,pp.32-36.

[13]Selwyn Piramuthu, "RFID mutual authentication protocols," Decision Support Systems, Vol.50, Issue 2, January 2011, pp.387-393.

[14] Su Mi Lee, Young Ju Hwang, Dong Hoon Lee, Jong In Lim, "Efficient Authentication for Low-Cost RFID Systems," Lecture Notes in Computer Science. Berlin, vol.3480, pp. 619-627,2005.

[15] Yong Ki Lee, Ingrid Verbauwhede, "Secure and Low-cost RFID Authentication Protocols," Proceedings of the 2nd IEEE Workshop on Adaptive Wireless Networks, 2005.

[16] Kaleb Lee, "A Two-Step Mutual Authentication Protocol Based on Randomized Hash- Lock for Small RFID Networks," 2010 Fourth International Conference on Network and System Security, pp. 527 – 533.

[17] Eun Young Choi, Su Mi Lee, Dong Hong Lee, "Efficient RFID Authentication Protocol for Ubiquitous Computing Environment," Embedded and Ubiquitous Computing, vo1.3832, pp.945-954, 2005.

[18] He Lei, Lu Xin-mei, Jin Song-he, Cai Zeng-yu, "A One-way Hash based Low-cost Authentication Protocol with Forward Security in RFID System," 2010 2nd International Asia Conference on Informatics in Control, Automation and Robotics (CAR 2010)[2],pp.269 – 272.

[19] J. H. Ha, S. J. Moon, J. Y. Zhou, and J. C. Ha, "A new formal proof model for RFID location privacy," in: S. Jajodia and J. Lopez, editors, Proceedings of 13th European Symposium on Research in Computer Security – ESORICS'08, LNCS 5283, Springer – Verlag, pp. 267 – 281,2008.

[20] Da-Zhi Sun, Ji-Dong Zhong, "A hash-based RFID security protocol for strong privacy protection," IEEE Transactions on Consumer Electronics (2012) Vol.58, Issue: 4, pp.1246 – 1252.

[21] Liang Huan qi, "Research of Mutual Authentication Protocol for RFID Based on Hash Function and Public Key," South China University of Technology, 2012.

[22] Jianliang Meng, Ze Wang, "A RFID Security Protocol Based on Hash Chain and Three-Way Handshake," 2013 International Conference on Computational and Information Sciences,pp.1463 – 1466.

[23] Yanfei Liu, Sha Feng, "Scalable Lightweight Authentication Protocol with Privacy Preservation," 2014 Tenth International Conference on Computational Intelligence and Security, pp.474 – 478.

[24] T. Li, W. Luo, Z. Mo, and S. Chen, "Privacy-preserving RFID authentication based on cryptographical encoding," IEEE INFOCOM,2012, pp. 2174-2182.

[25] G. Avoine, L. Buttyan, T. Holczer, and I. Vajda, "Group-Based Private Authentication," IEEE International Symposium on World of Wireless, Mobile and Multimedia Networks, 2007, pp. 1-6.

[26] Prosanta Gope and Tzonelih Hwang, "A realistic lightweight authentication protocol preserving strong anonymity for securing RFID system," Computers & Security, Vol.55, November 2015, pp.271-280.

[27] Prajnamaya Dass, Hari Om, "A secure authentication scheme for RFID Systems," Procedia Computer Science, Vol.78, 2016, pp. 100-106.

[28] Jung-Sik Cho, Young-Sik Jeong and Sang Oh Park, "Consideration on the brute-force attack cost and retrieval cost: A hash-based radio-frequency identification (RFID) tag mutual authentication protocol," Computers & Mathematics with Applications, Vol.69, Issue 1, January 2015, pp. 58-65.

[29] Dang Nguyen Duc and Kwangjo Kim, "Defending. RFID authentication protocols against DoS attacks," Computer Communications, Vol.34, Issue 3, 15 March 2011, pp. 384-390.

Quad-rotor UAV Control Method Based on PID Control Law

Yang sen[1,2], Wang Zhongsheng[3]

[1] Department of UAV Engineering, Ordance Engineering College, Shijiazhuang,

China Email: 568657132@qq.com

[2] School of Automation Science and Electrical Engineering, Beihang University, Beijing, China, Email: 568657132@qq.com

[3] School of Computer Science and Engineering, Xi'an Technological University,

Xi'an 710021, China, Email:59483672@qq.com

Abstract. This paper studies on the dynamics model and control method of quad-rotor UAV for research. Firstly analyzes the dynamic characteristic of quad-rotor UAV and establishes the nonlinear dynamics model of quad-rotor UAV; and then applies the PID control to three channels of pitch, roll and yaw based on the established model, and the simulation results show that PID control is effective for the quad-rotor UAV control with the ideal conditions. Finally analyzes the results of PID control under the circumstance that the data form feedback channel is polluted by noise, which lay the foundation for the improvement of the PID control law.

Keywords: quad-rotor,dynamics model, PID

1. Introduction

Quad-rotor UAV is a kind of butterfly, coaxial type, vertical take-off and landing multi-rotor aircraft. Compared with other types of UAV, it has lots of unique advantages [1]: vertical take-off and landing, hovering, flying in arbitrary direction, adapting to many kinds of takeoff and landing site, etc. Its unique performance makes it have broad application space in military and civilian fields. In the aspect of military, Quad-rotor UAV can be used to perform both tasks of destruction and non-combat missions such as investigation, positioning, communications relay, etc. In the aspect of civil, quad-rotor UAV in monitoring of atmospheric environment, the traffic situation, exploration and resource distribution, detecting electric power line, etc have broad application prospects [2].

Due to quad-rotor UAV movement characteristics present a nonlinear, strong coupling, time-varying, exploring practical flight control method is of great value. Control algorithm design is the core content of quad-rotor UAV flight control, and PID as a classic control algorithm has the advantages of simple structure, easy to implement, which has been widely applied in engineering practice [3]. Therefore, to carry out the quad-rotor UAV control method based on the PID control law is not only theoretical research significance, and lay a foundation for quad-rotor UAV to engineering practical. Aiming at

the quad-rotor UAV flight control problem, this paper carry out the research work mainly from the modeling methods, control algorithm and the simulation experiment and other aspects.

2. Foundation of the Dynamic Model of the Quad-Rotor Uav

The motion of UAV can be divided into 6 degrees of freedom, including 3 degrees of freedom of linear motion and 3 degrees of freedom of angle motion around the center of mass[4]. According to Newton’s second law, the dynamic equations of UAV are as follows:

$$\vec{F} = m\frac{d\vec{V}}{dt} \tag{1}$$

$$\vec{M} = \frac{d\vec{H}}{dt} \tag{2}$$

Where $\vec{F}$ represents force acted on the quad-rotor UAV, m is the mass of the UAV, $\vec{V}$ indicates the velocity of the center of mass of the UAC, $\vec{M}$ is resultant moment of force of the UAV and $\vec{H}$ is moment of momentum of UAV relative to the ground coordinates.

2.1 Linear Equation of Motion

The force acted to UAV includes gravity, lift of the rotor and the air resistance.

$$G = mg \tag{3}$$

$$F_i = \frac{1}{2}\rho C_i \omega_i^2 = k_i \omega_i^2 \tag{4}$$

$$D_i = \frac{1}{2}\rho C_d \omega_i^2 = k_d \omega_i^2 \tag{5}$$

Where G is the gravity of the UAV, F_i , $i \in \{1,2,3,4\}$, is the lifting force of the rotor i, D_i is the resistance of the rotor i, C_i is the lift coefficient of the rotor, C_d is the resistance coefficient of the rotor, ω_i is the angular velocity of the rotor i.   is the lift coefficient and k_d is the resistance coefficient.

$\vec{F}$, the resultant lift of the quad rotors, is as follows:

$$\vec{F} = R\begin{bmatrix} 0 \\ 0 \\ \sum_{i=1}^{4} F_i \end{bmatrix} = \begin{bmatrix} \cos\psi\sin\theta\cos\phi + \sin\psi\sin\phi \\ \sin\psi\sin\theta\cos\phi - \sin\phi\cos\psi \\ \cos\theta\cos\phi \end{bmatrix}\sum_{i=1}^{4} F_i \tag{6}$$

Substitute equation (6) into (1):

$$\begin{cases} \ddot{x} = \left[\left(\text{üüü}\psi\text{üüüü}\theta \quad \phi + \quad \psi \quad \phi \right)\sum_{i=1}^{4} F_i - K_1\dot{x} \right] m^{-1} \\ \ddot{y} = \left[\left(\text{üüü}\psi\text{üüüü}\theta \quad \phi - \quad \phi \quad \psi \right)\sum_{i=1}^{4} F_i - K_2\dot{y} \right] m^{-1} \\ \ddot{z} = \left[\left(\cos\theta\cos\phi \right)\sum_{i=1}^{4} F_i - K_3\dot{z} \right] m^{-1} - g \end{cases} \tag{7}$$

Where (x, y, z) is the location of the center of mass of the UAV, $K_i (i = 1,2,3)$ is the total resistance

coefficient and g is gravitational acceleration.

2.2 The Angular Motion Equation

The relation between the angular velocity of ruler angle $(\dot{\phi},\dot{\theta},\dot{\psi})$ and the angular velocity of the fuselage (p,q,r) is as follows:

$$\begin{bmatrix}\dot{\theta}\\ \dot{\phi}\\ \dot{\psi}\end{bmatrix}=\begin{bmatrix}p+p\sin\phi\tan\theta+r\cos\phi\tan\theta\\ q\cos\phi-r\sin\phi\\ q\sin\phi\sec\theta+r\cos\phi\sec\theta\end{bmatrix} \tag{8}$$

Assuming that the shape of the quad-rotor UAV is symmetrical, the mass distribution is uniform, it can be assumed that the center of gravity of the UAV is located at the center of the quad-rotor UAV. According to the calculation of the angular momentum, the motion equation of the angle of the quad-rotor UAV is as follows:

$$\begin{bmatrix}M_x\\ M_y\\ M_z\end{bmatrix}=\begin{bmatrix}\dot{p}I_x-\dot{r}I_{xz}+qr(I_z-I_y)-pqI_{xz}\\ \dot{q}I_y-pr(I_x-I_z)+(p^2-r^2)I_{xz}\\ \dot{r}I_z-\dot{p}I_{xz}+pq(I_y-I_x)+qrI_{xz}\end{bmatrix} \tag{9}$$

Where M_x,M_y,M_z respectively represents the component of the resultant external angular momentum of the UAV around the axis of X,Y,Z .

According to equation (9):

$$\begin{bmatrix}\dot{p}\\ \dot{q}\\ \dot{r}\end{bmatrix}=\begin{bmatrix}\left[M_x+\left(I_x-I_z\right)qr\right]/I_x\\ \left[M_y+\left(I_z-I_x\right)pr\right]/I_y\\ \left[M_z+\left(I_x-I_y\right)pr\right]/I_z\end{bmatrix} \tag{10}$$

Finishing equation (9) and equation (10):

$$\begin{cases}\ddot{\phi}=\left[M_x-\dot{\theta}\dot{\psi}\left(I_z-I_y\right)\right]/I_x\\ \ddot{\theta}=\left[M_y-\dot{\phi}\dot{\psi}\left(I_x-I_z\right)\right]/I_y\\ \ddot{\psi}=\left[M_z-\dot{\phi}\dot{\theta}\left(I_y-I_x\right)\right]/I_z\end{cases} \tag{11}$$

According to the 'X' flight model of UAV and theorem of momentum:

$$\begin{bmatrix}M_x\\ M_y\\ M_z\end{bmatrix}=\begin{bmatrix}l\left(F_1+F_4-F_2-F_3\right)\\ l\left(F_1+F_3-F_2-F_4\right)\\ \lambda\left(F_1+F_2-F_3-F_4\right)\end{bmatrix} \tag{12}$$

Where l is the distance between the motor shaft and the center of mass of the UAV, λ is the coefficient which link the lift and the twisting moment.

Assuming the input of the system of the quad-rotor UAV as follows:

$$U=\begin{bmatrix}U_1\\U_2\\U_3\\U_4\end{bmatrix}=\begin{bmatrix}F_1+F_2+F_3+F_4\\F_1+F_4-F_2-F_3\\F_1+F_3-F_2-F_4\\F_1+F_2-F_3-F_4\end{bmatrix} \tag{13}$$

Where U_1 is the vertical controlled quantity, U_2 is the roll controlled quantity, U_3 is the pitch controlled quantity and U_4 is the yaw controlled quantity.

Integrate equation (11), (12), (13):

$$\begin{cases}\ddot{\phi}=U_2 l I_x^{-1}\\ \ddot{\theta}=U_3 l I_y^{-1}\\ \ddot{\psi}=U_4 \lambda I_z^{-1}\end{cases} \tag{14}$$

Assuming that the flight environment of the quad-rotor UAV is indoor or breeze outside, the resistance coefficient in equation (7), $K_i(i=1,2,3)$ will be negligible. Then integrate equation (14) and equation (7):

$$\begin{cases}\ddot{x}=\left[\left(\cos\psi\sin\theta\cos\phi+\sin\psi\sin\phi\right)U_1\right]m^{-1}\\ \ddot{y}=\left[\left(\sin\psi\sin\theta\cos\phi-\sin\phi\cos\psi\right)U_1\right]m^{-1}\\ \ddot{z}=\left[\left(\cos\theta\cos\phi\right)U_1\right]m^{-1}-g\\ \ddot{\phi}=U_2 l I_x^{-1}\\ \ddot{\theta}=U_3 l I_y^{-1}\\ \ddot{\psi}=U_4 \lambda I_z^{-1}\end{cases} \tag{15}$$

3. The Control Method of the Quad-Rotor UAV Based on PID Control Law

The principal structure of the PID controller is as shown in Figure 1[5].

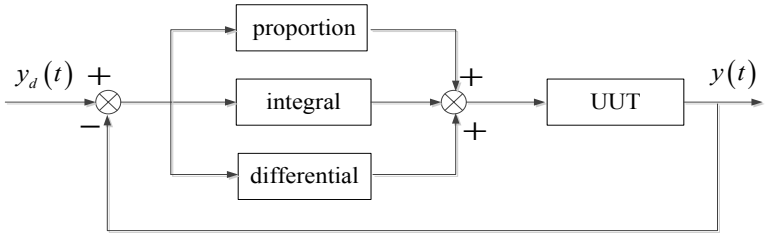

Figure.1 Program block diagram of PID

Where $y_d(t)$ is set point, $y(t)$ is the real output of system. PID controller use the error value between $y_d(t)$ and $y(t)$.

$$e(t)=y_d(t)-y(t) \tag{16}$$

The control law is as follows:

$$u(t) = k_p\left(e(t)\right) + k_i\int_0^t e(t)\,\mathrm{d}t + k_d\frac{\mathrm{d}\left(e(t)\right)}{\mathrm{d}t} \tag{17}$$

Where k_p is proportionality coefficient, k_i is integral coefficient and k_d is differential coefficient.

Exert PID control to the pitch, yaw, roll channel respectively. The structure drawing of PID control of the roll channel is as shown in the Figure 2 [6].

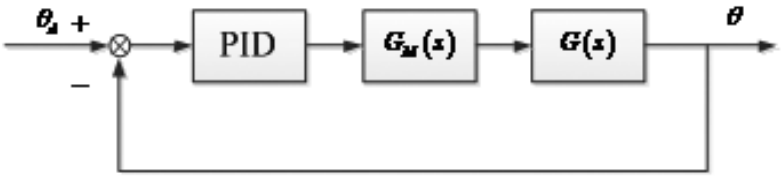

Figure.2 PID control flow chart of Roll

Where $G_M(s)$ is the transfer function of the electrical machine and $G(s)$ is the transfer function of the quad rotor UAV.

The step response exerting PID control to the pitch, yaw, roll channel respectively is as shown in the Figure3, 4, 5. And the control quality is as shown in the table 1.

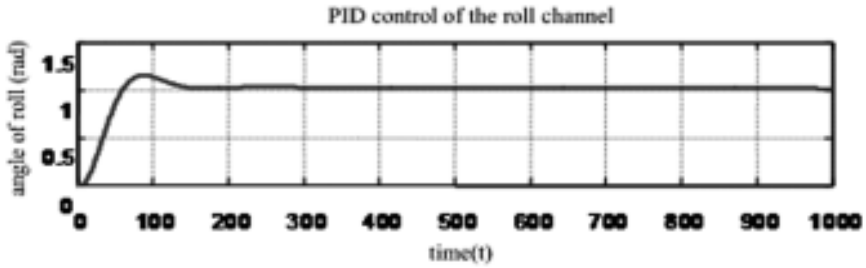

Figure.3 PID control of the roll channel

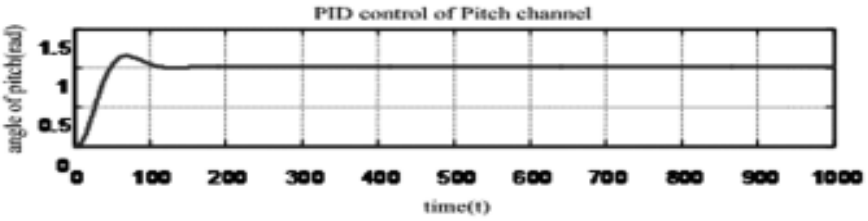

Figure.4 PID control of the pitch channel

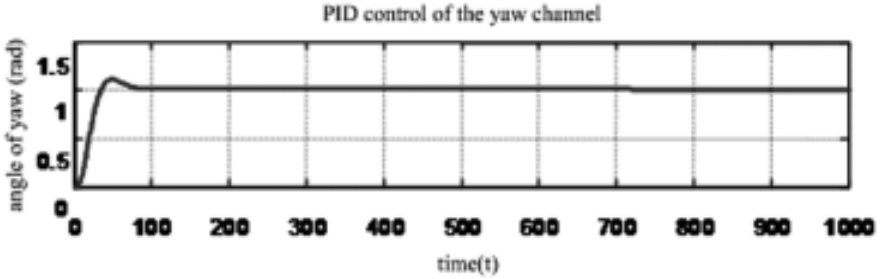

Figure.5 PID control of the yaw channel

Table 1 PID control quality

channel	k_p	k_i	k_d	risetime	overshoot
Roll	0.89	1.87×10^{-2}	0.073	0.38	15.4%
Pitch	0.73	1.45×10^{-2}	0.079	0.29	15.3%
Yaw	0.12	4.5×10^{-2}	0.078	0.21	11.3%

According to the response of the three channel and control quality, PID control method is efficient to control the quad-rotor UAV under the ideal environment.

But in the real flight, the sensor data of the feedback channel are easily polluted by measurement noise. The response of the roll channel polluted by the noise is shown in the figure 6. It is necessary to study the control method under the condition that the sensor data are polluted by noise.

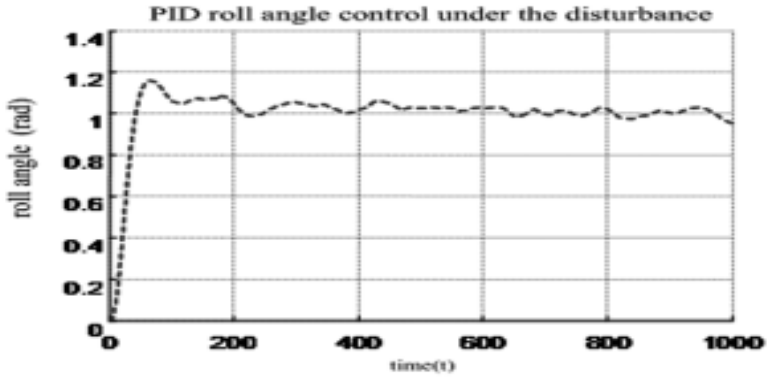

Figure.6 PID control result with noise interference

4. Conclusion

In this paper, the dynamic model of quad-rotor UAV is established, and the PID controllers of the pitch, yaw and roll channels are designed. The simulations reveal that PID control method is efficient to control the quad -rotor UAV under the ideal environment. Finally, taking the roll channel as an example to analysis the result of PID control with the noise disturbance in sensor data, laying the foundation to study the new control method under the condition that the sensor data are polluted by noise.

References

[1] YUE Jilong, ZHANG Qingjie. Research Progress and Key Technologies of Micro Quad-Rotor UAVs[J]. Electronic Optics & Control, 2012,17 (10): 46-52.

[2] Daniel Mellinger, Quentin Lindsey, Vijay Kumar. The GRASP Multiple Micro-UAV Test bed [J]. Robotics & Automation Magazine, IEEE.2010 17(3): 54-65.

[3] Bouabdallah S, Noth A, Siegwart R. PID vs LQ Control Techniques Applied to an Indoor Micro Quadrotor [C]// IEEE International Conference on Intelligent Robots and Systems,2004 : 2451-2456.

[4] Li Jie, QI Xiao-hui. Design and implementation of flight control system for small quad-rotor[J]. CHINA MEASUREMENT & TEST, 2014, 02: 90-93.

[5] Liu Jinkun. Advanced PID Control MATLAB Simulation[M]. Beijing: Electronic Industry Press, 2013.

[6] Rong Xu. Sliding Mode Control of a Quadrotor Helicopter[C]// Proceedings of the 45th IEEE Conference on Decision & Control Manchester Grand Hyatt Hotel, 2006, 13(15): 4957-4962.

Application of Computational Tools to Analyze and Test Mini Gas Turbine

Haifa El-sadi* , Anthony Duva

Mechanical Engineering and Technology
Faculty of Engineering and computer science
Wentworth Institute of Technology
Boston, MA, USA

Corresponding author Email: elsadih@wit.edu

Abstract. Performance analysis and testing of the Mini Gas Turbine was carried out in Wentworth Institute of Technology's Thermodynamics Laboratory. The computational tool allows students to focus on more design-oriented problems. Furthermore, students had the ability to see immediate results to variations of the design conditions as well as different parameters that would affect the mini turbine. This project was carried out as a senior design project (Capstone), the students updated the existing data acquisition system, writing a new data acquisition program in LabVIEW, installing new pressure and temperature sensors, and performing a first and second law of thermodynamics analysis on the engine in Engineering Equation Solver. In order to update the existing data acquisition system, new NI SCB-68 connector blocks were implemented along with NI USB-6251 terminals. The new hardware is operated through a LabVIEW program running on a new laptop designated and mounted to the mini jet turbine housing. Instrumentation, testing, and calibration are the three main milestones for this project As a result, The Inlet Mass Flow Rate numeric indicator value is calculated, not measured. The calculated value is dependent on the measured values of Compressor Inlet Temperature (T1), Compressor Inlet Static Pressure (Ps), and Compressor Inlet Dynamic Pressure (Pt-Ps). However, the pressure, temperature and thrust were tested as a function of RPM. The mini turbine engine is ready to be used in student experimental settings. Feedback from students proves that the use of different tools significantly enhances the student learning experience and encourages the students to use different theory from different courses, make the course more dynamic, and motivate the students to learn the material.

Keywords: LabVIEW, Engineering Equation solver (EES), Mini-turbine, Pressure

1. Introduction

The turbine engine discussed throughout this research is a self-contained turbojet engine.This engine operates on a Brayton cycle. The Brayton cycle depicts the air-standard model of a gas turbine power cycle. A simple gas turbine is comprised of three main components: a compressor, a combustor, and a turbine. According to the principle of the Brayton cycle, air is compressed in the compressor. The air is then mixed with fuel, and burned under constant pressure conditions in the combustor. The resulting hot gas is allowed to expand through a turbine to perform work. Most of the work produced in the turbine is used to run the compressor and the rest is available to run auxiliary equipment and produce

power [1].

Gas turbine engines include internal passages which serve to channel the cooling air from compressors to the different components to be cooled. The research on the flow in a corotation radial inflow cavity was pioneered by Owen et al. [2]. They used integral momentum techniques for flows in a rotating cylindrical cavity. Firouzian et al. [3, 4] studied the flow and heat transfer in the cavity. Their results revealed the complicated source-sink flow feature in a radial inflow rotating cavity. One of the concerns in turbomachine is the pressure loss in the cavity; different ways to minimize the pressure loss have been explored. Chew et al. [5] has used fins to reduce the pressure loss. On the other hand, X. Liu [6] has studied the flow in a corotation radial inflow cavity between turbine disk and coverplate. Also, the flow field in a preswirled cooling air supply to a turbine rotor has been investigated by Oliver et al. [7, 8].

An analysis on this engine provides important performance characteristics such as thrust, compressor performance, turbine performance (work and power, expansion ratio, turbine efficiency), combustion/ emission analysis, and overall isentropic efficiency. In order to perform an analysis on this engine, several quantities at specific locations are needed. Sensors are instrumented on this engine at the compressor inlet, compressor outlet, turbine inlet, turbine exit, and exhaust to collect data on the temperature and pressure at each location. This data is then used to perform a performance analysis on the engine. In addition, there are sensors on this engine to monitor thrust, RPM, and fuel flow rate.

Shown below in Figure 1 is a cross section of the engine with main components labeled.

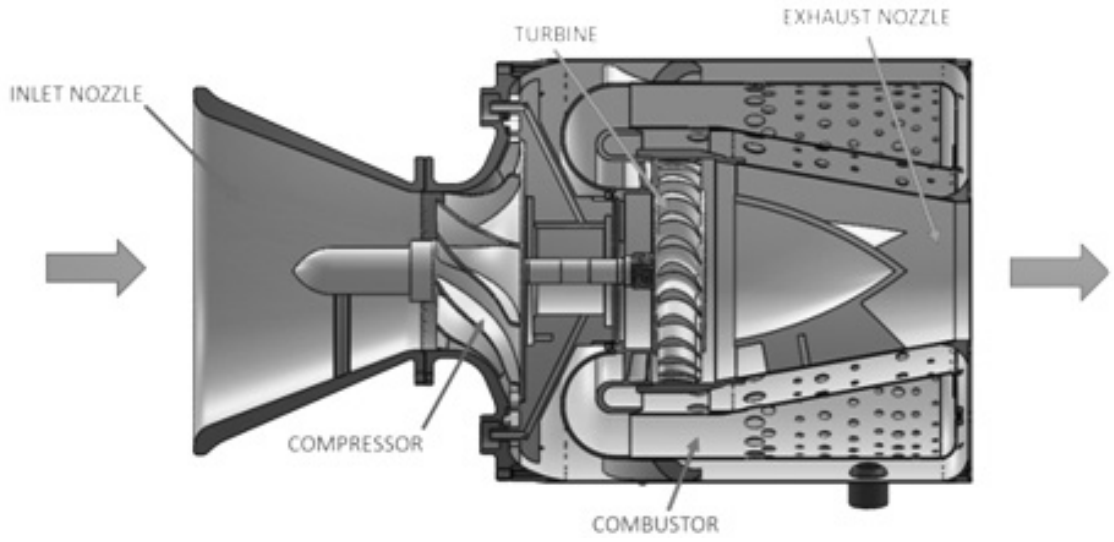

Figure.1 Turbine Engine Layout (Brayton Cycle)

Figure 2 below shows the location of each temperature and pressure being measured on the engine.

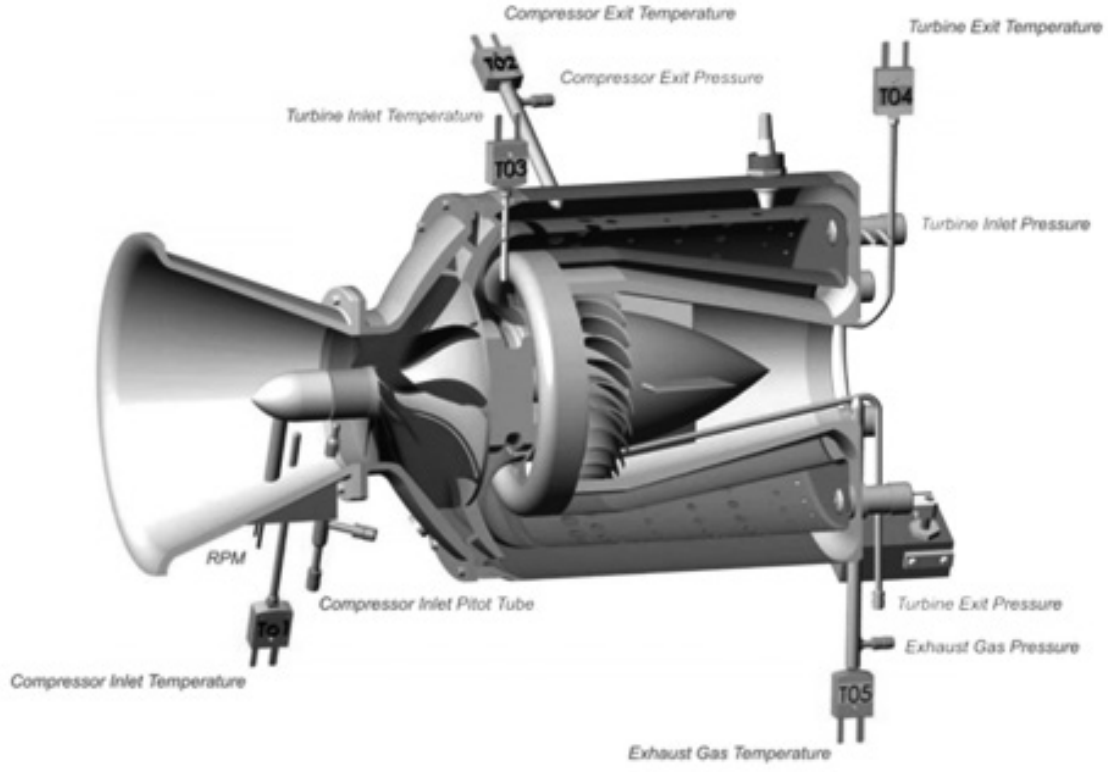

Figure.2 Engine Instrumentation Locations

Shown below in Table 1 are the specifications of the engine.

Table 1 Engine Manufacturer Specifications

Manufacturer	Turbine Technologies, Ltd.
Model Number	2000DX
Max. RPM	90,000
Max. Exhaust Temperature	720 C
Pressure Ratio	3.4:1
Specific Fuel Consumption	1.18 lb./lb.-hr

The Turbine Technologies Mini Gas Turbine in the Wentworth Institute of Technology thermodynamics lab is in great need of an instrumentation overhaul. Due to the high cost of replacing the data acquisition system completely, our team will be replacing it ourselves. The current DAQ system is outdated and incompatible with current software on the computer it is paired to. A new set of DAQ hardware will be paired with a new computer running a LabVIEW program to collect the data. Our team's goals also include calibration of pressure transducers and thermocouples for accurate measurement. Our team will then run a 1st and 2nd law of thermodynamics on the system using Engineering Equation Solver (EES).

The mini gas turbine in the thermodynamics lab is a fantastic resource that is going un-used. Many students can benefit from the mini turbine's technical sophistication. Benefits include but are not limited

to technical understanding, conceptual understanding, and practical application. With the recent creation of the Aerospace Engineering Minor at Wentworth, this machine could open the eyes to many young engineers and give them the ability to have a future in the aerospace industry. Turbine propulsion is used on various aircraft, but dominates the commercial jet and military jet industries.

The main problem of this project is to overhaul the instrumentation of the mini gas turbine and have it ready to be run for students. Instrumentation, testing, and calibration are the three main milestones for this project. A technical lab will be produced for thermodynamics students to run.

2. Instrumentaion

Figure 3 below shows the laptop system mounted and installed.

Figure.3 Laptop and Monitor Installed

the new DAQ has several additional components which are much larger than the old system a much larger mounting bracket was necessary. After modeling all of the current system components in SolidWorks, a sheet metal bracket was designed to fit all of the DAQ components without interfering with any of the existing surrounding components.

Figure 4 below shows the design of the new DAQ setup.

Figure.4 DAQ Components Installed

During the course of this project, there were many sensors that needed to be changed or added. The preexisting DAQ system was capable of collecting temperature and pressure readings from the various mini-turbine engine stages; however, there was room for improvement. One of the main additions made to the instrumentation was implementing a new pressure transducer to read the static pressure at the inlet of the nozzle. The pitot-static mast style device can be seen below in figure 5:

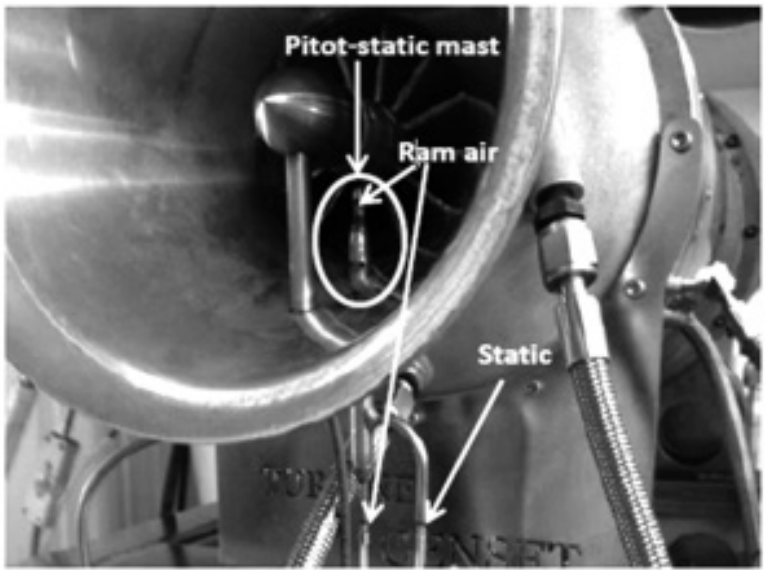

Figure.5 Inlet Pitot Tube Current Set-Up

The basis of this project is to transition the new hardware and supported LabVIEW software. The hardware chosen for the task are the NI SCB-68 and NI USB-6251. Two of each have been implemented in the DAQ system.

While attempting to calibrate the thrust strain gauge, significant noise to the NI chassis was experienced. The pre-existing set-up had the wires from the strain gauge splitting between the meter and the NI chassis. While the out-put signal from the strain gage was filtered through the DP25-S, it was not filter through the NI chassis. To remedy the issue, the DP25-S was replaced with a DP25-S-A which had the correct analog signal output. With the new signal analog signal output, there was no noise experienced from the thrust strain gage and meter. Below the new meter can be seen:

3. Testing

Figure 6. LabVIEW Data Acquisition Front Panel User Interface (Plot Tab)

In order to calculate the Inlet Mass Flow Rate to the turbine engine, the static pressure is needed. The static pressure is obtained by connecting a pressure transducer directly to the static pressure port on the inlet pitot tube. Next, the density of the air is calculated using this static pressure. The air velocity is calculated next using the Dynamic Pressure which is the difference between the total pressure and the static pressure. The Mass Flow Rate is finally obtained knowing the density, velocity and cross sectional area of the inlet nozzle at the location of the pitot tube. This calculation is performed in the LabVIEW program (Figure 77). See following report section for mass flow rate governing equations.

The fuel flow rate is determined from measuring the fuel pressure. If the fuel pressure as well as the fuel properties are known, the flow rate can be determined. The Inlet Mass Flow Rate numeric indicator

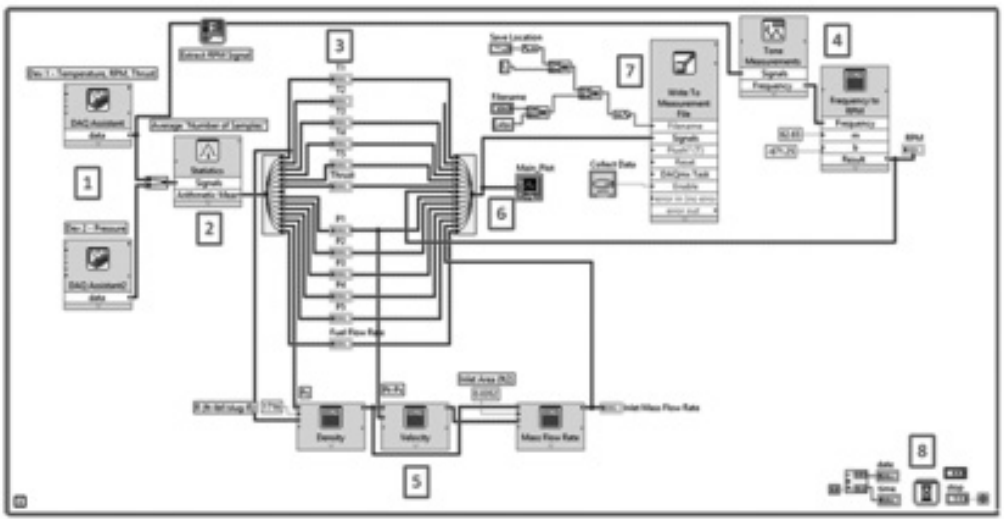

Figure.6 LabVIEW Block Diagram

value is calculated, not measured. The calculated value is dependent on the measured values of Compressor Inlet Temperature (T1), Compressor Inlet Static Pressure (Ps), and Compressor Inlet Dynamic Pressure (Pt-Ps). Using Express Formula functions, the density of the air is first calculated, then the velocity of the air is calculated, and finally the Inlet Mass Flow Rate can be calculated. The following equations are contained within these functions for Density (ρ), Velocity (v) and Mass Flow Rate ($\dot{m}$).

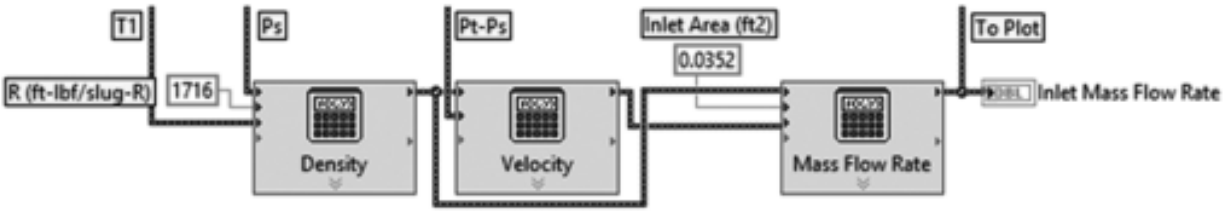

Figure.7 Mass Flow Rate Calibration

Where,
A = Compressor Inlet Area
R = Ideal Gas Constant for Air

$$\rho = \frac{(P_s+14.7)144}{R(T_1+460)}\ (slug/ft^3) \quad (1)$$

$$v = \sqrt{\frac{2P_1*144}{\rho}}\ (ft/s) \quad (2)$$

$$\dot{m} = \rho A v\ (slug/s) \quad (3)$$

Figure 8 shows the inlet mass flowrate vs. RPM

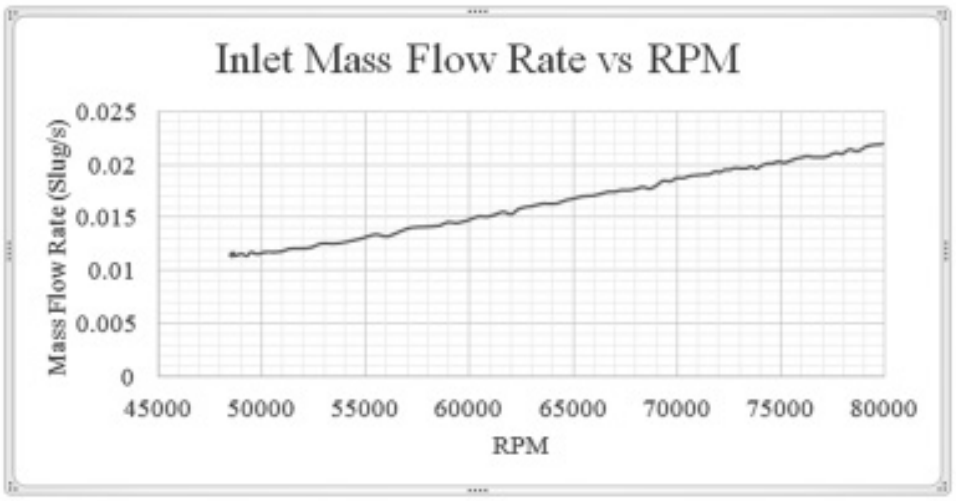

Figure.8 Engine Testing Data Plot – Inlet Mass Flow Rate vs RPM

A sample set of data collected from an engine test run is shown in figure 9 through

Figure 11. These plots contain important characteristics of the engine such as the relationship between engine RPM and Thrust, Temperature, Inlet Mass Flow Rate, and Pressure.

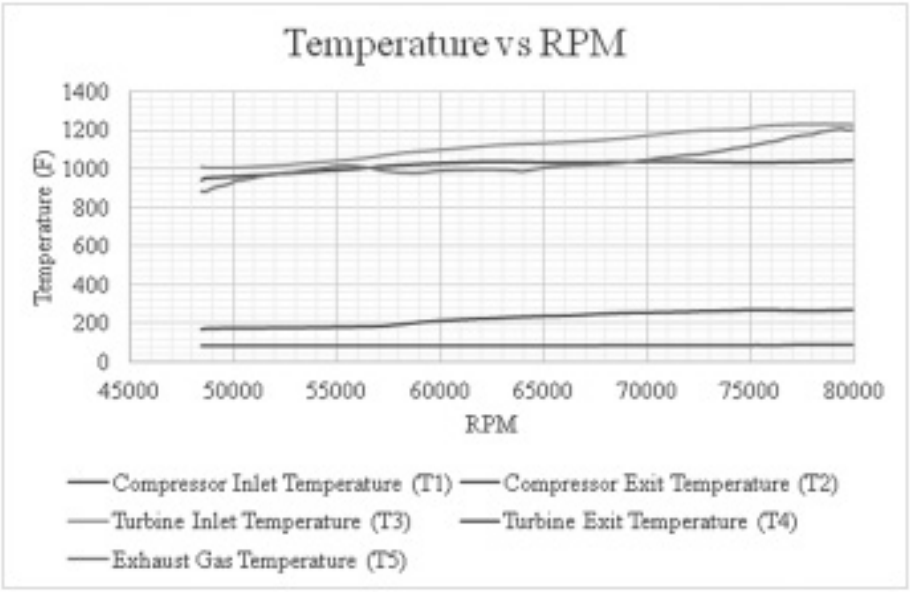

Figure.9 Engine Testing Data Plot – Thrust vs RPM

4. Engineering Equation Solver (EES)

One of the critical tasks was to create a program in EES which analyzes the engine using the first and second laws of thermodynamics. Ideally this program would be displayed on the second monitor so you can take the data directly from LabView and plug it into the EES program. After plugging in the different temperatures and pressures as inputs in the EES program, it will calculate the compressor efficiency, turbine efficiency, overall efficiency of the engine and the thrust of the engine. A diagram window interface was created in EES to make it easy for the user to run the program without understanding the entirety of the code. Figure 12 below shows the equations window section of the EES program. Figure.12 EES code

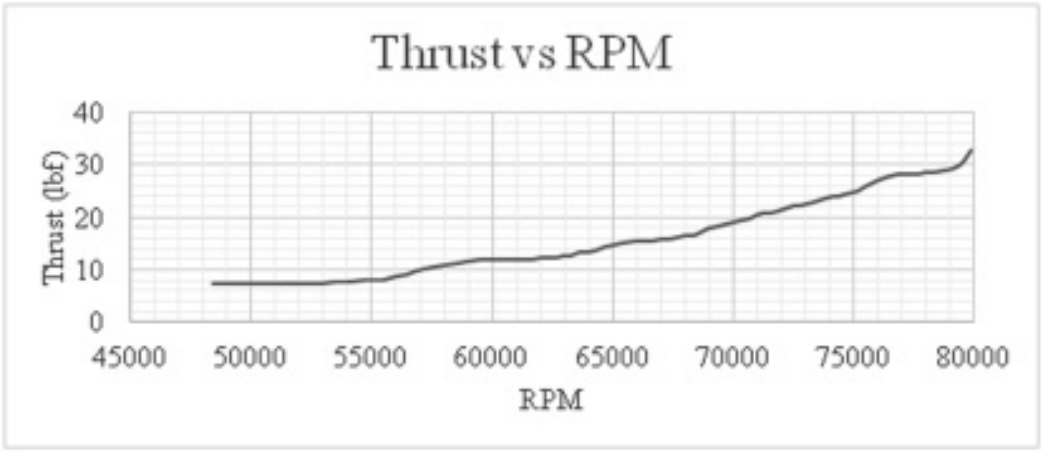

Figure.10 Engine Testing Data Plot – Temperature vs RPM

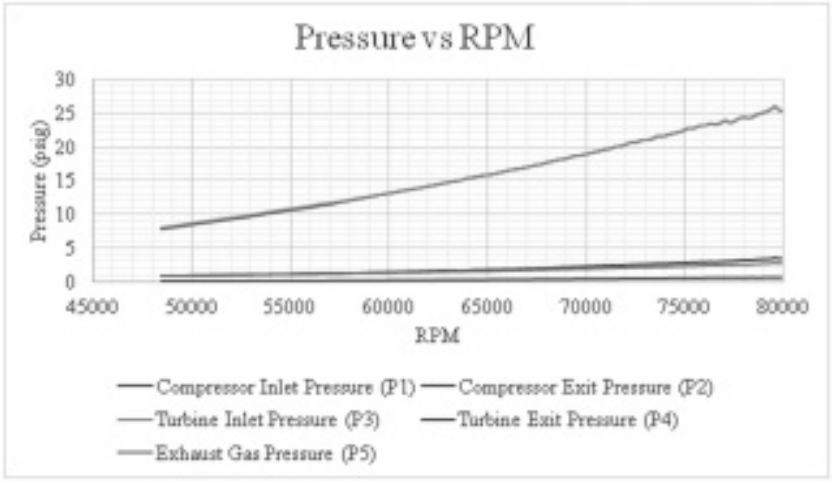

Figure.11 Engine Testing Data Plot – Pressure vs RPM

5. Conclusion

This paper explored the use of computational tools to enhance the students' understanding of the different gas turbine engine processes and apply the theory such as conservation of mass and energy which were learned in different courses such as Thermodynamics and fluid mechanics. The computational tool such as EES allows the students to focus on the fundamental concepts of energy equation and second law of thermodynamics to yield quicker final results. The completion of this capstone project produced quality and timely task completion. The mini turbine engine is now ready to be used in student experimental settings. Each data acquisition component of the system is calibrated including all thermocouples and pressure

transducers, RPM measurement and thrust measurement. The LabVIEW program will be used for real time data display and data acquisition of the complete run cycle of the system. Using this data exported to Excel by the LabVIEW program, these values can be inputted into the first and second law of thermodynamics EES

program to determine the efficiencies of the compressor, turbine, and the overall system as well as the work done by the system in BTU/hr.

The senior students completed their tasks and sub-tasks and achieved their final goal. These tasks and sub-

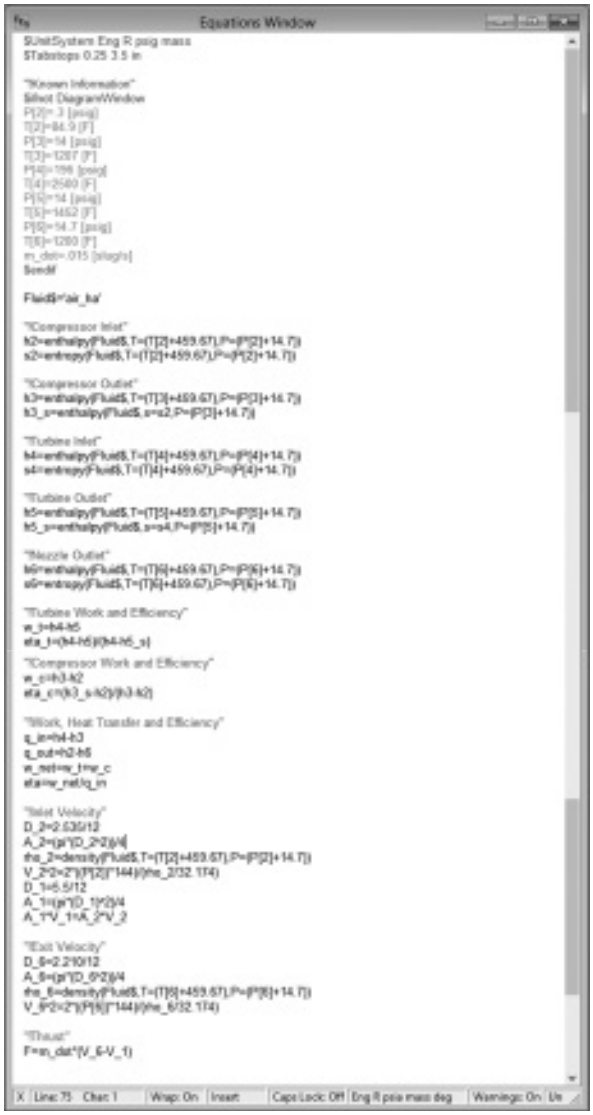

Figure.12 EES code

tasks include but are not limited to preliminary research and component identification, mounting of a new laptop arm and laptop, design and manufacturing of a mounting bracket for the DAQ hardware, an EES program, a DAQ and user-friendly display LabVIEW program. It can be concluded that using senior students. Feedback from students, proved that the use of computational tools signi**fi**cantly enhances the student learning experience while motivating the students to learn the di**ff**erent mini turbine processes.

References

[1] Moran, Michael J., and Howard N. Shapiro. Fundamentals of Engineering Thermodynamics. Seventh ed. New York: Wiley, 2011. Print

[2] [1] Owen, j.m., Pincombe, J.R. and Rogers, R.H., “Source-sink flow inside a rotating cylindrical cavity”, J. Fluid Mech., vol.155, 1985, 233-265.

[3] Firouzian, M.O., Owen, J.M., Pincombe, J.R. and Rogers, R.H., “Flow and heat transfer in a rotating cylindrical cavity with a radial inflow of fluid. Part 1: The flow structure”, Int. J. Heat and Fluid

Flow, vol.6, 1985, 228-234.

[4] Firouzian, M.O., Owen, J.M., Pincombe, J.R. and Rogers, R.H., "Flow and heat transfer in a rotating cylindrical cavity with a radial inflow of fluid. Part 2: Velocity, pressure and heat transfer measurements", Int. J. Heat and Fluid Flow, vol.7, 1986, 21-27.

[5] Chew, J.W., Farthing, P.R., Owen, J.M. and Stratford, B., "The use of fins to reduce the pressure drop in a rotating cavity with radial inflow", J. Turbomachinery, vol. 111, 1989, 349-356.

[6] X. Liu, "Flow in a corotation radial inflow cavity between turbine disk and coverplate", Int. Gas Turbine & Aeroengine Congress & Exhibition, Orlando, Florida, 1997.

[7] Oliver Popp, Horst Zimmermann, and J. Kutz, "CFD-analysis of coverplate receiver flow", Int. Gas Turbine & Aeroengine Congress & Exhibition, Birmingham,UK,1996.

[8] Haifa El-sadi, Grant Guevremont, Remo Marini, Sami Girgis, "CFD Study of hpt blade cooling flow supply systems", ASME Turbo Expo 2007: Power for Land, Sea and Air,May 14-17, 2007, Montreal, Canada

The Research of Direct Torque Control Based on Space Vector Modulation

Su Xiaohui , Chen Guodong and Xu Shuping

School of Computer Science and Engineering, Xi'an Technological University, 710021 China

Email: suxh666@163.com

Abstract. In order to solve the conventional direct torque control contradiction between the dynamic and static performance ,a permanent magnet synchronous motor system direct torque control architecture is proposed based on space vector modulation strategy . In this method flux and torque are controlled through stator voltage components in stator fluxlinkage coordinate axes and space vector modulation is used to control inverters.The simulation verifies that SVM-DTCis capable of effectively improving the steady state performance and keeping the excellent dynamic performance of theconventional DTC system simultaneously and remain the switching frequency constant.

Keywords: Simulation, Direct torque control, Space vector modulation.

1. Introduction

Direct torque control (DTC) has been widely used in the field of control of permanent magnet synchronous motor (PMSM), because it has the advantages of simple structure and fast dynamic response of the torque, which has been paid more and more attention in recent years [1-3].Conventional direct torque control is based on the torque, flux hysteresis controller output and a 60° stator flux linkage angle based on the signal, according to certain rules from the prefabricated switch table select the appropriate space voltage vector on the motorTorque, flux linkage for Bang-Bang control [4].However, according to this way of selecting the voltage vector can not meet the system of torque and flux linkage of the double request, will have a larger torque and flux ripple [5].In addition, the conventional DTC method can cause the output of the hysteresis controller and the position of the stator flux linkage signal to be constant over multiple sampling periods, resulting in the same switch state of the inverter during these sampling periods, and thus the switching frequency of the system is changedNot constant, the capacity of the power device can not be fully utilized [6].Space Vector Modulation (SVM) is used to obtain the desired arbitrary voltage vector by combining adjacent effective voltage vector and zero-voltage vector in one sampling period, and the voltage vector is linearly adjustable [7].

2. Space Vector Modulation Algorithm

There are eight switching states for three-phase voltage source inverters, corresponding to six active voltage vectors: U1 (100), U2 (110), U3 (010), U4 (011), U5 (001), U6 (101) And two zero-voltage vectors U7 (000), U8 (111). Space vector modulation is applied to the motor is based on three-phase symmetrical sinusoidal voltage supply AC motor generated by the ideal circular flux trajectory as the

base, through the eight basic space voltage vector to the equivalent reference voltage vector so that the actual motor The air-gap trajectory approaches the ideal circle.

As shown in Fig. 1, in the coordinate system, the first sector is used as an example to synthesize the reference vector with two adjacent voltage vectors U1, U2 and zero vectors U0 (U7 and U8). According to the volt-second balance principle:

$$\mathbf{U}_1 T_1 + \mathbf{U}_2 T_2 + \mathbf{U}_0 T_0 = \mathbf{U}_s^* T_s \tag{1}$$

Where, T1, T2, respectively U1, U2 role of time, T0 is zero vector of time, T5 for the PWM cycle. The meaning of formula (1) is that the integral effect produced by the vector in T5 time is the same as the integration effect of U1, U2 and zero vector U0.

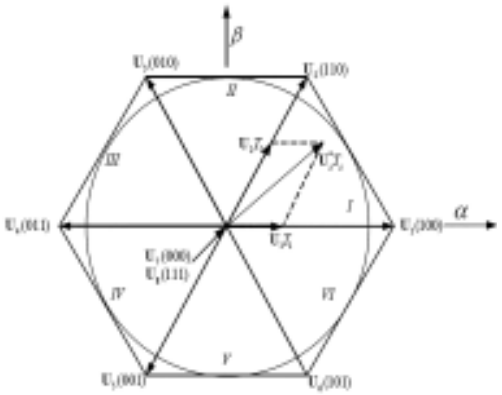

Figure.1 space voltage vector and sector

(1) U1, U2 and in axis decomposition obtained:

$$\begin{cases} T_1 = \dfrac{T_s}{2U_d}(3U_\alpha - \sqrt{3}U_\beta) \\ T_2 = \sqrt{3}\dfrac{T_s}{U_d}U_\beta \\ T_0 = T_s - T_1 - T_2 \end{cases} \tag{2}$$

The amplitude of the fundamental voltage of the output voltage increases linearly with time, and the time T0 of the zero vector U0 decreases gradually, but the following relationship should be satisfied:

$$\begin{cases} T_1 + T_2 \le T_s \\ T_0 \ge 0 \end{cases} \tag{3}$$

Similarly, in the remaining five sectors, the basic space voltage vector will change with the region of the corresponding changes. This allows SVM technology to synthesize any required space voltage vectors.

Space vector modulation is to use a certain frequency ($1/T_s$) and amplitude ($T_s/2$) of the equivalent time triangular wave to modulate A, B, C three-phase switching time T_{cm1}, T_{cm2}, T_{cm3} ,that is, the modulation signal. From the basic modulation principle of SVM, the maximum linear range of SVM is the inscribed circle shown in Fig.1, that is, the space vector modulation in the inscribed circle is linear modulation, while the over-inscribed circle is overmodulation . The following simulation and

experimental analysis and comparison of different reference voltage vector in the case, SVM modulation signal and output line voltage waveform and the relationship between.

3. Dynamic Control of Stator Flux Linkage

Figure 2 depicts the relationship between the stator flux linkage and the space voltage vector in the motor operation and the relationship between the stator flux in a single sampling period T5Dynamic control process stator flux.

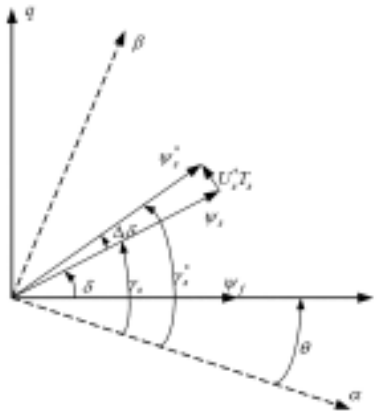

Figure.2 flux linkage diagram

In Fig. 2, the phase angle γ_s of the stator flux vector $\boldsymbol{\varnothing}_s$ at the present moment can be estimated by the flux estimator in the stator two-phase stationary coordinate system $\alpha\beta$,If the control system gives the reference flux linkage $\boldsymbol{\varnothing}_s^*$ with the phase angle γ_s^* , the stator flux linkage $\Delta\delta$ angle ahead of the current time, if the actual flux vector arrives at the reference flux linkage at the next sampling time, a space voltage vector $\mathbf{U}_s^*$ as shown in the figure should be applied in the time period of the sampling period T5, the reason for this is that the magnitude and phase angle of the applied space voltage vector U5 * can be calculated from equations (4) ~ (7) by moving the end points of the flux vector in the direction of the applied space voltage vector.

$$U_{s\alpha}^* = \frac{\left|\boldsymbol{\varnothing}_s^*\right|\cos(\gamma_s+\Delta\delta)-\left|\ _s\right|\cos\gamma_s}{T_s}+R_s i_{s\alpha} \approx \frac{\left|\ _s^*\right|\cos(\gamma_s+\Delta\delta)-\left|\ _s\right|\cos\gamma_s}{T_s} \tag{4}$$

$$U_{s\beta}^* = \frac{\left|\boldsymbol{\varnothing}_s^*\right|\sin(\gamma_s+\Delta\delta)-\left|\ _s\right|\sin\gamma_s}{T_s}+R_s i_{s\beta} \approx \frac{\left|\ _s^*\right|\sin(\gamma_s+\Delta\delta)-\left|\ _s\right|\sin\gamma_s}{T_s} \tag{5}$$

$$\left|\mathbf{U}_s^*\right| = \sqrt{U_{s\alpha}^{*\,2}+U_{s\beta}^{*\,2}} \tag{6}$$

$$\varphi_s^* = \arctan(U_{s\beta}^*/U_{s\alpha}^*) \tag{7}$$

Where $U_{s\alpha}^*$ and $U_{s\beta}^*$ are the components of the reference voltage vector $\mathbf{U}_s^*$ in the two-phase stationary coordinate system $\alpha\beta$, respectively, $\left|\mathbf{U}_s^*\right|$ and φ_s^* , respectivelyis the amplitude and phase angle of $\mathbf{U}_s^*$. The stator flux vector magnitude and phase angle, torque can be calculated by the following formula:

$$\begin{cases}\psi_{s\alpha} = \int (u_{s\alpha} - R_s i_{s\alpha})dt \\ \psi_{s\beta} = \int (u_{s\beta} - R_s i_{s\beta})dt \end{cases} \tag{8}$$

$$|\psi_s| = \sqrt{{\psi_{s\alpha}}^2 + {\psi_{s\beta}}^2} \tag{9}$$

$$\gamma_s = \arctan(\psi_{s\beta} / \psi_{s\alpha}) \tag{10}$$

$$T_e = \frac{3}{2} N_p (\psi_{s\alpha} i_{s\beta} - \psi_{s\beta} i_{s\alpha}) \tag{11}$$

The subscripts α and β are the components of each physical quantity on the $\alpha\beta$ -axis of the stator two-phase stationary coordinate system.

4. Direct Torque Control of Space Vector Modulation

The structure diagram of the direct torque control system (SVM-DTC) of permanent magnet synchronous motor based on space vector modulation is shown in Fig.3, Where the reference flux calculation model element and the space voltage vector modulation element SVM replaces the flux linkage in a conventional DTCand a torque hysteresis controller and switch table.

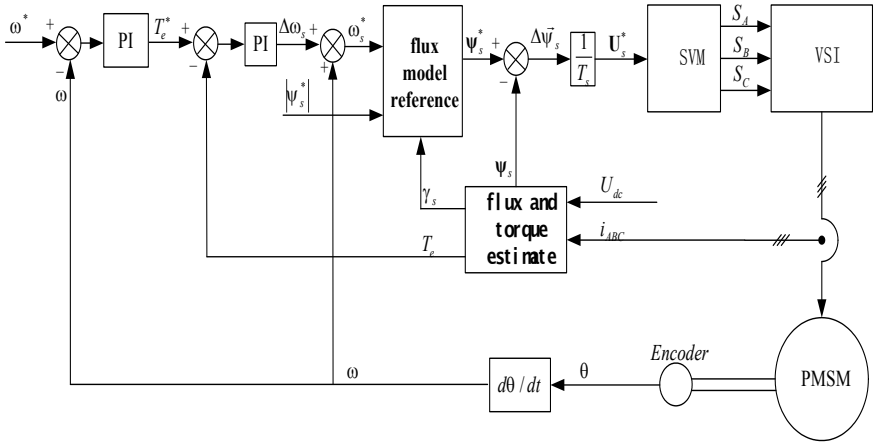

Figure.3 SVM-DTC block diagram of the structure

In Fig. 3, the difference between the reference angular velocity ω_s^* and the feedback angular velocity ω is output to the reference torque command T_e^* via a PI regulator.As the steady-state stator flux rotation speed and the rotor speed of rotation is the same, that is, synchronous speed ω , and when the reference torque or load torque in the dynamic process of mutation, the two speeds will be significantly inconsistent, the stator the flux rotation speed is significantly faster than the rotor rotation speed, there is a difference between the two rotational speed difference $\Delta\omega_s$ .Thus, the difference between the reference torque T_e^* and the estimated torque T_e can be output by a PI regulator, which is the stator flux rotational speed increment $\Delta\omega_s$,to reflect the dynamic change of the torque in real time.Thus, the total rotational speed ω_s^* of the flux linkage in one sampling period can be determined by the steady-state rotation speed ω and the rate of changeOf the rotational speed difference $\Delta\omega_s$, that is, the system should be in

the next sampling period given the flux reference speed.After obtaining the total flux rotation speed ω_s^* , the reference flux vector $\boldsymbol{\psi}_s^*$ given in the next sampling period can be obtained by referring to the flux linkage calculation model.The reference flux vector $\boldsymbol{\psi}_s^*$ and the estimated flux vector $\boldsymbol{\psi}_s$ of the current time can be calculated in the next sampling cycle should be applied to the space voltage vector $\mathbf{U}_s^*$, space voltage vector $\mathbf{U}_s^*$ and then through the space voltage vector modulation unit SVM to generate PWM pulse signal S_A , S_B and S_C , the final control voltage source inverter VSI drive permanent magnet synchronous motor.This new structure has the following advantages: PI regulator parameter adjustment is easy, and will not make the entire control system is running difficult.The product $\Delta\delta$ of the stator flux angle at the next time can be obtained by multiplying the flux rotation speed ω_s^* and the sampling period T5. Therefore, it is possible to adjust T5 todetermine $\Delta\delta$, which is easy to implement in the actual system.

5. Simulation Analysis

The SVM-DTC control of permanent magnet synchronous motor (PMSM) based on the above-mentioned principle is established by Matlab / Simulink simulation softwareSystem model.The simulation motor parameters are: UN = 220v; NP = 4; Rs = 2.875 ohms; Ld = 8.5mH; Lq = 8.5mH;F = 0.175Wb.Specific simulation conditions are set to: no-load start, the initial speed 1200r / min, 0.1s step to 1400 r / min,The load was applied to the 2 N • m at 0.2 s.

Figures 4 to 6 show the performance comparison of the conventional DTC and SVM-DTC simulation results, respectively.As can be seen from the figure,The response time of this control system is very short, almost no overshoot, which is the direct torque control of the outstanding advantages.From the torqueWaveform, the control mode of dynamic response is very fast, steady-state SVM-DTC torque fluctuations more stable, which canIt is seen from the current waveform that the current waveform of the SVM-DTC is closer to the sine wave than the conventional DTC current waveform.These differences is that the conventional DTC can only be controlled by selecting six basic active space voltage vectors and a hysteresis controller and SVM-DTC can use SVM to arbitrarily linearly combine the required space voltage vector to by real-time sampling calculation can be more precise control of the stator flux linkage.

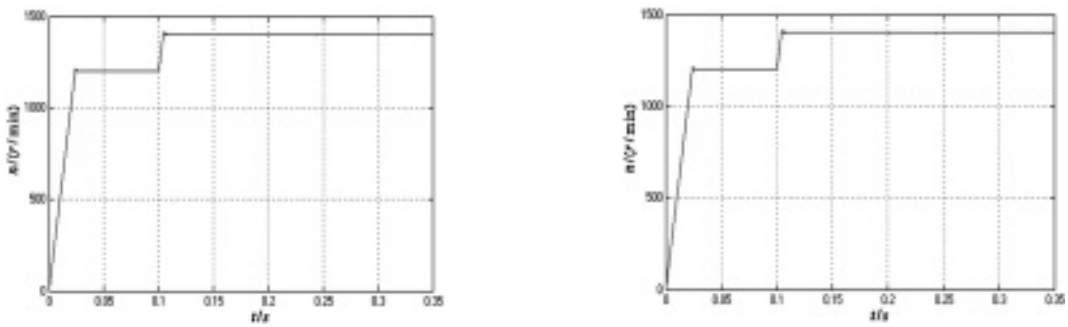

(a) Conventional DTC velocity response curve (b) SVM-DTC velocity response curve

Figure .4 two kinds of control speed response curve

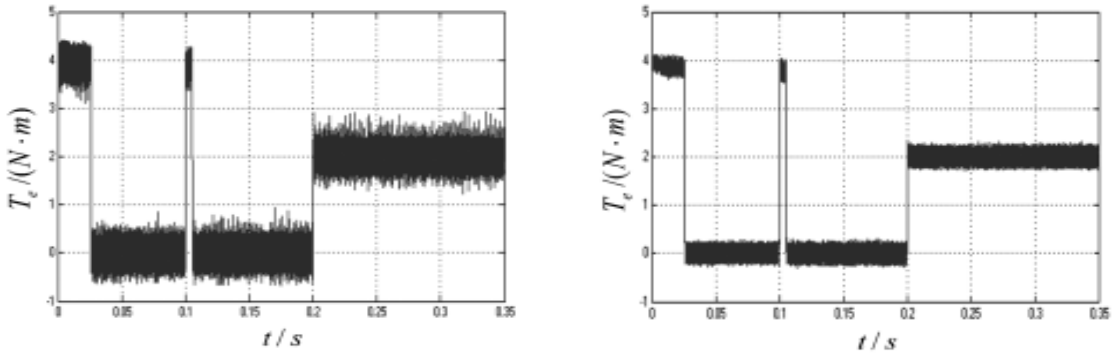

(a) Conventional DTC torque response curve (b)SVM-DTC torque response curve

Figure.5 two kinds of control torque response curve

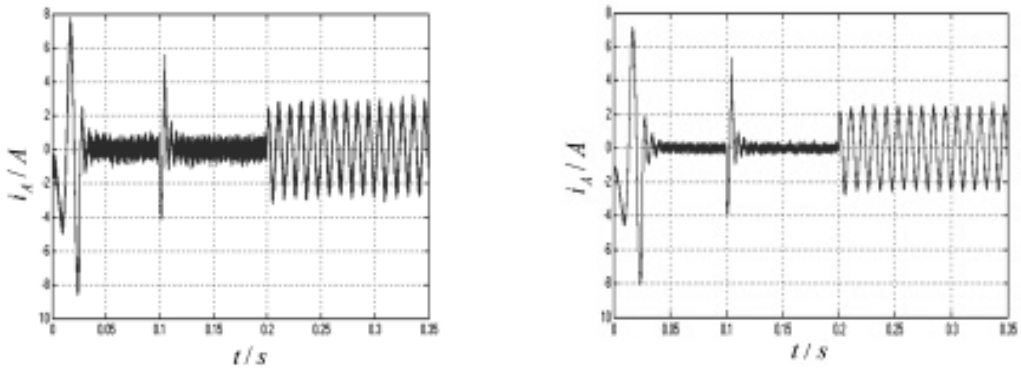

(a)Conventional DTC Phase Current Curves (b)SVM-DTC phase current curve

Figure.6 two kinds of control phase current curve

Torque Figure 7 for the SVM-DTC control process of the motor torque angle δ waveform of the change, we can see that the torque angle is electromagnetic torque changes consistent.In most steady-state processes, the torque angle δ is in the vicinity of a fixed value to do a small wave and the torque angle also changes rapidly in the dynamic process of rapid torque change.

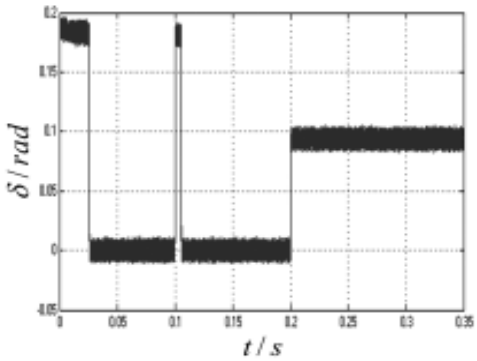

Figure.7 Torque angle δ curve

6. Conclusion

In order to solve the contradiction between dynamic and static performance of conventional direct torque control, that is, the contradiction between torque, fast response of flux linkage and torque, and large steady-state pulsation of flux linkage, this paper proposes a space vector based on space vector (PMSM) direct torque control (SVM-DTC), the principle and implementation of the scheme are discussed in detail. It is pointed out that the conventional DTC can only control the motor torque and flux linkage with a limited basic voltage vector, but none of the basic space voltage vectors can completely compensate the flux and torque errors in the system at the same time. Vector Modulation (SVM) is a promising solution. Secondly, the basic principle of SVM is expounded briefly. The SVM algorithm under different reference voltage vector input is analyzed, simulated and experimented. The SVM algorithm and its application are discussed in detail. Implementation has a clearer understanding. Finally, the SVM-DTC is discussed in detail, including the structure of the control system, the dynamic control process of the stator flux vector, the method of flux and torque estimation and the calculation model of the reference flux, etc. Theoretically, And the best compensation principle of flux error. Finally, the realization of SVM-DTC is studied, and compared with conventional DTC, the correctness of the control strategy is verified. Simulation results show that compared with conventional direct torque control, SVM-DTC has the advantages of faster dynamic response of conventional DTC and more stable steady-state operation while keeping the switching frequency of power devices constant. Because SVM-DTC has low hardware requirements and good control performance, it can effectively solve the contradiction between dynamic and static performance of conventional DTC, so it has good application prospects.

Acknowledgment

The authors wish to thank the cooperators. This research is partially funded by the Project funds in shaanxi province department of education (15JF019) and the Project funds in shanxi province department of science industrial projects(2015GY067).

References

[1] Zhang Wei, Michael S,Branicky, Stephen M, Phillips,Stability of Networked Control Systems, IEEE Control Systems Magazine1 February 2001, (21)： 84-99.

[2] Goodwin C, Juan Carlos Aguero,ArieFeuer, State Estima2tion for Systems Having Random Measurement Delays UsingErrors in Variables, The 15th Triennial World Congress1Barcelona,Spain, 2002.

[3] Lee Kyung Chang,Lee Suk, Remote Controller Design of Networked Control System Using Genetic Algorithm, ISIE 2007， Pusan， KOREA in IEEE, 2007: 1845-1850.

[4] AlmutairiNaif B， Chow Moyuen, PI Parameterization Using Adaptive Fuzzy Modulation (AFM) for Networked Control Systems - Part I : Partial Adaptation [J],IEEE Proceedings of IECON 2008,Sevilla， Spain， 2008. 3152-3157.

[5]Huang J Q , Lew is FL, Liu K A, Neural predictive control for telerobotswith time delay [J]. Journal of Intelligent and Robotic System s, 2000, 29： 1- 25.

[6]Lian Fengli1 Analysis, Design, Modeling,and Control of Networked Control Systems, Ph.D. thesis,The University of Michigan,2001.

[7] Huang J Q , Lew is FL, Liu K A, Neural predictive control for telerobotswith time delay [J]. Journal of Intelligent and Robotic System s, 2008, 29： 1- 25.

About the Author

Su xiaohui, (1970-11), male (the Han nationality), Shaanxi Province, Working in Xi'an technological university, Vicect professor, the research area is computer control.

Correspondence Address

(School of Computer Science and Engineering , Xi'an Technological University)

Postal Code: 710021 Tel: 13759907360

Email: suxh666@163.com

Behavior Control Algorithm for Mobile Robot Based on Q-Learning

Shiqiang Yang[1], Congxiao Li[2]

[1,2] Faculty of Mechanical and Precision Instrument Engineering, Xi'an University of Technology, Xi'an, P.R.China. 710048,

Email: [1]yangsq@126.com, [2]congcong_0901@126.com

Abstract. In order to adapt to navigation in unknown environment, the mobile robot must have intelligent abilities, such as environment cognition, behavior decision and learning. The navigation control algorithm is researched based on Q learning method in this paper. Firstly, the corresponding environment state space is divided. The action sets mapping with states are set. And the reward function is designed which combines discrete reward returns and continuous reward. The feasibility of this algorithm is verified by computer simulation.

Keywords: Q-learning, navigation, behavior control, simulation

1. Introduction

With the development of intelligent control technology, the mobile robot autonomous navigation control algorithm in unknown environment has become one of the interesting researches in the field of artificial intelligence[1,2]. The mobile robot must have more intelligent abilities, such as environment cognition, behavior decision and learning, to adapt to navigation in unknown environment[3]. Because of the uncertainty of the environment information and the lack of prior knowledge, the robot navigation in unknown environment becomes more complex and difficult. Reinforcement learning is a kind of mapping study between environment states to actions[4]. It hopes to take the actions which can get the largest cumulative award by learning. So, it is a kind of autonomous learning to adapt to the environment that takes environment feedback as the input. It is a good idea that makes a learning agent achieves goal by the interaction with the environment. An agent must perceive the environment and take correct actions to complete the assignment. At the same time, the agent must get one or more environment information about the target state in learning.

The reactive robot navigation control method is researched based on Q learning by the interaction between robot and the environment to adapt unknown different environment. The mobile robot navigation control strategy is represented in this paper.

2. Q Learning Algorithm

Reinforcement learning algorithm is a kind machine learning algorithms between supervised learning

and unsupervised learning. It is a kind of online learning based on reward and punishment mechanism. It learns environment based on deterministic or uncertain returns without model. It adjusts the parameters of the environment through the feedback of learning environment to the system. The mathematical model of reinforcement learning algorithm is based on the Markov chain and dynamic programming. It is a kind of strategy selection optimization method based on trial and error behavior.

Q-learning algorithm is a kind of typical model of reinforcement learning method. Learning agent has experienced ability to select the optimal action in the action sequence in Markov environment. The state estimation value function at different times is achieved while learning to optimize an iterative calculation function, so that the most optimal strategy is obtained. Q-learning is a kind of incremental online learning process. The map of "state - action" is used to iteration Q-learning. It should be ensure that the convergence of each iteration learning process.

The value of $Q(s,a)$ should be initialized in Q-learning process first. An action a should be choose obeying certain strategy, such as epsilon-greedy or the Boltzmann strategy, according to the learning agent initial state s to get the next state s'. And instantaneous reward r is achieved. The value of Q function is updated following the renewal rules. When agent access to the end of the target state or meet the correct conditions to end, the Q algorithm complete one cycle learning. Agent would continue the iteration cycle until the end of learning.

The optimal function values are approximated by optimizing value of the iterative function $Q(s,a)$ in Q-learning process. The renewal rules in Q-learning process are as formula (1) and formula (2).

$$Q(s_t,a_t) \leftarrow Q(s_t,a_t) + a\Delta Q(s_t,a_t) \tag{1}$$

$$Q(s_t,a_t) = (1-a)Q(s_t,a_t) + a[r_{t+1} + \gamma \max_{a\in A} Q(s_{t+1},a)] \tag{2}$$

Where a represents learning step. r_{t+1} represents the instantaneous rewards while the action a_t is performed in the process from the state s_t to state s_{t+1}. γ represents the discount rate of the $\max_{a\in A} Q(s_{t+1},a)$.

A lot of episodes are contained in Q-learning process. And they all repeat the following steps[5].

Step 1: observe the current state s_t;

Step 2: choose and perform an action a_t;

Step 3: observe the next state s_{t+1};

Step 4: receive a transient signal of rewards and punishments r_{t+1};

Step 5: update the value of Q function following to the formula (2);

Step 6: turn to the next moment, $t \leftarrow t+1$.

3. The Design of Q-Learning System for Mobile Robot Navigation

It needs two main functions, to avoid obstacles and to move to target, while the robot reactively

navigating in an unknown environment. The design of the Q-learning system from the robot model, environment state, action space, and reward in return to make it intelligent. For the convenience of description and to simplify the algorithm, the obstacles which site the 180° range only ahead the robot are considered. Obstacles position is divided into three directions: the left, right and ahead.

3.1 The division of the environment state

Q-learning is based on the discrete Markov decision model. So discretizing the continuous environment space into limited environment unit is needed for mobile robot navigation by Q-learning. It discretizes the environment from two aspects, the distance from robot to the obstacle and the angle from the robot to the target.

The environment is divided into three states according to the distance from robot to the obstacle:

$$s_{d-ro}=\begin{cases} sf & d_{R-O}>d_{sf} \\ m & d_{\min}\le d_{R-O}\le d_{sf} \\ d_g & d_{R-O}<d_{\min} \end{cases} \tag{3}$$

Where d_{R-O} represents the distance between the robot and the obstacles. And d_{R-O} is always less than the maximum distance which robot could detect. d_{sf} is set to the minimum safe distance without obstacle avoidance. $d_{\min}$ is set to robot safety threshold.

Define the distance on the left side as $s_{LR\_O}=d_l$, which is the minimum distance of the left side to the barrier measured by the sensor. Define the distance of the obstacles ahead as $s_{FR\_O}=d_m$, which is the minimum distance to obstacles ahead. Define the distance of the right obstacles as $s_{RR\_O}=d_r$, which is the minimum distance of the right side to the barrier.

The environment state is divided into the following eight states by the perspective of the angle from robot to target:

$$s_{a\_rg}=\{\mathrm{NVB},\mathrm{NB},\mathrm{NS},\mathrm{NVS},\mathrm{PVS},\mathrm{PS},\mathrm{PB},\mathrm{PVB}\} \tag{4}$$

Where NVB represents the target lies on the left rear of the robot within a range of 180°-135° counter clockwise. NB represents that the target locates on the robot left rear within the range of 135°-90°. NS represents that target lies on the left rear within the range of 45°~0°. $\{\mathrm{PVS},\mathrm{PS},\mathrm{PB},\mathrm{PVB}\}$ represent the case that the target lies on the robot right, it is just the reverse to the above. So the mobile robot state can be expressed as $s_{a\_rg}\in\{NVB,NB,NS,NVS,PVS,PS,PB,PVB\}$ .The definition of the eight states can be shown as the following.

$$s_{a-rg}=\begin{cases} NVB & -\pi\le \arg<-3\pi/4 \\ NB & -3\pi/4\le \arg<-\pi/2 \\ NS & -\pi/4\le \arg<-\pi/4 \\ NVS & -\pi/4\le \arg<0 \\ PVS & 0<\arg<\pi/4 \\ PS & \pi/4\le \arg<\pi/2 \\ PB & \pi/2\le \arg<3\pi/4 \\ PVB & 3\pi/4\le \arg<\pi \end{cases} \tag{5}$$

Where a_{rg} represents the angle between the forward direction and the direction from current point to the target point.

In summary, the environment state set S by discretization can be expressed as:

$$S=s_{a\_rg}\cup s_{d\_ro} \tag{6}$$

3.2 The definition of robot action

Autonomous mobile robot motion can be decomposed into translational motion and rotation motion. So the robot action set should be defined according to the rotation motion and translation motion. The concrete are defined as follows.

$$A = \{a_1, a_2, a_3, a_4, a_5\} \tag{7}$$

Where a_1 represents that the robot contrarotates for 45° and the mobile robot moves step is Step long, but Step=0. This means it just makes a pure rotation without shift. a_2 represents rotating for 15° counterclockwise and the mobile robot moves Step, but Step=0. a_3 represents the robot rotate for 0° and the mobile robot moves Step, Step= STEP(STEP for setting the robot moving step length unit). This means the robot make a pure shift without rotation. a_4 represents rotating for clockwise 15° and Step=0. a_5 represents rotating for clockwise 45° and Step=0.

3.3 The setting to reward function

Reward in return is immediate return to the robot for taking an action in a state. It can not evaluate the action is good or not in global, but reward function setting is a key factor to Q-learning system to get the corresponding strategy. It' s the unique useful information can be used in the strategy learning. Reward return function setting is the key to Q-learning system and learning strategies. A simple discrete efficient reward function is proposed after the above environment states division by the distance to obstacle and angle to target.

$$r_{a\_rg} = \begin{cases} -2 & s_{a\_rg} = NVB \quad or \quad s_{a\_rg} = PVB \\ -1 & s_{a\_rg} = NB \quad or \quad s_{a\_rg} = PB \\ 1 & s_{a\_rg} = NS \quad or \quad s_{a-rg} = PS \\ 4 & s_{a\_rg} = NVS \quad or \quad s_{a\_rg} = PVS \end{cases} \tag{8}$$

$$r_{d\_ro} = \begin{cases} 5 & s_{d\_ro} = sf \\ -1 & s_{d\_ro} = m \\ -5 & s_{d\_ro} = dg \end{cases} \tag{9}$$

Where r_{a_rg} represents the rewards in state s_{a_rg} . And r_{d_ro} represents the rewards in state s_{d_ro} .

Continuous reward in return for each action is set according the distance from current position to the target to guide robot towards the goal quickly. The specific design of the reward pay back system is shown as follows:

$$r_{d\_rg} = R_0 * Setp * \cos(a_t) / d_t \tag{10}$$

Where R_0 is the initial parameter values which depends on the value of the reward in return shown above. And a_t represents the angle from the moving direction to target point at the time t . The d_t represents the distance from the robot location to the target at the time t . The value of reward return r_{d_rg} is increasing while robots getting closer and closer to target.

4. Reactive Navigation Algorithm Based on Q-Learning and Simulation

The learning algorithm is introduced into the autonomous mobile robot reactive navigation control. Q-learning steps are as follow:

Step 1: Define state space and action space in the simulation environment. The reward return follows formula (8) and (9) above. Point (10, 15) sees as initial starting location and 0° as the attitude angle. The point (42, 30) sees as the target point. Initialize the parameters in Q-learning: Step = 1, $Q(\mathrm{s},\mathrm{a})=0$, $e(\mathrm{s},\mathrm{a})=0$ to all map state-action;

Step 2: Observe the current state s_t ;

Step 3: Select an action a_t according to the Boltzmann distribution action selection mechanism, and then execution;

Step 4: Observe the new state s_{t+1} and get reward $r(s_t,a_t)$;

Step 5: Calculate the value: $\delta \leftarrow r(s_t,a_t)+\max_{a\in A} Q_{t-1}(s_{t+1},a)-Q(s_t,a_t)$, $e_t(s_t,a_t)\leftarrow 1$;

Step 6: Calculate the Q-function: $Q_t(s,a)\leftarrow Q_{t-1}(s,a)+a\delta e_t(s,a)$;

Step 7: Judge whether the distance from robot to obstacle is less than the safe distance in the new state s_{t+1} . If the distance is less than the safe distance, turns back to the starting point and restart from the second step. Whether to reach the target point should be judged if it is greater than the safe distance. If it is true, then end the iteration, or turn to the second step to continue.

Two different simulation environments are set up to verify the feasibility of this above algorithm. The position (x, y) is represented for vertical and horizontal coordinates in simulation. The robot is simplified to a point and the obstacles are simplified to solid circles. Many random arrangement circular obstacles are in the environment. Robot starting point lies in the lower left corner in the simulation environment and the target is located in upper right, and both of them are shown as “ ☆ ”. The location of robot is shown as “※” in the simulation figure, and the line of “※” shows robot path from the initial starting point to the target.

As shown in Fig. 1 is the first circle learning process based on the Q learning, 30 obstacles are arranged random in the simulation. It can be seen that robot is always move to the target with much repetition. The path is extremely unreasonable and the robot fails to reach the target at last.

The results after 237 learning cycles are shown in Fig. 2. A feasible path is found from the chaotic state shown in figure 1, and robot arrives at the target safely. This path is better than the first learning circle apparently.

The simulation environment is changed in Fig. 3 and Fig. 4. The number of obstacles is 40 with random arrangement.

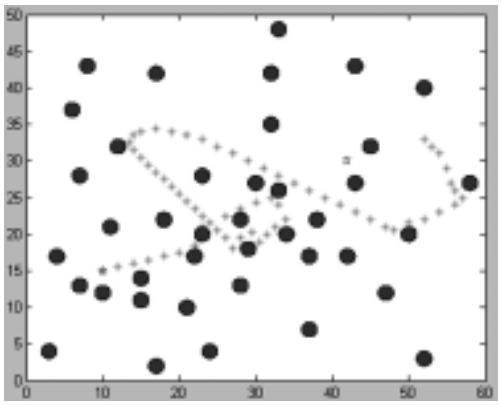

Fig.1 Simulation after 1st cycles learning

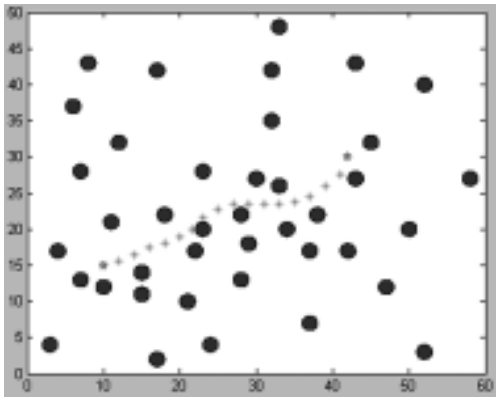

Fig.2 Simulation after 237 cycles learning

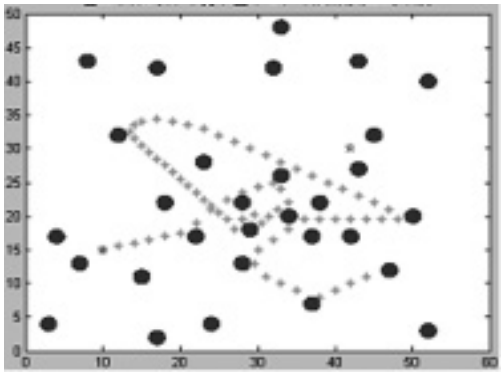

Fig.3 Simulation after 1st cycle learning

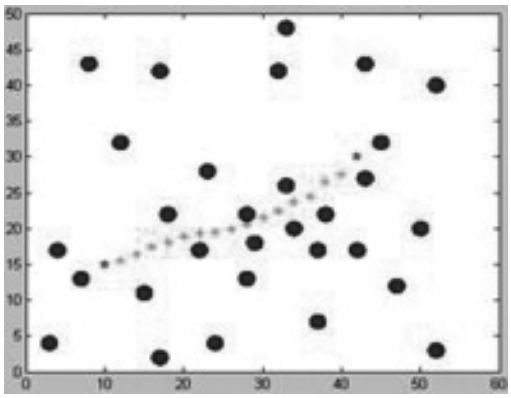

Fig.4 Simulation after 237 cycles learning

It can be seen that the path is in chaos after 1st cycle learning. The robot arrive at the target after 237 cycles learning. The path is feasible and safe.

According to the different unknown environments simulation, it can be seen that the robot behavior control algorithm based on Q-learning can adapt to the changes of the environment. Robot can get a feasible path by the online learning. Reactive navigation based on Q-learning has the effective path optimization.

5. Summary

The mobile robot navigation method is researched based on Q-learning method in unknown environment. The method to divide the environment state, to set the action sets and to set reward function are discussed. The Boltzmann selection mechanism is adopted for the learning process to action selection. The simulation results show that the reactive autonomic navigation approach based on the Q-learning can adapt to complicated unknown environment, this method is effective and feasible.

References

[1] Guo Rui, Wu Min, Peng Jun,etc. A new Q learning algorithm for multi-agent systems. Acta automatica sinica, Vol.33, No.4, p. 367-372, 2007

[2] LIAN Chuanqiang, XU Xin , WU Jun, LI Zhaobin. Q-CF multi-Agent reinforcement learning for resource allocation problems. CAAI Transactions on Intelligent Systems, Vol.6, No. 2, p.95-100, 2011

[3] FANGMin，LI Hao. Heuristically Accelerated State Backtracking Q－Learning Based on Cost Analysis. PR & A, Vol.26, No.9, p. 838-844, 2013

[4] HU Jun, ZHU Qing-bao. Path planning of robot for unknown environment based on prior knowledge rolling Q-learning. Control and Decision, Vol.25, No.9, p.1364-1368,2010

[5] J. C. H. Watkins Christopher, Dayan Peter. Q-learning. Machine Learning, Vol.8, No.3, p.279-292,1992

Author Brief and Sponsors

Shiqiang Yang is PhD. and associate professor in mechnical engineer department of Xi'an University of Technology. And his research interest is on mobile robot control. This work was financially supported by the National Natural Science Foundation of China (Grant No.51475365), the Scientific Research Program Funded by Shaanxi Provincial Education Department (Program No.2013JK1000).

Method of Determining Relevance of Changing Processes of Condition Building Parameters

Anna Doroshenko[1,a *], Andrey Volkov[1,b]

[1]Moscow state university of civil engineering, 129337, Russia, Moscow, Yaroslavskoe shosse 26

Email: [a]pochta.avd@gmail.com, [b]rector@mgsu.ru

Abstract. In the modern world it is increasingly referred to the concept of intelligent building. Intelligent building referred to above all energy-efficient building, using alternative energy sources, as well as equipped with modern energy efficient technologies that reduce the energy consumption of the building in general. But for all the time and does not set forth a definition of intelligence buildings, which leads to different opinions and approaches to the understanding of the term.

Keywords: Intelligent building, energy efficient technologies, the energy consumption, intelligence buildings.

1. Introduction

The original generic approach to the formal definition of the term "intelligence" of buildings in terms of abstract cybernetics involves the calculation of an abstract intelligence quotient and abstract building automation rate:

Abstract Intelligence quotient of buildings is determined by the following formula [1]:

$$BIQ=\frac{Q(R_1)}{Q(R)} \quad (1)$$

where Q – function of the considered set (measure of the set).

Abstract coefficient of buildings automation is determined by the following formula [2]:

$$BAQ=\frac{Q(P_2)}{Q(P_1)} \quad (2)$$

P – set of all change processes of parameters and their values of the building;

P1 – a subset of the change processes in values of the observed parameters of the building, P1P;

P2 – a subset of managed processes change the values of the observed parameters of a building, P2P1;

R – set of management processes change of values the observed parameters of the building (the building process parameter control);

R1 – a subset of the change control process of values the observed parameters of the building (building parameters management processes), functional (F) adaptive own state space X1, R1R.

Q – function of the sets under consideration [1].

The sets are calculated as shown in the formulas (3) – (6) [2].

$$Q(R) = \sum_{r \in R} C_r \quad (3)$$

$$Q(R_1) = \sum_{r \in R_1} C_r \quad (4)$$

$$Q(P_1) = \sum_{r \in P_1} C_r \quad (5)$$

$$Q(P_2) = \sum_{r \in P_2} C_r \quad (6)$$

Quantifying the significance of changes in the process parameters for the processes of heat exchange in building is calculated according to the formula [7]:

$$C_r = \frac{E_i}{\sum_{i=1}^{n} E_i} \quad (7)$$

where Ei – energy capacity of the process adopted for the period

2. Method

There is a question of forming method of the unique determination of energy capacity of change processes of the values of building parameters.

Problem is to generate a set of expressions that define the energy capacity of the known types of processes for engineering systems.

As part of the work covered such types of buildings as:

• Residential apartment buildings

• Residential townhouses

• Public buildings

3. Discussion

Engineering systems have been considered in the work in accordance with the normative documents of the Russian Federation

Heating, ventilation and air conditioning, are considered in accordance with SNIP 41-01, water supply and sanitation systems are considered in accordance with SNIP 2.04.01 and SNIP 02.04.02, electric power systems are considered in accordance with the PUE.

Structurally proposed set of expression has the form shown in the table 1.

Table 1 The structure of the expression of certain sets of processes energy capacity

№	Engineering system	Type of engineering system	Expression
1		Heaters radiator	$E=f_{1-1}$
2		Convection	$E=f_{1-2}$
3		Air heating	$E=f_{1-3}$
4	Ventilation system	Natural ventilation system	$E=f_{2-1}$
5		Forced ventilation system	$E=f_{2-2}$
6		Supply and exhaust ventilation system	$E=f_{2-3}$
7		The system of supply and exhaust ventilation with air recirculation	$E=f_{2-4}$
8		The system of supply and exhaust ventilation air recuperation	$E=f_{2-5}$
9	The air conditioning system	Air-cooling	$E=f_{3-1}$
10		Air heating	$E=f_{3-2}$
11		Air humidification by irrigation	$E=f_{3-3}$
12		Air steam humidification	$E=f_{3-4}$
13	The water supply system	Cold water supply	$E=f_{4-1}$
14		Hot water supply	$E=f_{4-2}$
15	The sewerage system	Sewerage system without heat recovery	$E=f_{5-1}$
16		Sewerage system with heat recovery	$E=f_{5-2}$
17	Gas supply system	Gas supply system	$E=f_{6-1}$

Using normative documents consider air heating by means of radiators (point 1 of Table 1). Where heating consists of two types: air-heating and heating walls

Air-heating is defined by the formulas (8 – 9).

$$Q_{air} = G_{air} c_{air} \rho_{air} (T_{out\ temp.} - T_{in\ temp..}) \quad (8)$$

$$E_{air} = \frac{ky_{p.} H_{p.} Q_{air}}{c_w (T_{w.end} - T_{w.initial})} / (\eta_{n.} \eta_{p.}) \quad (9)$$

Where: – thermal power required for heating the air in the radiator heating system, W;

– air consumption,;

– specific heat of air, J/(kg*0C);

ρ_{air} – air density in kg/m^3;

$T_{out\ temp.}$ – outdoor air temperature, 0C;

$T_{in\ temp.}$ – indoor air temperature, 0C;

and E_{air} – electric power needed to supply the coolant in the radiator heating system for heating the air, W;

K – the safety factor;

y – the proportion of the pumped liquid, N/m³;

Hp – the pump head, m;

η_n – pump efficiency;

η_p – transfer coefficient;

C_w – specific heat of water, J/(kg*0C);

$T_{w.end}$ – end water temperature, 0C;

$T_{w.initial}$ – initial water temperature, 0C.

Heating walls is defined by the formulas (10 – 11).

$$Q_w = kF(T_{in} - T_{out}) \quad (10)$$

$$E_w = \frac{k_s y H_p Q_w}{c_w(T_{w.end} - T_{w.initial})} / (\eta_n \eta_p) \quad (11)$$

Q_w – thermal power required for heating the walls of the radiator heating system, W;

K – heat transfer coefficient,W/(m2*0C);

F – wall area, m2;

T_{in} – indoor air temperature, 0C;

T_{out} – outdoor air temperature, 0C;

E_w – electric power needed to supply the coolant in the radiator heating system for heating the walls, W;

K_s – the safety factor;

$y_{П.B}$ – the proportion of the pumped liquid, N/m³;

H_p – the pump head, m;

η_n – pump efficiency;

η_p – transfer coefficient;

C_w – specific heat of water, J/(kg*0C);

$T_{w\,end}$ – end water temperature, 0C;

$T_{w\,initial}$ – initial water temperature, 0C.

4. Conclusion

The presence of such a set of expressions avoids subjective evaluations in determining significance of

the individual processes change the value of the building parameters. The inclusion of the proposed set in the method of determining BIQ and BAQ allows an objective comparison of "intelligence" of different buildings and different types of buildings.

The prospect of work is the development of computer technology, realized in the automated calculation of the energy capacity and then quantify the significance of the processes of engineering systems. This computer technology will be the first step of the automated designing, implementing a formal approach to the definition of "intelligence" of buildings.

5. Acknowledgements

This work was financially supported by the Ministry of Russian Education (state task #2014/107)

References

[1] A.A.Volkov, D.E. Namiot, M.A. Shneps-Shneppe, On the tasks of creating an effective infrastructure for habitat. // International journal of open information technologies. - 2013. - V7 (1). - pp. 1-10.

[2] J Duffy,W Beckman, Thermal processes using solar energy. - M .: Mir, 1977.

[3] M.M. Brodach, Heat Energy optimization orientation and size of the building. // Proceedings of the Research Institute for Building Physics. M., 1987. The heat treatment and durability of buildings.

[4] P.P.Denisov, Influence index space-planning solutions building on the heat consumption. - „Housing " 1981, № 1.

[5] B.I. Giyasov, The impact of infrastructure development on the urban living environment // Vestnik MGSU. - 2012 - V4

[6] Volk, R., Stengel, J., Schultmann, F. Building Information Modeling (BIM) for existing buildings - Literature review and future needs (2014) Automation in Construction, 38, pp. 109-127.

[7] Wang, X., Chong, H.-Y. Setting new trends of integrated Building Information Modelling (BIM) for construction industry (2015) Construction Innovation, 15 (1), pp. 2-6.

[8] Shanmuganathan, S. BIM - A global consultant 's perspective (2013) Structural Engineer, 91 (11), pp. 102-104.

[9] Volkov, A. General information models of intelligent building control systems: Scientific problem and hypothesis (2014) Advanced Materials Research, 838-841, pp. 2969-2972.

[10] Volkov, A. General information models of intelligent building control systems: Basic concepts, determination and the reasoning (2014) Advanced Materials Research, 838-841, pp. 2973-2976.

[11] Volkov, A.A., Sedov, A.V., Chelyshkov, P.D. Modelling the thermal comfort of internal building spaces in social buildings (2014) Procedia Engineering, 91, pp. 362-367.

[12] Volkov, A., Chelyshkov, P., Sedov, A. Application of computer simulation to ensure comprehensiv